

**ISTANBUL TECHNICAL UNIVERSITY ★ GRADUATE SCHOOL OF SCIENCE**  
**ENGINEERING AND TECHNOLOGY**

**INVESTIGATION OF GEARTRAIN IMPACT NOISE IN DIESEL ENGINES**

**M.Sc. THESIS**

**Ali TATAR**

**Department of Mechanical Engineering**

**Machine Dynamics, Vibration and Acoustics Programme**

**MAY 2015**



**ISTANBUL TECHNICAL UNIVERSITY ★ GRADUATE SCHOOL OF SCIENCE**  
**ENGINEERING AND TECHNOLOGY**

**INVESTIGATION OF GEARTRAIN IMPACT NOISE IN DIESEL ENGINES**

**M.Sc. THESIS**

**Ali TATAR**  
**(503121414)**

**Department of Mechanical Engineering**

**Machine Dynamics, Vibration and Acoustics Programme**

**Thesis Advisor: Prof. Dr. Kenan Yüce ŞANLITÜRK**

**MAY 2015**



**İSTANBUL TEKNİK ÜNİVERSİTESİ ★ FEN BİLİMLERİ ENSTİTÜSÜ**

**DİZEL MOTORLARDA DIŞLI DARBE GÜRÜLTÜSÜNÜN İNCELENMESİ**

**YÜKSEK LİSANS TEZİ**

**Ali TATAR  
(503121414)**

**Makina Mühendisliği Anabilim Dalı**

**Makina Dinamiği, Titreşim ve Akustiği Programı**

**Tez Danışmanı: Prof. Dr. Kenan Yüce ŞANLITÜRK**

**MAYIS 2015**



**Ali Tatar**, a **M.Sc.** student of ITU **Graduate School of Science Engineering and Technology** student ID **503121414**, successfully defended the **thesis** entitled “**INVESTIGATION OF GEARTRAIN IMPACT NOISE IN DIESEL ENGINES**”, which he prepared after fulfilling the requirements specified in the associated legislations, before the jury whose signatures are below.

**Thesis Advisor :**     **Prof. Dr. Kenan Yüce ŞANLITÜRK**     .....  
Istanbul Technical University

**Jury Members :**     **Prof. Dr. İsmail Ahmet GÜNEY**     .....  
Istanbul Technical University

**Dr. Egemen TINAR**     .....  
Arçelik A.Ş

**Date of Submission : 04 May 2015**  
**Date of Defense : 28 May 2015**



*To my grandmother,*



## **FOREWORD**

First of all, I would like to gratefully thank to my thesis supervisor, Prof. Dr. Kenan Yüce Şanlıtürk for his invaluable guidance, suggestion and endless support as well as his endless patience. I cannot forget his encouragement and motivation for me during my thesis study. He has influenced me with his great knowledge, experience, creativity and management capability. It is a great honour to be his student for me.

I would like to thank to Prof. Dr. Ahmet Güney who is also the jury member of this thesis. First, he endeared NVH to me with his undergraduate course in ITU. Therefore, he has become an important person during my career.

I would like to thank to Dr. Alfred Rust who is NVH technical specialist in AVL List GmbH. I cannot forget his support and interest during my researches and studies in Graz.

This project was conducted at the Engine Dynamometer Test Center of Ford OTOSAN, therefore I would like to thank all employees of Engine Dynamometer Test Center.

I would like to thank my friends who always support me with their best wishes. It is not possible to forget some supports at hard times. These invaluable supports belong to Yunus Emre Torun and Gürkan Tutu. I would like to thank them again.

Lastly, I would like to thank my family for their patience during my thesis study. Especially, my grandmother, who grew me, is the real owner of this thesis due to her invaluable support, patience and love. No one deserves this gratitude more than her.

May 2015

Ali TATAR  
(Mechanical Engineer)



## TABLE OF CONTENTS

	<u>Page</u>
<b>FOREWORD</b> .....	<b>ix</b>
<b>TABLE OF CONTENTS</b> .....	<b>xi</b>
<b>ABBREVIATIONS</b> .....	<b>xiii</b>
<b>LIST OF TABLES</b> .....	<b>xv</b>
<b>LIST OF FIGURES</b> .....	<b>xvii</b>
<b>SUMMARY</b> .....	<b>xix</b>
<b>ÖZET</b> .....	<b>xxiii</b>
<b>1. INTRODUCTION</b> .....	<b>1</b>
1.1 Problem .....	2
1.2 Literature Review .....	3
1.3 Objectives and Outline of Thesis .....	7
<b>2. THEORY</b> .....	<b>11</b>
2.1 Gears.....	11
2.2 Geartrain Noise .....	12
2.2.1 Gear meshing noise .....	13
2.2.2 Gear impact noise.....	14
2.2.2.1 Backlash effect on gear impacts.....	15
2.2.2.2 Mathematical model of gear impacts .....	16
2.3 Dynamic Model of the Gear System .....	16
2.3.1 Gear contact dynamic model.....	18
2.3.2 Gear drive system model.....	19
2.3.3 Nonlinear dynamic model of geartrain .....	20
2.4 Torsional Vibration Analysis of Crankshaft for Six Cylinder Engine .....	22
2.5 Vibration & Acoustic Analysis Method.....	25
2.5.1 Sound pressure level .....	25
2.5.2 Fourier analysis .....	25
2.5.3 Cepstrum analysis .....	27
2.5.4 Envelope analysis.....	28
2.5.4.1 Hilbert tranform .....	28
<b>3. NUMERICAL ANALYSIS OF GEARTRAIN IMPACTS</b> .....	<b>29</b>
3.1 Geartrain Impact Impulse Method .....	30
3.1.1 Geartrain modelling in AVL Excite Timing Drive .....	31
3.1.2 Determination of critical gear meshes .....	34
3.1.3 Effect of engine speed on impact impulses.....	35
3.1.4 Backlash effect on impact impulses.....	36
3.1.5 Effect of gear loading on impact impulses.....	36
3.1.6 Effect of fuel pump phasing on impact impulses.....	37
3.2 Torsional Vibration Analysis of Crankshaft .....	39
3.2.1 Multi-body engine model.....	39
3.2.2 Multi-body dynamic analysis result .....	40

<b>4. EXPERIMENTAL STUDY OF GEARTRAIN IMPACT NOISE .....</b>	<b>43</b>
4.1 Engine Dynamometer Noise & Vibration Tests.....	44
4.1.1 Vibration and acoustic measurement comparisons .....	47
4.1.2 Acoustic camera measurements .....	50
4.1.3 Investigation of backlash effect.....	54
4.1.4 Fuel pump phasing .....	58
4.1.5 Torsional vibration measurement of crankshaft.....	64
4.1.6 Cylinder pressure variation effect on torsional vibrations .....	65
4.2 Investigation of Housing Effect.....	67
4.2.1 Housing FRF measurements .....	67
4.3 Vehicle Exterior Noise Tests.....	69
4.3.1 Gear loading effect.....	69
4.3.2 Adjustable idler backlash changing effect .....	73
4.3.3 Effect of idle speed.....	75
4.4 Advanced Signal Processing Applications .....	76
4.4.1 Time domain signal analysis of hot idle data.....	76
4.4.2 Envelope analysis of hot idle data.....	77
4.4.3 Modulation frequency analysis of hot idle data .....	79
4.4.4 Cepstrum analysis of hot idle data .....	80
<b>5. CONCLUSIONS AND RECOMMENDATIONS .....</b>	<b>81</b>
5.1 Conclusions .....	81
5.2 Future Reccomendations .....	82
<b>REFERENCES .....</b>	<b>85</b>
<b>CURRICULUM VITAE .....</b>	<b>89</b>

## ABBREVIATIONS

<b>Acc</b>	: Accelerometer
<b>ARCT</b>	: Acoustic Relevant Contact Time
<b>CAD</b>	: Computer Aided Design
<b>CAE</b>	: Computer Aided Engineering
<b>CRS</b>	: Common Rail System
<b>CT</b>	: Close Throttle
<b>EKM</b>	: Einfachst-Klapper-Modell
<b>EO</b>	: Engine Order
<b>FFT</b>	: Fast Fourier Transform
<b>FRF</b>	: Frequency Response Function
<b>HD</b>	: Heavy Duty
<b>HT</b>	: High Temperature
<b>ICP</b>	: Integrated Circuit Piezoelectric
<b>MDOF</b>	: Multi Degree of Freedom
<b>Mic</b>	: Microphone
<b>NVH</b>	: Noise, Vibration, Harshness
<b>PAS</b>	: Power Assisted Steering
<b>PBN</b>	: Pass By Noise
<b>POT</b>	: Partial Open Throttle
<b>PS</b>	: Pferdestärke
<b>PTO</b>	: Power Take Off
<b>RotExc</b>	: Rotational Excitation
<b>RPM</b>	: Revolutions per minute
<b>SHGE</b>	: Shaft / Gear
<b>SOHC</b>	: Single Over Head Cam
<b>SPL</b>	: Sound Pressure Level
<b>WOT</b>	: Wide Open Throttle



## LIST OF TABLES

	<u>Page</u>
<b>Table 3.1</b> : Names of gear meshes.....	34
<b>Table 4.1</b> : Engine specification.....	43
<b>Table 4.2</b> : Geartrain meshing frequency.....	49
<b>Table 4.3</b> : Oilpump backlash value.....	54
<b>Table 4.4</b> : Hot idle sound pressure level of backlash iterations.....	55
<b>Table 4.5</b> : Full load speed sweep sound pressure level of backlash iterations. ....	57
<b>Table 4.6</b> : Cylinder to cylinder peak pressure variation .....	66
<b>Table 4.7</b> : Sound pressure level comparison of gear loading. ....	72
<b>Table 4.8</b> : Sound pressure level comparison of idler backlash effect.....	73



## LIST OF FIGURES

	<u>Page</u>
<b>Figure 1.1</b> : Pass-by noise (PBN) contributions of 13L heavy-duty truck [1].	1
<b>Figure 2.1</b> : (a) Spur gears [19]. (b) Helical gears [20].	11
<b>Figure 2.2</b> : Timing drive noise characteristic [24].	12
<b>Figure 2.3</b> : Signatures of gear whine and gear rattle [26].	13
<b>Figure 2.4</b> : Backlash effect on gear impact noise (Crocker’s graph) [3].	15
<b>Figure 2.5</b> : Gear backlash [31].	15
<b>Figure 2.6</b> : Gear contact dynamic model [28].	18
<b>Figure 2.7</b> : Definition of transmission error [28].	19
<b>Figure 2.8</b> : Gear drive dynamic model [28].	19
<b>Figure 2.9</b> : The nonlinear dynamic model [13].	20
<b>Figure 2.10</b> : Nonlinear meshing contact model at gear mesh [13].	21
<b>Figure 2.11</b> : A six cylinder engine crankshaft [36].	22
<b>Figure 2.12</b> : Multi-mass model of six cylinder engine [36].	22
<b>Figure 2.13</b> : Time and frequency domain [38].	27
<b>Figure 3.1</b> : Geartrain system of a 12.7 liter engine.	29
<b>Figure 3.2</b> : Acoustic relevant contact time [41].	31
<b>Figure 3.3</b> : AVL Excite geartrain dynamic model.	33
<b>Figure 3.4</b> : Determination of critical gear meshes.	35
<b>Figure 3.5</b> : Engine speed effect on total impact impulse.	35
<b>Figure 3.6</b> : Backlash effect on total impact impulse.	36
<b>Figure 3.7</b> : PAS pump loading effect on total impact impulse.	37
<b>Figure 3.8</b> : Fuel pump phasing effect on total impact impulse.	38
<b>Figure 3.9</b> : Multi-body engine model [44].	39
<b>Figure 3.10</b> : Torque fluctuation of crankshaft.	40
<b>Figure 3.11</b> : Angular acceleration FFT of crankshaft damper ring.	40
<b>Figure 4.1</b> : Torque curve of 12.7L HD diesel engine.	44
<b>Figure 4.2</b> : Semi-anechoic test cell with low-noise engine test bench [26].	45
<b>Figure 4.3</b> : Engine dynamometer configuration of 12.7 liter HD diesel engine.	45
<b>Figure 4.4</b> : Microphone positions in engine dynamometer.	46
<b>Figure 4.5</b> : (a) Brüel & Kjaer microphone Type 4188 [45]. (b) PCB Piezotronics ICP accelerometer Model HT 356B21 [46]. (c) LMS SCADAS 310 - UTP data acquisition system [47].	47
<b>Figure 4.6</b> : Accelerometer locations on engine.	48
<b>Figure 4.7</b> : Waterfall FFT vs time diagram of engine rear side mic and flywheel housing bottom accelerometer.	48
<b>Figure 4.8</b> : Waterfall FFT vs time diagram of engine left side mic and geartrain housing left accelerometer.	49
<b>Figure 4.9</b> : HEAD VISOR acoustic camera [49].	50
<b>Figure 4.10</b> : Screenshot of HEAD VISOR software.	50
<b>Figure 4.11</b> : Engine left side critical peak.	51

<b>Figure 4.12</b> : Engine right side critical peak. ....	51
<b>Figure 4.13</b> : Engine left side acoustic camera result.....	52
<b>Figure 4.14</b> : Engine right side acoustic camera result. ....	53
<b>Figure 4.15</b> : Oilpump gears of 12.7 liter HD diesel engine. ....	54
<b>Figure 4.16</b> : Engine rear microphone 1/3 octave of oil pump backlash iterations. .	55
<b>Figure 4.17</b> : Engine rear microphone FFT of oil pump backlash iterations. ....	56
<b>Figure 4.18</b> : Engine left mic waterfall FFT diagram of oilpump backlash iterations. .....	56
<b>Figure 4.19</b> : Oilpump backlash iteration comparison at engine rear microphone. ..	57
<b>Figure 4.20</b> : Fuel pump phasing tool. ....	58
<b>Figure 4.21</b> : Full load test 4 microphone average sound pressure level of phasing angles. ....	59
<b>Figure 4.22</b> : Full load test rear microphone sound pressure level of phasing angles. .....	60
<b>Figure 4.23</b> : Fuel pump phasing noise contribution on rear mic and four mic average. ....	60
<b>Figure 4.24</b> : Engine rail pressure for different phasing angles. ....	61
<b>Figure 4.25</b> : Engine torque level for different phasing angles.....	61
<b>Figure 4.26</b> : Fuel pump phasing full load speed sweep test FFT vs rpm campbell diagram of engine rear microphone. ....	62
<b>Figure 4.27</b> : Fuel pump phasing full load speed sweep test FFT vs rpm campbell diagram of flywheel housing accelerometer. ....	62
<b>Figure 4.28</b> : Fuel pump phasing idle SPL of rear mic and four mic average. ....	63
<b>Figure 4.29</b> : Torsional vibration damper of 12.7 liter engine. ....	64
<b>Figure 4.30</b> : Torsional vibration measurements of 12.7 liter HD engine. ....	64
<b>Figure 4.31</b> : Cylinder pressures of cylinders 1, 2, 5, 6. ....	66
<b>Figure 4.32</b> : Different flywheel housing designs. ....	67
<b>Figure 4.33</b> : Flywheel housing FRF measurement accelerometer locations. ....	67
<b>Figure 4.34</b> : Flywheel housings in Y direction: FRF sum. ....	68
<b>Figure 4.35</b> : Microphones locations for gear loading and idle speed changing test.	69
<b>Figure 4.36</b> : Microphones locations for adjustable idler gear backlash test. ....	69
<b>Figure 4.37</b> : Right mic waterfall FFT diagram of gear loading (impact noise). ....	71
<b>Figure 4.38</b> : Right mic waterfall FFT diagram of gear loading (meshing noise). ...	71
<b>Figure 4.39</b> : 1/3 octave comparison of PAS pump gear loading. ....	72
<b>Figure 4.40</b> : Adjustable idler of 12.7 liter engine. ....	73
<b>Figure 4.41</b> : 1/3 octave comparison of maximum and minimum idler backlash. ....	74
<b>Figure 4.42</b> : Rear mic waterfall FFT diagram of idler backlash effect.....	74
<b>Figure 4.43</b> : Rear mic waterfall FFT diagram of idler backlash effect.....	75
<b>Figure 4.44</b> : Time domain signals of accelerometer and microphone data. ....	76
<b>Figure 4.45</b> : Envelope spectrums of accelerometer (a) and microphone (b) data. ..	77
<b>Figure 4.46</b> : Envelope spectrums of fuel pump phasing data: the best case (a) and the worst case (b). ....	78
<b>Figure 4.47</b> : FFT spectrums of fuel pump phasing data: the best case (a) and the worst case (b). ....	78
<b>Figure 4.48</b> : Modulation frequency analysis of microphone data.....	79
<b>Figure 4.49</b> : Cepstrum envelope (Cepslope) analysis of accelerometer data. ....	80
<b>Figure 4.50</b> : Cepstrum envelope (Cepslope) analysis of microphone data.....	80

# **INVESTIGATION OF GEARTRAIN IMPACT NOISE IN DIESEL ENGINES**

## **SUMMARY**

Overall noise level of internal combustion engines has always been an important issue in the automotive industry due to the competition between automotive manufacturers as well as legislative regulations. Thus, automotive manufacturers aim to determine engine noise sources and their root causes before mass production, and also they take applicable precautions in order to prevent engine noise problems within the NVH considerations during design and development phases.

It is well known that diesel engines are noisier than gasoline engines since diesel engines have higher gas pressure in combustion chamber during combustion process compared to gasoline engines. This also affects mechanical noise problems in diesel engines, which can cause higher vibration and noise levels compared to those of gasoline engines. Therefore, overall noise levels of diesel engines are more crucial than those of gasoline engines.

Mainly, radiated noise of internal combustion engines are examined in two categories as combustion noise and mechanical noise. Geartrain noise is one of the most significant mechanical noise contributors in diesel engines, especially in heavy-duty diesel engines. Fundamentally, there are two important gear noise types in geartrains, which are classified as gear impact (rattle) noise and gear meshing (whine) noise. This thesis aims to focus on geartrain impact noise which is also referred to as gear hammering or rattle noise. Likewise, gear meshing noise is named as gear whine noise in the automotive industry. Gear meshing noise, a kind of tonal noise, frequency of which is proportional to the engine order hence its diagnosis is easier with NVH measurements. Gear impact noise, on the other hand, is known as broadband noise, therefore its root cause analysis is more difficult by gear fault diagnosis compared to root cause analysis of gear meshing noise.

The main reason for the occurrence of gear impact is that relative motion between gear teeth leads to loss of contact which in turn results in impact between gears creating impact noise. Moreover, speed and/or torque fluctuations of geartrain members and torsional vibrations of engine crankshaft and geartrain members dominate these gear impacts. Operating conditions in diesel engines are also important factor for radiation of impact noise from engine surfaces. Higher loads in the engine cause higher impacts between gears, hence gear impact noise increases with respect to loads. Especially, the gear impact noise becomes a significant noise source in engine full load conditions. On the other hand, gear impact noise becomes more audible at lower engine speed due to the low levels of combustion noise as well as low levels of other mechanical noise.

The main objectives of this thesis are to determine the effective parameters on geartrain impact noise in diesel engines and to understand the background theory of gear impacts. In the second chapter, background theory of gear impacts, dynamics,

noise and vibration are introduced, and torsional vibration analysis of crankshaft is described. Furthermore, vibration and acoustic analysis methods for experimental studies are presented. For the determination of effective parameters on geartrain impact noise in diesel engines, numerical and experimental studies, which are respectively presented in chapters three and four, are conducted on a six cylinder heavy-duty diesel engine, geartrain of which are made of spur gears.

Numerical analyses of geartrain impact are performed by using impact impulse method which is a special analysis method for the evaluation of impact noise level. Critical gear meshes in engine geartrain is determined by geartrain impact impulse analyses. The analysis results show that crankshaft gear and crankshaft idler gear mesh is the most critical gear mesh for geartrain impacts. Moreover, significant parameters on geartrain impacts, which are backlash, engine speed, gear loading and fuel pump phasing, are determined by the impact impulse analysis. As a result, gear loading and fuel pump phasing are determined as the significant factors on gear impacts rather than backlash effect.

Experimental studies of geartrain impact noise are conducted with the help of NVH tests in engine dynamometer and NVH tests on the vehicle. Impact noise source on the heavy-duty diesel engine is detected in acoustic dynamometer by using acoustic camera measurement and “vibration and acoustic measurement comparisons”. Results of experimental studies show that geartrain side of the heavy-duty diesel engine has the highest noise contribution to the overall noise level of the engine. Significant parameters on impact noise are experimentally investigated by fuel pump phasing test, backlash iteration test in engine dynamometer and gear loading test, idler backlash test and engine speed test on the vehicle. In accordance with the results of the numerical analyses, experimental results also confirm that fuel pump phasing has strong effect on gear impact noise at full load conditions and gear loading has significant effect on gear impact noise at idle operating condition. Moreover, it is observed experimentally that oilpump backlash has minor effect on geartrain impact noise compared to fuel pump phasing and gear loading effect. However, backlash effect on gear impact noise is clearly seen on the gear mesh between camshaft gear and camshaft idler gear.

Pressure variations between cylinders are also measured in engine dynamometer, and results show that cylinder to cylinder pressure variations occur in the heavy-duty engines. It is well known that cylinder to cylinder pressure variation has adverse effects on crankshaft torsional vibrations.

Housing FRF test is also another conducted experimental study in order to establish the housing effects on geartrain impact noise. Result of housing FRF tests show that design of housing has crucial effect on structural behavior of housing which can also cause higher noise radiation from housing surface due to the gear impacts.

Finally, torsional vibration analyses are carried out by both numerical analyses and experimental studies, and it is observed that combustion order, especially the combustion fundamental order, which is the third engine order for a six cylinder engine, dominates the crankshaft torsional vibrations. Likewise, envelope analysis and the new analysis method developed and named in this thesis as cepslope (cepstrum + envelope) reveal the repetition of the combustion orders. Furthermore, they prove that combustion fundamental order is one of the most important parameter on gear impacts.

In the conclusion chapter, numerical and experimental studies are evaluated and compared in order to determine the effective parameters on gear impact noise. At the end, geartrain design recommendations and future research recommendations for the subject of this thesis are expressed in some detail.



## DİZEL MOTORLARDA DIŞLI DARBE GÜRÜLTÜSÜNÜN İNCELENMESİ

### ÖZET

İçten yanmalı motorların gürültü seviyesi otomotiv sektöründe artan rekabet ve yasal düzenlemeler nedeniyle giderek önemli bir konu haline gelmektedir. Bundan dolayı, otomotiv firmalarında çalışan mühendisler motorlardaki gürültü kaynaklarını tespit edebilmek için çaba sarf etmektedirler. Özellikle seri üretime geçilmeden önce bu gürültü kaynaklarının ana sebebinin belirlenmesi çok önemlidir. Motordaki gürültü kaynakları tasarım aşamasında tespit edildikten sonra motordaki titreşim ve gürültüyü azaltmak için iyileştirmeler yapılmaktadır.

Dizel motorların benzin motorlarına nazaran daha gürültülü olarak çalıştıkları bilinen bir olgudur. Esasında bunun nedeni dizel motorlarda yanmanın benzin motorlarına göre yüksek basınçlarda gerçekleşmesidir. Özellikle ağır vasıta dizel motorlarda çok yüksek silindiriçi basınçları oluşmaktadır. Bu yüksek silindiriçi basınçlar dizel motorlardaki mekanik gürültünün de artmasına sebebiyet vermektedir. Ayrıca bu yüksek silindiriçi basınçlardan dolayı dizel motorlarda titreşim ve gürültü seviyeleri benzin motorlarına göre daha yüksek olmaktadır. Sonuç olarak, dizel motorların gürültü seviyesi benzin motorlarına kıyasla daha fazla önem arz etmektedir.

İçten yanmalı motorlarda gürültü esas olarak iki grupta incelenmektedir. Bunlar yanma gürültüsü ve mekanik gürültülerdir. Motorlarda zaman ayar dişlileri mekanik gürültüye neden olan en önemli parçalarından biridir. Özellikle ağır vasıta motorlarda krank milinden kam miline ve diğer tahrik edilen motor parçalarına güç ve kuvvet aktarımı dişli sistemleriyle gerçekleştirilebilmektedir. Bunun nedeni ağır vasıta motorlarda aktarılan kuvvet ve gücün yüksek olmasıdır. Kayış veya zincir sistemlerinin kullanılması bu denli yüksek güç ve kuvvetlerin krank milinden kam miline aktarılmasında fiziksel kısıtlamalar nedeniyle mümkün olmamaktadır. Aksi takdirde zincir ve kayış sistemleri kullanıldıklarında, yüksek kuvvetlerden dolayı bu sistemlerde dayanım ve ömür problemlerinin oluşacağı aşikardır.

Temel olarak, dişli gürültüsü iki gruba ayrılmaktadır. Bu gürültüler dişli tıkırdama (rattle) ve dişli uğultu (whine) gürültüsüdür. Bu tez çalışmasında bu iki gürültüden biri olan dişli tıkırdama gürültüsü incelenmiştir. Dişli tıkırdama gürültüsünün ana nedeni dişliler arasındaki boşluktan kaynaklı çarpma olduğu için bu tez kapsamında dişli darbe gürültüsü olarak ifade edilmiştir. Ayrıca tıkırdama şanzımanlarda yüksüz dişlilerde gevşek parça titreşmesi olarak ifade edildiği için, motorlardaki zaman ayar dişlileri için dişli darbe gürültüsü ifadesinin kullanılmasının daha uygun olacağına kanaat getirilmiştir. Bununla birlikte motorlarda tam yük durumunda zaman ayar dişlilerinde en yüksek darbe gürültüleri oluşmaktadır. Bu açıdan bakıldığında şanzımanlardaki yüksüz dişlilerde oluşan tıkırdama gürültüsüyle motor zaman ayar dişlilerinde tam yükte etkisi daha fazla gözükürken darbe gürültüsü birbirinden ayrılmaktadır. Diğer önemli dişli gürültüsü olan dişli uğultu gürültüsü dişli kavrama frekansıyla ilişkilidir. Dişli uğultu gürültüsü dar bant bir gürültüdür; başka bir deyişle tonal bir karaktere sahiptir. Bu gürültü tipi motor dönüş hızına bağlı olduğu için

mertebe takibi metoduyla teşhis edilmesi dişli darbe gürültüsünün tespit edilmesine göre daha kolaydır. Çünkü dişli darbe gürültüsü geniş bantlı bir gürültüdür. Ayrıca bu gürültünün frekansı motor hızına bağlı olarak da değişmez. Bundan dolayıertebe takibi metoduyla motorlardaki dişli darbe gürültüsünün tespiti mümkün değildir. Özetle motorlarda dişli darbe gürültüsünün tespit edilmesi oldukça zordur.

Dişli darbe gürültüsünün oluşmasındaki ana neden dişli çiftlerinin birbirleri arasındaki teması kaybederek dişli boşlukları arasında birbirlerine göre göreceli olarak yaptıkları hareketlerdir. Dişlilerin birbirleri arasındaki teması kaybederek yaptıkları bu göreceli hareketler dişliler arasında çarpmaya neden olmaktadır. Bu çarpma da dişlilerdeki darbe gürültüsünün oluşmasının nedenidir. Bunlarla birlikte dişlilerdeki hız, tork dalgalanmaları ve burulma titreşimleri dişliler arasında oluşan çarpma kaynaklı darbe gürültüsünü tetiklemektedir. Dizel motorlardaki yük durumu dişli darbe gürültüsünün yayılması üzerindeki diğer bir önemli faktördür. Motor yük durumu arttıkça dişli darbe gürültüsü yüksüz duruma göre daha yüksek seviyede olmaktadır. Öte yandan, dişli darbe gürültüsü rölanti çalışma koşulunda daha duyulur hale gelmektedir. Bunun nedeni ise yüksüz ve düşük hız durumlarında yanma gürültüsünün ve diğer gürültülerin etkisini kaybetmesidir. Böylelikle dişli darbe gürültüsü, yanma gürültüsüyle ve diğer gürültülerle maskelenemeyerek duyulabilir hale gelmektedir.

Bu tezin ana amacı dizel motorlardaki dişli darbe gürültüsü üzerinde etkili olan faktörlerin belirlenmesi ve dişli darbesinin arka planındaki tezinin ortaya konulmasıdır. Tezin ikinci bölümünde dişli dinamiği, dişli darbesi, dişli gürültü ve titreşimi ile ilgili teorik bilgiler verilmiştir. Altı silindirli bir motor için krank milinin burulma titreşimi analizi izah edilmiştir. Ek olarak krankşaft burulma titreşimi analizinin teori kısmında anlatılmasının nedeni krankşaft burulma titreşimi üzerinde etkili olan faktörün dişli darbesi üzerinde de etkili olmasındandır. Deneysel çalışmaların incelenmesinde kullanılmak üzere titreşim ve akustik analiz metotları da bu bölümde gösterilmiştir. Dizel motorlarda dişli darbe gürültüsü üzerinde etkili olan parametrelerin tespiti için altı silindirli bir ağır vasıta motor üzerinde yapılan sayısal ve deneysel çalışmalar sırasıyla tezin üçüncü ve dördüncü bölümlerinde detaylıca anlatılmıştır. Bahsi geçen altı silindirli ağır vasıta motorun zaman ayar dişlilerinin hepsi alın dişlilerden oluşmaktadır. Helisel dişlilerden oluşan zaman ayar dişlileri bu tez kapsamında incelenmemiştir.

Motor zaman ayar dişlilerindeki darbe seviyesinin belirlenmesi için sayısal çalışmalardan ilki özel bir metot olan çarpma itme (impact impulse) metoduyla yapılmıştır. Bu metotta fizik derslerinden temel olarak bilinen itme – momentum prensibi kullanılmaktadır. Dişliler arasında çarpma esnasında oluşan kuvvetin çarpma süresi boyunca integralinin alınmasıyla çarpma itme değerleri elde edilmektedir. Ayrıca bu metot sayısal olarak zaman ayar dişlilerinde darbe açısından kritik dişli çiftlerinin belirlenmesine yardımcı olmaktadır. Altı silindirli dizel motorda yapılan çarpma itme analiziyle krankşaft dişlisi ve krankşaft avare dişlisi arasında oluşan darbe seviyesinin en yüksek değere sahip olduğu belirlenmiştir. Aslında bunun nedeni krankşaftının üzerindeki burulma titreşimlerinin ve hız düzensizliğinin diğer dişlilere göre daha fazla olmasındandır. Bunlardan başka motor zaman ayar dişlilerinin darbeleri üzerinde etkili olan parametrelerden dişli yükleme etkisi, yakıt pompası fazlama etkisi, motor hızı etkisi ve dişli boşluğu etkisi çarpma itme metodu analiziyle incelenmiştir. Bu analizlerle yakıt pompası fazlamasının ve dişli yüklemenin dişli darbe gürültüsü üzerinde en fazla etkiye sahip olduğu tespit edilmiştir. Dişli yüklemesinin dişli darbe gürültüsünü azaltma yönünde etkisi olduğu

gözlemlenmiştir. Yakıt pompası fazlamasının ise fazlama açısına göre dişli darbe gürültüsü üzerinde olumlu veya olumsuz etkisi olabilmektedir. Sonuç olarak ise dişli yükleme ve yakıt pompası fazlamasının, dişli boşluğuna kıyasla dişli darbe gürültüsü üzerinde daha fazla etkisi olduğu görülmüştür.

Motor zaman ayar dişlilerindeki darbe gürültüsünün incelenmesi için deneysel çalışmalar motor akustik dinamometresinde ve araç üzerinde yapılmıştır. Altı silindirli dizel motorun darbe gürültüsü kaynakları akustik kamera kullanılarak motor akustik dinamometresinde tespit edilmiştir. Ayrıca ivmeölçer ve mikrofon ölçümleriyle de akustik kamera ölçümleri doğrulanmıştır. Akustik kamera ölçümleriyle motorda zaman ayar dişlilerin bulunduğu taraf olan motorun arka tarafı en yüksek gürültü seviyesine sahip bölge olarak belirlenmiştir. Ayrıca darbe gürültüsüne neden olan frekanslar da akustik kamera, ivmeölçer ve mikrofon ölçümleriyle belirlenmiştir. Sayısal çalışmalarda kullanılan çarpma itme analizlerine benzer şekilde yakıt pompası fazlaması ve dişli boşluğu etkileri motor akustik dinamometresinde, dişli yükleme, dişli boşluğu ve motor hızı etkileri ise araç üzerinde deneysel olarak incelenmiştir. Sonuç olarak yakıt pompası fazlamasının ve dişlilerin yüklenmesinin dişli darbe gürültüsü üzerinde çok önemli etkisi olduğu deneysel olarak ispatlanmıştır. Ayrıca yağ pompasına güç aktaran dişli çiftinin dişli boşluğunun azaltılmasının darbe gürültüsü üzerinde az bir etkisi olduğu gözlemlenmiştir. Bununla birlikte, kritik dişli çiftlerinde dişli boşluk değerlerinin kaydırılabilir averse dişlisiyle değiştirilmesinin dişli darbe gürültüsü üzerinde dikkate değer bir etkisi olduğu gözlemlenmiştir. Dişli boşluğu arttıkça dişli darbe gürültüsünün de paralel bir şekilde arttığı görülmüştür. Sonuç olarak dişli boşluğunun darbe gürültüsü üzerinde etkisinin kritik dişlilerde daha fazla olduğu görülmektedir.

Motor silindirleri arasında oluşan basınç farkları krankşaft üzerindeki burulma titreşimlerini arttıran önemli faktörlerdendir. Motor dinamometresi testleri kapsamında silindiriçi basınçlar da ölçülmüştür. Sonuç olarak silindirler arasında basınç farklılıklarının olduğu deneysel olarak gözlemlenmiştir.

Motor zaman ayar dişlilerin bulunduğu muhafazalar dişli darbe gürültüsünün yayılmasında önemli rol oynamaktadırlar. Muhafazalar üzerine kaburga tasarımı yapılarak yapısal davranışları değiştirilebilmektedir. Bu amaç doğrultusunda değişik tasarımdaki muhafazalar üzerinde çekiç testi yapılarak muhafazaların yapısal davranışları incelenmiştir. Muhafazaların yapısal davranışlarının değişik tasarımlarla dikkat çekici bir şekilde değiştiği görülmüştür. Özellikle darbe frekanslarıyla çakışan muhafazaların doğal frekansları, tasarım değişiklikleriyle kontrol edilebilmektedir.

Teori bölümünde gösterilen krankşaft burulma titreşimi analizi sayısal ve deneysel çalışmalarla da yapılmıştır. Motor ateşleme frekansının temel harmonisinin burulma titreşimleri üzerinde tetikleyici unsur olduğu sayısal ve deneysel çalışmalarla gösterilmiştir. Benzer şekilde, ileri sinyal işleme yöntemlerinden olan envelope analizi ve cepstlope (cepstrum + envelope) analiziyle de motor ateşleme frekansının tekrarlamasının dişli darbe gürültüsü üzerinde tetikleyici bir etkiye sahip olduğu gösterilmiştir. Sonuç olarak, 6 silindirli bir motor için 3 olan motor mertebesinin dişli darbesini tetiklediği ispatlanmıştır.

Tezin sonuç kısmında sayısal ve deneysel çalışmalarla elde edilen sonuçlar detaylı olarak ele alınmıştır. Motor zaman ayar dişlileri için yazarın tasarım önerileri ve gelecekte bu konuyla ilgili yapılabilecek çalışmalar ifade edilmiştir.



## 1. INTRODUCTION

Noise, vibration and harshness (NVH) topics have been considered major problem areas for automotive companies. Automotive manufacturers aim to minimize overall noise level of their vehicles in order to meet the customer satisfaction and vehicle noise legislations, which lead automotive companies to develop quieter vehicles. Actually, overall noise level of an internal combustion engine is an important issue in the automotive industry as engine noise is considered to be one of the major sources in vehicle total noise level. Automotive companies do lots of NVH tests on vehicles and in engine acoustic dynamometers before the mass production in order to meet the pass-by noise legislation that is vital for automotive manufacturers. In Figure 1.1, it is seen that engine has the highest noise contribution on vehicle total noise level based on pass-by noise test. That's why NVH engineers pay a lot of attention to engine noise during their NVH improvement studies on vehicles.

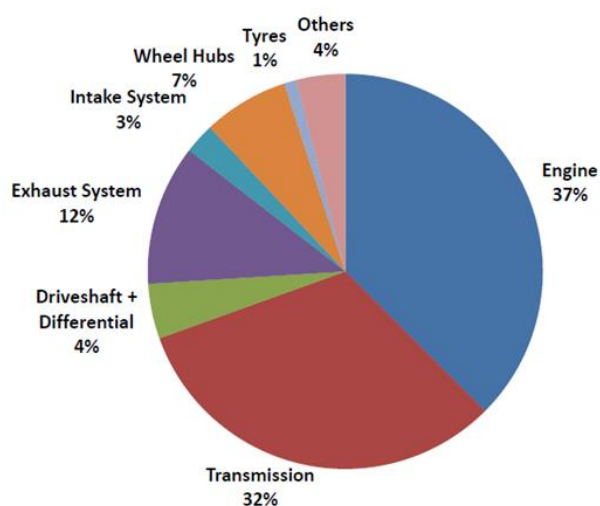


**Figure 1.1** : Pass-by noise (PBN) contributions of 13L heavy-duty truck [1].

Engine noise is classified in two categories such as mechanical noise and combustion noise in the base engine NVH development activities. Geartrain noise is one of the most important mechanical noise contributors in internal combustion engines, moreover it consists of gear impact (rattle) noise and gear meshing (whine) noise. Especially, the geartrain impact noise is considered as the most difficult root cause

analysis problem in heavy-duty (HD) diesel engines. Reducing the geartrain noise is highlighted as one of the important NVH topics in order to improve mechanical noise in HD diesel engines.

## **1.1 Problem**

Diesel engines are commonly used as heavy-duty engines because of the higher torque demand which is also the main reason for using gear drive as timing drive system instead of other timing drive options. There are mainly three types of timing drive systems in engines such as gear, chain and belt drive systems. Gear drive system, also called as geartrain, is one of the most commonly used drive systems in heavy-duty engines. Higher power and torque transmission from crankshaft to camshaft cannot be achieved by belts or chains due to the physical limitations. In other words, chains or belts are not convenient power transmission systems in HD diesel engines. Therefore, gear drives are essential timing drive system in HD diesel engines. Power can be transmitted from crankshaft to other components such as camshaft and fuel pump by geartrain in heavy duty diesel engines. On the other hand, using geartrain in HD diesel engines brings some noise problems such as "whine" and "rattle". Gear impact noise, which is also called as gear rattle noise, is commonly encountered problems in the automotive industry. Gear impact noise becomes more audible especially during idle operation conditions due to the low levels of combustion noise and other mechanical noise when the engine speed is low. Impact forces between the gear mesh pairs result in geartrain vibration and noise which is usually classified as gear impact noise in engines. Gear impact noise propagates from geartrain to the engine environment by transfer paths. Moreover, impact forces between gears can cause fatigue life and fracture problems. Operating conditions, gear properties and engine components also affect the gear impact noise.

Due to design principles, internal combustion engines cannot provide uniform torque during engine operation because of the combustion process. Therefore, there exists both torque and speed fluctuations in internal combustion engines, which can be controlled but cannot be completely eliminated in practice. As a result, crankshaft is directly affected from torque fluctuations hence the gears between crankshaft and camshaft, main parts of the geartrain, are excited and this leads to impact forces between gears.

In recent years, injection pressures have been increased in order to obtain higher levels of power from diesel engines and this resulted in higher impact forces between gears. This has made the geartrain a significant noise contributor. As a result, most of the automotive companies' product development teams have started to work collaboratively for reducing this geartrain noise. This thesis is also contributing to this overall objective.

## **1.2 Literature Review**

The main aim of conducting a literature survey in this thesis is to find out the previous work and research related to the problem described above and to determine the fundamental background theory and the accumulated knowledge in this field. In addition, performing a literature survey can yield ideas for possible future works. The literature survey presented here can also provide valuable information to the researchers who might carry on the investigation about general gear impact noise not necessarily for diesel engines only.

A. Rust [1] showed the key parameters of heavy-duty engine NVH development in his NVH workshop presentation. He stated that engine noise is the highest noise contributor in pass-by noise test and geartrain is one of the most important mechanical noise contributors in HD diesel engines. Most importantly, optimization of fuel pump phasing is suggested for reducing geartrain impact excitation.

S.N. Dogan [2] focused on transmission rattle noise and he explained root causes and definition of rattling noise in transmission with a gear test rig and the EKM (Einfachst-Klapper-Modell) simulation program. Rattling noise is explained as backward and forward motions of unloaded gears within their functional clearances in consequence of engine induced torsional vibration. EKM simulation program uses basic impact law for modelling gear rattle. Furthermore, EKM program can calculate the rattle noise level by assuming the proportion between impact impulse and rattle noise level. In addition, in EKM program, impact impulses are multiplied with a correlation factor for a direct comparison with measured airborne noise level. A backlash model and an axial clearance model are offered for loose gears synchronizing rings in this study. As an important result, gear backlash, axial clearance and main center distance have significant effect on rattle noise, that was proven by both experimental tests and EKM simulation program. Moreover, the axial

impacts and torsional impacts of loose parts were tried to be minimized experimentally in this study. It can be said that EKM simulation program provide a quite successful correlation with the measured noise level in Dogan's study.

Esmaeli and Subramaniam [3] do a geartrain rattle research related to engine timing geartrain concepts and proposal in their master thesis. This study is also a useful design guide for engine timing geartrain. In this thesis study, geartrain designs of different automotive companies were introduced so as to illustrate various geartrain concepts. They pointed out that increased injection pressure in engines has a significant effect on geartrain noise due to the gear impacts. Moreover, it is indicated that type of fuel injection system plays an important role on geartrain noise. Torsional vibrations in geartrain were expressed as a source of gear rattle noise. They also gave further information about gear material properties, concepts and redesign layouts for engine timing drive system in the consideration of rattling noise. For instance, it is specified that reducing gear mesh number may decrease the noise and vibration in the geartrain, that is a simply kind of redesign layout. In addition, other redesign layouts were proposed such as bevel gear timing system in order to minimize geartrain noise. Similarly, they showed that scissor gear concepts can be used to eliminate backlash effect. In other words, scissor gears are used to keep the gear pairs always in contact hence preventing the rattling motion. To conclude, future geartrain concepts and precautions against rattling noise are introduced in this master thesis.

Crocker et al. [4] clearly showed the effect of backlash size and constant torque loading effect on geartrain rattle noise by numerical and experimental studies. An ADAMS simulation and experimental study on a 10-liter diesel engine were compared in order to determine the rattle noise level based on different parameters in their study. They presented results, demonstrating that rattle noise can rapidly increase up to a critical backlash value and then it will sharply decrease. Additionally, it is asserted that inertias of idler gears and ancillary drives have less effect on rattle noise. On the other hand, experimental studies revealed that loading gear mesh by alternator as a constant torque device considerably decreases geartrain rattle noise. It is also claimed that higher injection pressure in fuel pump can cause torque variation with respect to time. Therefore, gear rattle noise between gear meshes occurs in engine gear drive system. As a summary, effective parameters for

reducing geartrain rattle noise in diesel engines, which can be ordered as backlash size and gear loading, are identified by computer aided simulations and experimental measurements in this study.

Structural vibration excitation mechanisms of timing gear impacts were investigated in order to determine the affecting parameters on gear impact noise in a 3-cylinder engine by Wilhelm et al. [5]. Torque variations of components such as fuel pump and camshaft in gear drive system were specified as the significant factor on gear impacts. Structural vibration measurements and acoustic measurements were performed in full load and no load conditions for the purpose of determining the timing gear impact mechanism in this study. Wilhelm et al. explained that drive component vibrations such as torsional vibrations in gear shafts result in impacts between gears. In addition, these vibrations occur irregularly due to the phase difference between engine rotation and vibrations of geartrain components. In fact, fuel pump, valvetrain and crankshaft generate torque fluctuations on gears, which lead to vibrations in the geartrain. As an important consequence, they state that impacts between gears excite natural frequencies of geartrain system, which can be seen as free vibrations of individual geartrain members.

Bailey and Fussner [6] performed experimental studies related to effects of gear design parameters on geartrain impact noise in diesel engines. Three different gear sets were tested in a 3.3L four cylinder diesel engine and vibration and acoustic measurements were made. According to this study, gear material, contact ratio, tooth thickness, bearing clearance and gear backlash were indicated as influential parameters on geartrain rattle noise. For example, internal damping properties of materials were expressed as typical control parameters for noise reductions in this study. In addition, it is suggested that increasing gear thickness could be beneficial for reducing geartrain noise owing to the fact that gear backlash is reduced by increasing gear thickness. It was also claimed that the usage of anti – backlash gears could decrease the torsional vibration of the engine. Furthermore, frequency analyses were made in experimental studies in order to determine the gear design parameters effecting the critical frequencies.

Gao et al. [7] analyzed geartrain noise in a large diesel engine, which originated from meshing noise and impact noise. Authors indicate that vibration and noise at geartrain side are generated by gear impacts between backlashes due to fuel pump

and combustion borne torque fluctuations. Crankshaft and camshaft torsional vibrations also lead to the gear impacts. In this study, A-weighted sound power level of engine sides were experimentally calculated by intensity scanning method and calculated results showed that geartrain side has the highest sound power level over engine body. Acoustic measurements showed that gear impacts generated broadband noise, the amplitude of which was higher than that generated at gear meshing frequencies. Moreover, FRF measurements were made on gearwheels by using an instrumented hammer in order to determine the resonance frequencies in geartrain. FRFs were compared with camshaft torque autospectrum and a correlation was obtained between FRF measurements of cam gear and autospectrum of camshaft torque in constant load speed sweep test condition. In addition, a MATLAB programme was developed in order to simulate camshaft dynamics. This MATLAB program provides opportunity for calculating camshaft torque and cam gear meshing force. Zero backlash (anti-backlash) gear and camshaft damper simulations were done by using this MATLAB programme. Simulation results revealed that camshaft damper and anti-backlash provide improvements on geartrain impact noise.

Glyniadakis et al. [8] studied on air compressor rattle noise of diesel engines. By using anti-backlash gear in air compressor gear, angular displacement and velocity fluctuations of anti-backlash gear were analyzed in order to understand the effect of anti-backlash gear on rattle noise.

Ozguven and Houser [9] published a comprehensive review of mathematical model of gears dynamic models in 1988, which is still acceptable review for the investigation of gear dynamics. This paper examines the mathematical model of gears in five groups which are simple dynamic factor models, models with flexible teeth, models for gear dynamics, models for gear rotor dynamics and models for torsional vibrations.

Singh et al. studied on non-linear dynamic behavior of a geared system. They focused on a geared system with backlash and periodically time-varying mesh stiffness and rolling element bearings with clearance type non-linearities [10]. There are also some studies in the literature about non-linear dynamic models of geartrain systems which consist of periodically time-varying mesh stiffnesses. Dynamic response of geartrain systems are affected due to the periodically time-varying mesh stiffness [11-13].

Gear housing effect on the radiation of gear impact noise is demonstrated by some studies. It is stated that gear housing has a dominant effect on the level and frequency content of the emitted noise of the gear unit due to the gear teeth impacts [14-16].

Ozguven [17] provided some brief information about gear noise in his noise control book. He stated that gear noise depends on gear type such as helical or spur, gear design such as gear profile, gear quality as well as gear manufacturer. Tooth vibration and impacts between teeth can be underlying causes for gear noise. Gear housing effect is also considered to be significant due to the overlapping risk of its natural frequencies with gear meshing frequency.

Bodden et al. [18] showed the time structure of gear rattle in a transmission system. They also developed a new method to analyze gear rattle based on modulation analysis. They also demonstrated that gear rattle is directly related to cylinder firing. In order to show cylinder firing effect, they tried two cases, engaged clutch and not engaged clutch, in their vehicle test. As expected, when transmission was deactivated, in other words when clutch was not engaged, gear rattle decreased. Moreover, amplitude of cylinder firing impacts decreased.

### **1.3 Objectives and Outline of Thesis**

The main aims of this thesis are to understand the background theory of gear impacts and to determine the effective parameters on “geartrain impact noise in heavy-duty diesel engines”. Also, determination of gear impact characteristic is within the objectives of this study. Therefore, experimental studies and numerical analyses have been performed on a heavy-duty diesel engine for the determination of geartrain impact noise parameters. Geartrain with spur gears are investigated in this thesis. Numerical and experimental studies are also practised for spur gears. This thesis consists of five chapters comprising introduction, theory, numerical analyses, experimental studies and conclusion parts.

In the introduction chapter, geartrain impact noise problem is defined and importance of geartrain impact noise in diesel engines is introduced. Previous research about geartrain impact noise in diesel engines are explained in the literature review section. Furthermore, research about gear impact problem in other machines such as transmission and other gear noises such as meshing (whine) noise are presented in

the literature review section. By reviewing the literature, essential parameters affecting gear impacts and impact noise are identified. Available information in the literature outlined the scope of this thesis.

In the second chapter, background theory of geartrain noise is substantially classified as gear meshing noise and gear impact noise. Some mathematical models of gear impact noise are presented and gear dynamics theory are explained in order to relate with gear impacts. It is worth stating that gear contact dynamic and gear drive system are the fundamental components of gear dynamics. In addition, torsional vibration problem of six cylinder heavy duty engine is presented in this chapter. Furthermore, vibration and acoustic analysis methods are summarised in the last section of the theory chapter so as to understand the acoustic analysis, fourier transform, envelope analysis, modulation analysis and cepstrum analysis which are frequently used in experimental studies.

In the third chapter, numerical analysis of geartrain impact is conducted in order to determine the significant parameters on geartrain impact noise. This chapter consists of two main sections which are geartrain impact impulse method and torsional vibration of crankshaft. Geartrain impact impulse method is a special analysis method in order to evaluate impact noise level of geartrain system. This method is used in AVL Excite Timing Drive software which is also a commercial software, developed by AVL Research and Engineering Company. First, a geartrain model for the six cylinder engine is developed in AVL Excite Timing Drive software and then impact impulse analysis is conducted. Critical gear meshes are determined by using impact impulse analysis. Finally, the most significant parameters on gear impacts such as engine speed, backlash, gear loading and fuel pump phasing are determined by the impact impulse analysis. In the second section of numerical analysis, torsional vibration analysis of crankshaft is carried out by establishing multibody engine model in AVL Excite software.

In the fourth chapter, experimental studies of geartrain impact noise are performed with the help of NVH tests in engine dynamometer and vehicle. First of all, impact noise source on engine is identified in acoustic dynamometer by using acoustic camera measurement and “vibration and acoustic measurement comparisons”. As in numerical analysis part, significant parameters on impact noise are experimentally investigated by fuel pump phasing test, backlash iteration test, torsional vibration

measurement of crankshaft in engine dynamometer, and gear loading test and engine speed test on vehicle. Housing frequency response function is also measured in order to find out housing effects on geartrain impact noise. Time domain, envelope, modulation and cepstrum analyses are also conducted in this chapter.

In the fifth chapter, conclusions and recommendations are presented for geartrain impact noise in diesel engines. Numerical and experimental studies are also compared in this part in order to introduce the significant parameters on geartrain impacts. In addition, design recommendations for geartrain of heavy-duty diesel engines with the consideration of gear impact noise are expressed. Finally, some recommendations are provided for possible futures studies on this subject.



## 2. THEORY

### 2.1 Gears

Gears are among the most important machine elements in engineering. Power and motion transmission from one side to other side can be achieved by using gears. They are also fundamental building blocks for torque and speed conversions in machines. Two types of gears are mostly utilized in the engine geartrain system. They are named as spur gears and helical gears, which are shown in Figure 2.1.

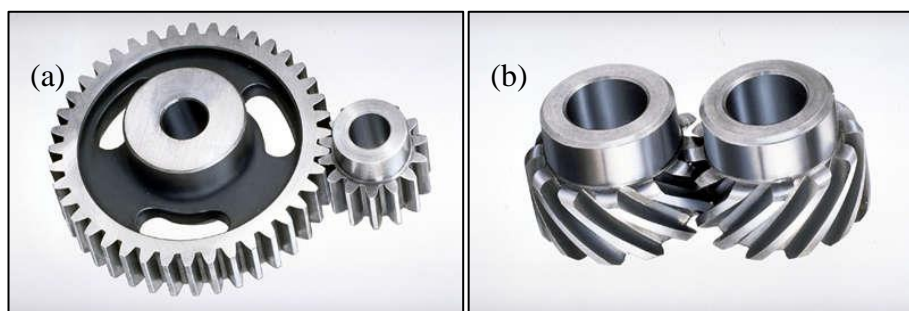


**Figure 2.1 :** (a) Spur gears [19]. (b) Helical gears [20].

Generally, helical gears have more advantages than spur gears. First of all, helical gears have higher contact ratio compared to that of spur gears. As an additional information, contact ratio describes the average number of teeth during the contact time in which a tooth joins in contact and leaves the contact with the mating gear relative to the pitch [3]. As a result of higher contact ratio, helical gears are less sensitive to geometric deviations than spur gears so they can be used in high speed applications [21]. By considering gear noise, helical gears operate quieter than spur gears because of higher contact ratio [3]. Moreover, helical gears can withstand higher loads compared to spur gears due to the load distribution over higher number of teeth in helical gears [22].

There are also disadvantages of using helical gears. First, helical gears are more expensive than spur gears. Second, helical gears create axial forces which cannot occur in spur gears. In addition, helical gears consist of helix angle, hence manufacturing helical gears are more difficult than spur gears [3].

## 2.2 Geartrain Noise

The geartrain is a kind of timing drive system, which consists of several gears such as auxiliary gears, drive gears and idler gears. The main objective of using a geartrain system in an internal combustion engine is to transmit mechanical power from crankshaft to camshaft and driving valvetrain synchronously with cranktrain [23]. Other types of timing drive systems are belt and chain drive systems, which are not suitable for transmitting higher load from crankshaft to camshaft due to the possible durability risks. However, as shown in Figure 2.2, belt and chain drive systems work quieter than gear drive system especially at lower engine speeds. Gear drive systems are utilized in heavy-duty diesel engines owing to the higher importance of durability rather than engine noise.

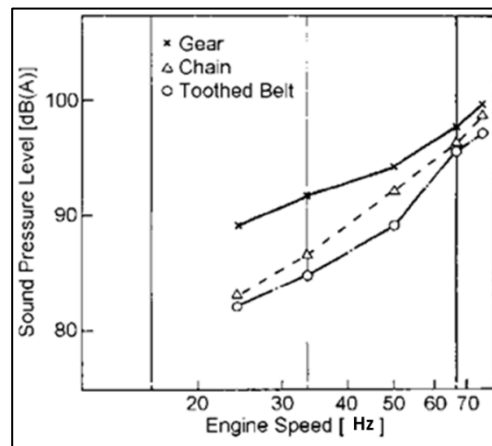


**Figure 2.2 :** Timing drive noise characteristic [24].

Gears generate noise due to several reasons such as error in the gear profile, surface roughness, impact of tooth, sliding and rolling friction, bearings, churning of the lubricant and windage [25]. Moreover, gear design, gear quality and type of gear have effects on gear noise [17].

Mainly, two noise types can be observed in geartrain system. They are called as gear rattle and whine noise which are commonly used terms in the industry. Instead of gear rattle, gear impact can also be used. Similarly, instead of whine noise, the term "meshing noise" is also used in the literature. Frequency characteristics of these two types of noise are presented in Figure 2.3. Gear meshing noise is a tonal noise which can also be described as narrowband noise. Moreover, frequency of meshing noise depends on engine speed. As can be seen from Figure 2.3, gear meshing noise is especially significant at higher engine speeds. On the other hand, gear impact noise

(rattle noise) is more significant at lower engine speeds and it is also a broadband noise, i.e., it is seen in a wide frequency range.

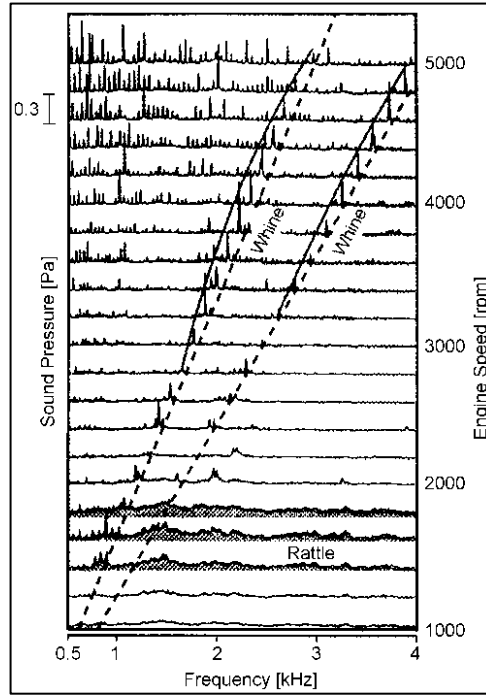


**Figure 2.3 :** Signatures of gear whine and gear rattle [26].

### 2.2.1 Gear meshing noise

Gear meshing (whine) noise, which is excited by the transmission error at the gear mesh due to manufacturing errors and tooth deflection under load, occurs at the tooth meshing frequency as a result of elastic deformation of the loaded gear teeth [1, 26, 27, 28]. Gear meshing noise is defined as a narrowband noise as well tonal noise at the meshing frequency and at their harmonics. This gear meshing noise is also related to gear meshing tolerances, gear quality, tooth shape and contact ratio [29]. Transmission error, mesh stiffness variation and friction forces are also considerable excitation factors of gear meshing noise [29]. It is also worth stating that, from NVH point of view, it is a critical situation when the housing mode is excited by gear meshing frequency [17].

The tooth meshing frequency is expressed as [17];

$$f = \frac{N \cdot m}{60} \quad (2.1)$$

where  $f$  is tooth meshing frequency [Hz],  $m$  is the number of teeth of a gear and  $N$  is the rotational speed of the gear [rpm]

### **2.2.2 Gear impact noise**

Backward and forward relative motion between gear teeth by losing contact within their backlash leads to impact between gears due to the torsional vibrations of the engine [2]. As a result, these impacts between gear teeth cause impact noise which is characterised as broadband noise. Speed and torque fluctuations of geartrain members and torsional vibrations in geartrain dominate gear impacts and they increase the amplitude of torsional vibrations. Additionally, gear impact frequencies are also expected to be related to the natural frequencies of the geartrain torsional vibration modes.

Gear impact noise can be observed in both automotive gearbox (transmission) and timing gear drive system (geartrain) in internal combustion engines. Heavy impacts are particularly observed in geartrain system rather than transmission. Moreover, the gear impact noise becomes a significant noise source at engine full load conditions because higher heavy impacts are expected under full load condition. By the way, gear rattle in transmission due to the unloaded gears is different when compared to geartrain impacts. That's why impact word is preferred in this thesis instead of rattle word.

The engine cannot supply constant torque due to the transient combustion process in internal combustion engines, thus fluctuating torque is transmitted from the crankshaft to the camshaft and other drive components such as fuel pump, air compressor and power assisted pump. Crankshaft alternating torque and other drive components' alternating torques on the geartrain cause highly heavy tooth impacts between gears resulting in impact noise. Phasing difference between component vibrations and the engine cycles lead to increase of gear impacts. Torque fluctuations cause the gear teeth impacts in the geartrain, where high contact forces occur between the gears in a very short time. Moreover, increased cylinder pressure and fuel injection pressure increase the torsional excitations in the geartrain of diesel engines [3, 27]. The speed fluctuations mainly lead to gear impacts due to the engine firing order which is related with cylinder number. For a six-cylinder heavy-duty diesel engine, firing order would be three and the torsional vibration would be observed at third engine order frequency [30].

Constant friction forces between gears also affect geartrain impacts, but in a beneficial way. They provide considerable reduction of gear impact noise. However, friction has adverse effect on gear meshing noise.

### 2.2.2.1 Backlash effect on gear impacts

According to Crocker graph [4], backlash has significant effect on gear impacts as it is shown in Figure 2.4. Moreover, backlash also has beneficial effect, hence it is an optimization problem. For instance, lower backlash can cause jamming in gear meshes. However, if it is increased, gear impacts will increase first until a critical backlash value and then it will decrease sharply [3].

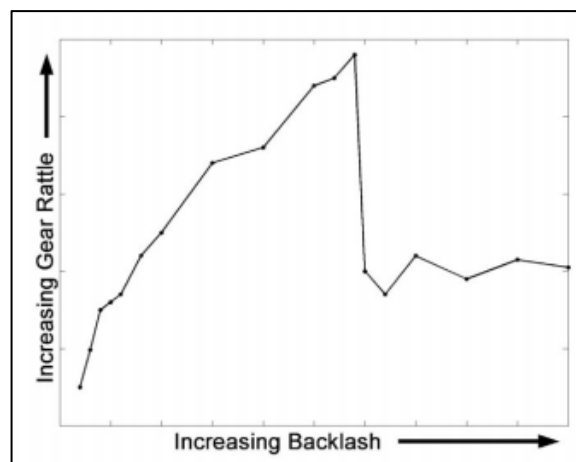


**Figure 2.4 :** Backlash effect on gear impact noise (Crocker's graph) [3].

As it is shown in Figure 2.5, backlash is described as the amount of clearance between gear teeth. The main purpose of having backlash is to prevent jamming between gear teeth hence optimizing backlash clearance is crucial in practice [3].

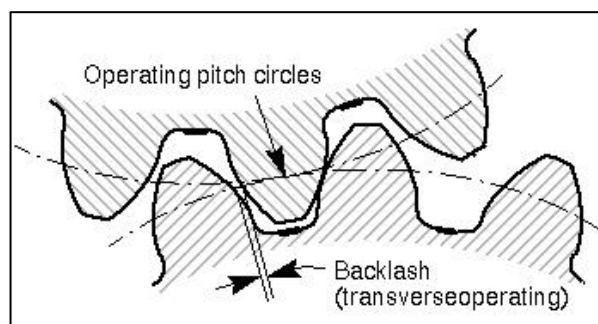


**Figure 2.5 :** Gear backlash [31].

Backlash can be minimized by meeting the gear manufacturing tolerances. Gear quality plays significant role for getting lower backlash value which is very difficult process to achieve. Gear coating is a commonly applied method in order to obtain

lower backlash value. Moreover, torsional springs can decrease the backlash between gears. They are also called as scissor gears, in other words, anti-backlash gears.

### 2.2.2.2 Mathematical model of gear impacts

Occurrence of gear impact can be expressed as a relationship between gear wheel inertia torque and drag torque which have crucial effect on gear impact noise. Speed fluctuation within backlash can lead to impacts between the gear teeth under operating conditions. If the angular acceleration is high enough to make the inertia torque at the driven wheel greater than its drag torque, impacts between gears can occur. Impact occurrence criteria can be expressed as [32];

$$J\dot{w} > T_{drag} \quad (2.2)$$

where  $J$  is moment of inertia of driven wheel,  $\dot{w}$  is angular acceleration of driven wheel,  $T_{drag}$  is drag torque acting on driven wheel. For instance, components such as air compressor, power assisted steering, power take-off and fuel pump can create friction torque in geartrain.

By using the equation (2.2), impact occurrence criteria can be explained in terms of a critical angular acceleration  $\dot{w}_{crit}$  where gear impact starts to occur [32];

$$\dot{w}_{crit} = \frac{T_{drag}}{J} \quad (2.3)$$

It is seen that impact is excited by angular acceleration. Torsional resonance plays considerable role on this angular acceleration.

## 2.3 Dynamic Model of the Gear System

Gear system is a mechanical system which can be expressed by mathematical models. By considering mechanical system dynamics [33], the mathematical model is built by using Lagrange's equation which is expressed as;

$$\frac{d}{dt} \left( \frac{\partial T}{\partial \dot{q}_k} \right) - \frac{\partial T}{\partial q_k} + \frac{\partial V}{\partial q_k} + \frac{\partial D}{\partial \dot{q}_k} = Q_k \quad (k = 1, 2, \dots, n) \quad (2.4)$$

where  $T$  is kinetic energy,  $V$  is potential energy,  $D$  is rayleigh dissipation function,  $q_k$  is generalized coordinates and  $Q_k$  is generalized forces.  $V$  can also be considered as

elastic potential energy for this system. In order to utilize the Lagrange equation, kinetic energy  $T$ , potential energy  $V$  and rayleigh dissipation function  $D$  need to be defined. Kinetic energy  $T$  is written as [33];

$$T = \frac{1}{2} \sum_{i=1}^p m_i \dot{r}_i^2 \quad (2.5)$$

where  $m_i$  is mass element and  $r_i$  is position vector. Elastic potential energy  $V$  is written as;

$$V = \sum_i \int_0^{v_i} k_i(u_i) u_i du_i \quad (2.6)$$

where  $k_i$  is stiffness element and  $u_i$  refers total displacement of stiffness element. For linear elastic force element, the potential energy is simplified as;

$$V = \frac{1}{2} \sum_{i=1}^p k_i u_i^2 \quad (2.7)$$

In order to define damping, Rayleigh dissipation function  $D$  is written as [33];

$$D = \sum_i \int_0^{\dot{u}_i} c_i(u_i) \dot{u}_i du_i \quad (2.8)$$

where  $c_i$  is damping element and  $\dot{u}_i$  refers refers total velocity of damping element. For linear elastic force element, the potential energy is simplified as;

$$D = \frac{1}{2} \sum_{i=1}^p c_i \dot{u}_i^2 \quad (2.9)$$

By using Lagrange equation, mechanical system's governing equation of motion can be expressed in matrix form as;

$$[M]\{\ddot{q}\} + [C]\{\dot{q}\} + [K]\{q\} = \{Q\} \quad (2.10)$$

where  $[M]$  is mass matrix,  $[C]$  is damping matrix and  $[K]$  is stiffness matrix,  $\{Q\}$  is the force vector and  $\{q\}$  is displacement vector.

### 2.3.1 Gear contact dynamic model

Gear contact dynamic model is significant for the determination of exact contact forces between gears for gear impacts. Researchers have offered several gear contact models. As seen in Figure 2.6, an advanced contact model is described by Singh et. al. [34]. This is the most commonly used gear contact model in the literature.

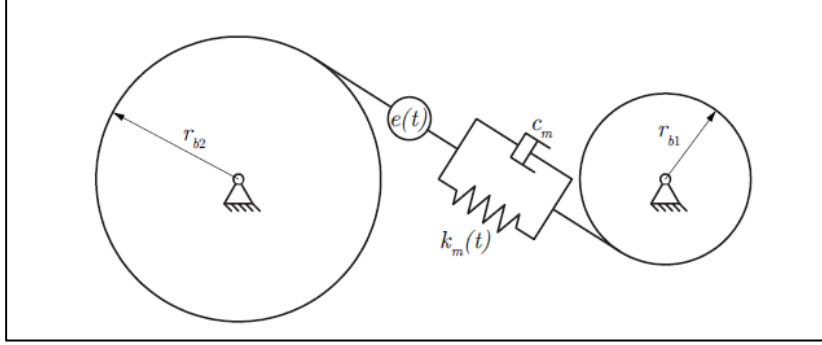


**Figure 2.6 :** Gear contact dynamic model [28].

The gear contact model in Figure 2.6 consists of a meshing stiffness  $k_m(t)$ , mesh damping  $c_m$  and meshing error  $e(t)$  as a time dependent displacement excitation. Backlash effect on mesh stiffness is considered by using time variant stiffness model. It is known that mesh stiffness becomes soft at the end of the contact and stiff at the middle of the contact.

By utilising the Lagrange equations dynamic equations of motion of the gear system are expressed as [35];

$$\begin{aligned} I_1 \ddot{\theta}_1 + c_{t1} \dot{\theta}_1 + k_{t1} \theta_1 &= T_1 - r_{b1} F_m \\ I_2 \ddot{\theta}_2 + c_{t2} \dot{\theta}_2 + k_{t2} \theta_2 &= -T_2 + r_{b2} F_m \end{aligned} \quad (2.11)$$

where  $I_1$  and  $I_2$  are mass moment of inertias,  $\theta_1$  and  $\theta_2$  are angular displacements,  $c_{t1}$  and  $c_{t2}$  are viscous damping coefficients,  $k_{t1}$  and  $k_{t2}$  are stiffness values of gears. Moreover,  $T_1$  and  $T_2$  are defined as rotational torques,  $r_{b1}$  and  $r_{b2}$  are gear base circle radius. Finally,  $F_m$  is gear meshing force which is expressed as [35];

$$F_m = c_m \dot{\delta} + k_m \delta \quad (2.12)$$

where  $c_m$  is meshing damping of gear pair, similarly  $k_m$  is meshing stiffness of gear pair and  $\delta$  is dynamic transmission error of gear tooth which is written as [35];

$$\delta = r_{b1}\theta_1 - r_{b2}\theta_2 - e(t) \quad (2.13)$$

where  $e(t)$  is known as meshing error. Transmission error is defined as the position difference between driven gear and driver gear. As it is seen in Figure 2.7 Transmission error is expressed as;

$$\text{Transmission Error} = r_{b1}\theta_1 - r_{b2}\theta_2 \quad (2.14)$$

The transmission error is considerably related to the transmitted torque by gears [20].

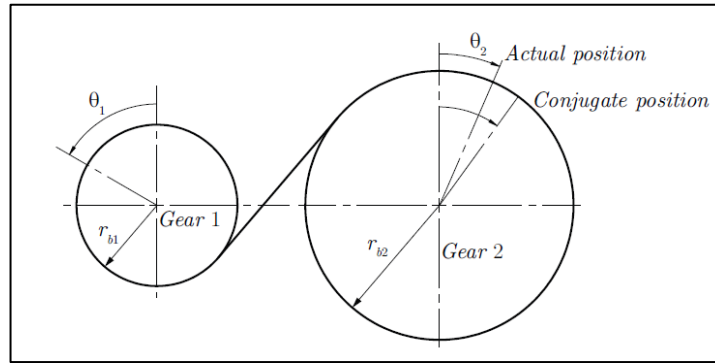


**Figure 2.7 :** Definition of transmission error [28].

### 2.3.2 Gear drive system model

Gear drive system can be modelled with gears, shafts and bearings for multi-body dynamic analysis. As it is seen in Figure 2.8, gear drive system model is expressed by using a shaft with a rigid gear where  $k_t$  spring element represents torsional and bending stiffness. Shaft is supported to bearing elements by  $k$  spring element. In addition, bearing elements consist of spring and damper elements. Damping of the shaft is also represented by the damper elements in the bearings [28].

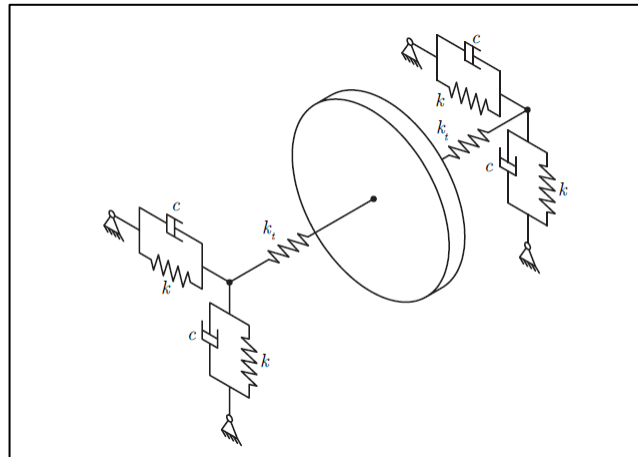


**Figure 2.8 :** Gear drive dynamic model [28].

### 2.3.3 Nonlinear dynamic model of geartrain

A nonlinear dynamic model of engine geartrain system, which consists of three gears and two meshes, is established by using gear contact dynamic model. Apparently, external forces are expressed as fluctuating torques in relation with the cycle combustion of the engine. In Figure 2.9, a nonlinear dynamic model is shown [13].

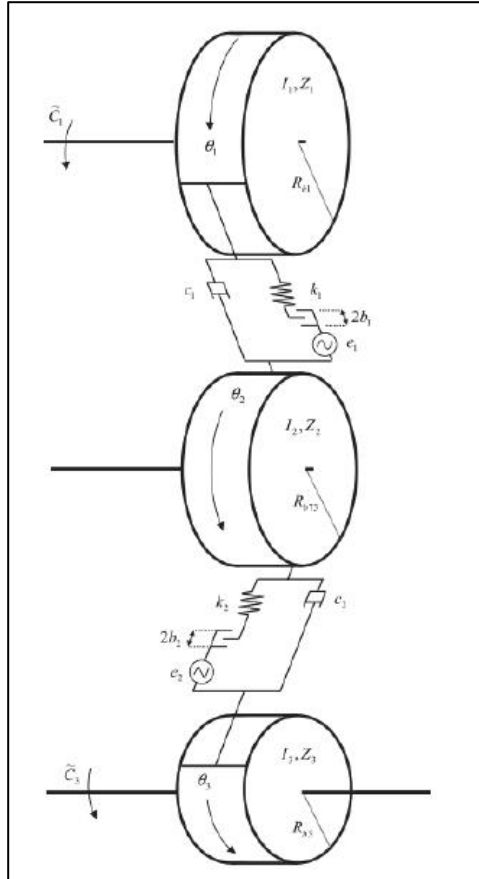


**Figure 2.9 :** The nonlinear dynamic model [13].

Energy equations and force equations are determined in order to obtain Lagrange equations. First of all, kinetic energy of this system is expressed as [13];

$$T = \frac{1}{2} (I_1 \dot{\theta}_1^2 + I_2 \dot{\theta}_2^2 + I_3 \dot{\theta}_3^2) \quad (2.15)$$

where  $T$  is kinetic energy of the system,  $I_j$  is the mass moment of inertia of gear and  $\dot{\theta}_j$  is angular velocity. Damping is also defined in terms of Rayleigh dissipation function as [13];

$$D = \frac{1}{2} (c_1 (r_{b1} \dot{\theta}_1 + r_{b1} \dot{\theta}_1)^2 + c_2 (r_{b2} \dot{\theta}_2 + r_{b3} \dot{\theta}_3)^2) \quad (2.16)$$

where  $r_{bj}\dot{\theta}_j$  is linear velocity term in gear mesh and  $c_j$  is damping coefficient of the mesh. Generalized fluctuating external forces are obtained from the virtual work  $\delta W$  which is expressed as [13];

$$\delta W = C_1\delta\theta_1 + C_2\delta\theta_2 + C_3\delta\theta_3 \quad (2.17)$$

where  $C_2\delta\theta_2$  is equal to zero due to there being no external force on second gear and  $C_j$  is the fluctuating part of the external torques.

The nonlinear elastic meshing force  $f_p$  is expressed as [13];

$$f_p(x_p) = k_p(t)g_p(x_p) \quad (2.18)$$

where,  $k_p(t)$  is periodically time-dependent mesh stiffness and  $g_p$  is described as [13];

$$g_p(x_p) = (x_p - b_p)H(x_p - b_p) + (x_p + b_p)H(-x_p - b_p) - s_p(t) \quad (2.19)$$

$x_p$  is also defined as;

$$x_p = (r_{bi}\theta_i + r_{bo}\theta_o) + e_p(t) \quad (2.20)$$

where  $e_p(t)$  and  $s_p(t)$  are periodic functions which include combined static transmission error and external mean torque effects. Moreover,  $b_p$  is the amount of backlash at gear mesh p. In addition,  $H$  is heaviside function and  $g_p$  is nonlinear displacement function. Nonlinear elastic meshing force can be seen in Figure 2.10.

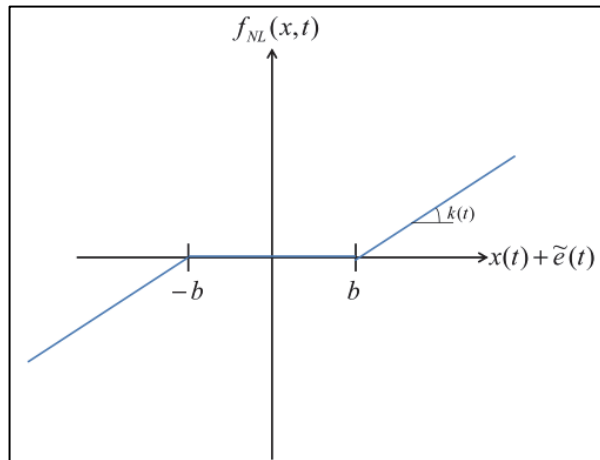


**Figure 2.10** : Nonlinear meshing contact model at gear mesh [13].

### 2.4 Torsional Vibration Analysis of Crankshaft for Six Cylinder Engine

The torsional vibrations are one of the most important problems in engines, especially in heavy-duty diesel engines. Crankshaft geometry and combustion process lead to torsional vibrations on crankshaft. In Figure 2.11, a six cylinder engine's crankshaft is shown.

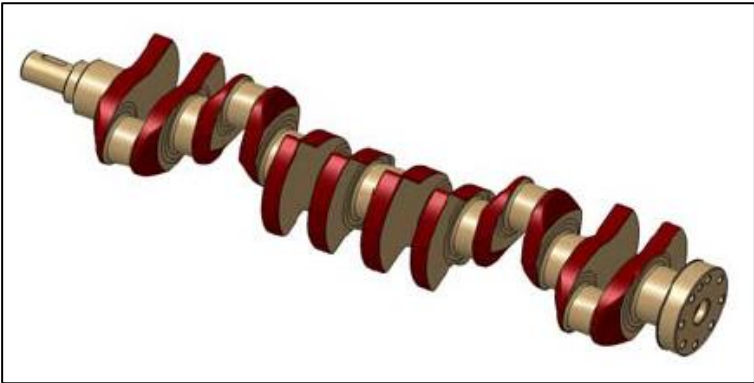


**Figure 2.11 :** A six cylinder engine crankshaft [36].

A crankshaft can be represented by a multi-mass model which can be used to create a dynamic model for the analysis of torsional vibrations. A multi-mass model of a six cylinder engine is then established with mass moments of inertia  $J_i$  and torsional flexibilities  $e_{i-j}$  as shown in Figure 2.12 [36].

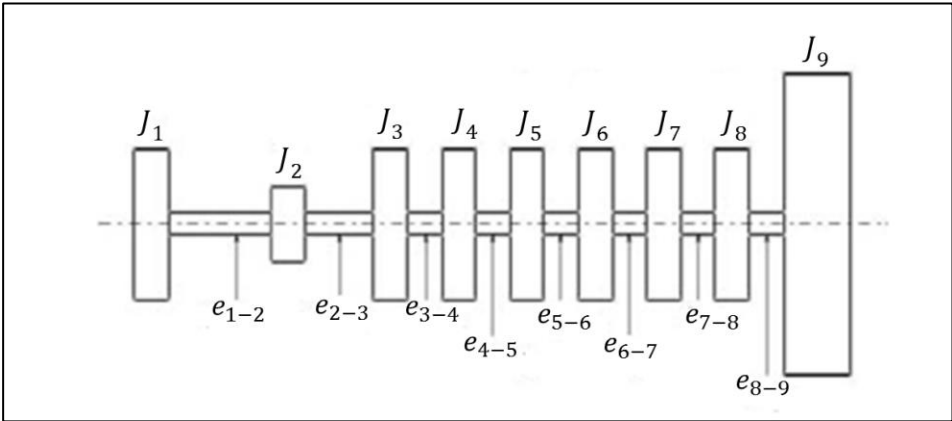


**Figure 2.12 :** Multi-mass model of six cylinder engine [36].

$J_1$  is crankshaft axis moment of inertia of auxiliary drives connected with crankshaft front end,  $J_2$  is moment of inertia of crankshaft front end with its tooth wheel, from  $J_3$  to  $J_8$  are moment inertia of crankshaft part and crankshaft axis moments of inertia connecting rod and piston assembly,  $J_9$  is moment of inertia of crankshaft rear end flywheel [36].

$e_{1-2}$  is torsional flexibility of auxiliary drives,  $e_{2-3}$  is torsional flexibility of crankshaft front end and first crank web, from  $e_{3-4}$  to  $e_{7-8}$  are torsional flexibilities of crankshaft webs,  $e_{8-9}$  is torsional flexibility of last crank web and rear end of crankshaft.

Lagrange equation is expressed as [33];

$$\frac{d}{dt} \left( \frac{\partial L}{\partial \dot{q}_i} \right) - \frac{\partial L}{\partial q_i} = 0 \quad (i = 1, 2, \dots, n) \quad (2.21)$$

where  $q_r$  is generalized coordinate,  $t$  is time and  $L$  is lagrangian function which is defined as;

$$L = T - V \quad (2.22)$$

where  $T$  is kinetic energy and  $V$  is potential energy. Equation of motion is written as [36];

$$J_i \ddot{q}_i + \frac{1}{e_{i-1,i}} (q_i - q_{i-1}) + \frac{1}{e_{i,i+1}} (q_i - q_{i+1}) = 0 \quad (i = 1, 2, \dots, n) \quad (2.23)$$

$e_{i,j}$  term donates flexibility matrix as  $[E]$ ,  $J_i$  donates mass matrix as  $[M]$  and  $q_i$  donates angular displacement vector as  $\{q\}$ . Stiffness matrix is also written in terms of flexibility matrix as;

$$[K] = [E]^{-1} \quad (2.24)$$

where it is seen that stiffness matrix is the inverse of flexibility matrix. Finally, the equation of motion for free vibration is rewritten in general matrix form as;

$$[M]\{\ddot{q}\} + [K]\{q\} = 0 \quad (2.25)$$

where  $[M]$  is a diagonal matrix written as;

$$[M] = \begin{bmatrix} J_1 & 0 & \dots & 0 & 0 \\ 0 & J_2 & \dots & 0 & 0 \\ \vdots & \vdots & \ddots & \vdots & \vdots \\ 0 & 0 & \dots & J_{n-1} & 0 \\ 0 & 0 & \dots & 0 & J_n \end{bmatrix} \quad (2.26)$$

Stiffness matrix  $[K]$  is also written as;

$$[K] = \begin{bmatrix} \frac{1}{e_{1,2}} & \frac{-1}{e_{1,2}} & & & & \\ e_{1,2} & e_{1,2} & & & 0 & 0 \\ -1 & 1 & + \frac{1}{e_{2,3}} & \dots & 0 & 0 \\ e_{1,2} & e_{1,2} & e_{2,3} & & & \\ & \vdots & & \ddots & & \vdots \\ & & & & \frac{1}{e_{n-2,n-1}} + \frac{1}{e_{n-1,n}} & \frac{-1}{e_{n-1,n}} \\ 0 & 0 & & & & \\ 0 & 0 & & & \frac{-1}{e_{n-1,n}} & \frac{1}{e_{n-1,n}} \end{bmatrix} \quad (2.27)$$

Assuming  $q(t)$  angular displacement vector as;

$$\{q(t)\} = \{u\}e^{i\omega t} \quad (2.28)$$

For harmonic motion,  $\ddot{q}(t)$  angular acceleration vector is defined as;

$$\{\ddot{q}(t)\} = -\omega^2\{u\}e^{i\omega t} \quad (2.29)$$

By substituting 2.28 and 2.29 equation in 2.25 equation, equation of motion in matrix form is rewritten as;

$$-\omega^2[M]\{u\}e^{i\omega t} + [K]\{u\}e^{i\omega t} = 0 \quad (2.30)$$

By ordering the terms, standart eigenvalue problem is obtained as;

$$\begin{aligned} ([K] - \omega^2[M])\{u\}e^{i\omega t} &= \{0\} \\ ([K] - \omega_r^2[M])\{\psi\}_r &= \{0\} \end{aligned} \quad (2.31)$$

This is the standard eigenvalue problem where  $\omega_r^2$  is eigenvalue and  $\{\psi\}_r$  is eigenvector. For the non-trivial solutions, determinant equation is written as;

$$\begin{aligned} \det|[K] - \omega^2[M]| &= 0 \\ \det|[K] - \lambda[M]| &= 0 \end{aligned} \quad (2.32)$$

Eigenvalues  $\omega_r$  and eigenvectors  $\{\psi\}_r$  can be determined by solving this eigenvalue problem. Eigenvalues donate natural frequencies of torsional vibration system and eigenvectors donate mode shapes of the torsional vibrations in crankshaft.

## 2.5 Vibration & Acoustic Analysis Method

### 2.5.1 Sound pressure level

Sound is a form of energy that propagates as pressure waves in water, air or elastic medium [17]. Sound pressure level is defined as [17, 37];

$$L_p = 10 \log \left( \frac{p}{p_0} \right)^2 = 20 \log \frac{p}{p_0} \quad (2.33)$$

where  $p_0$  is the reference pressure value which is  $20 \mu\text{Pa}$  ( $20 \cdot 10^{-6} \text{ Pa}$ ) [17, 37]. The sound pressure level  $L_p$  is a dimensionless number whose unit is decibel (dB). The total sound pressure level is also defined as [17, 37];

$$L_{pt} = 10 \log \left[ \sum_{i=1}^n 10^{L_{pi}/10} \right] \quad (2.34)$$

where  $n$  is the number of sound sources and  $L_{pi}$  is the sound pressure level of each source.

### 2.5.2 Fourier analysis

A periodic signal can be expressed as a sum of infinite series of sine and cosine terms. If  $x(t)$  is a periodic function with period  $T$ ,  $x(t)$  can be represented as [38];

$$x(t) = a_0 + 2 \sum_{k=1}^{\infty} \left( a_k \cos \frac{2\pi kt}{T} + b_k \sin \frac{2\pi kt}{T} \right) \quad (2.35)$$

where  $a_0$ ,  $a_k$  and  $b_k$  are known as Fourier coefficients which are written as [38];

$$a_0 = \frac{1}{T} \int_0^T x(t) dt \quad (2.36)$$

$$a_k = \frac{1}{T} \int_0^T x(t) \cos \frac{2\pi kt}{T} dt, \quad k \geq 0 \quad (2.37)$$

$$b_k = \frac{1}{T} \int_0^T x(t) \sin \frac{2\pi kt}{T} dt, \quad k \geq 1 \quad (2.38)$$

Discrete Fourier Transform is used for when the signal to be analyzed is in discrete form. If  $x_r$  represents discrete time domain data, its Discrete Fourier Transform is expressed as [38];

$$x_k = \frac{1}{N} \sum_{r=0}^{N-1} \left( x_r e^{-i\left(\frac{2\pi kr}{N}\right)} \right) \quad (2.39)$$

where  $t = rT/N$  and  $x_k = a_k - ib_k$ . Inverse Discrete Fourier Transform is similarly expressed by the inverse formula as [38];

$$x_r = \sum_{k=0}^{N-1} \left( x_k e^{i\left(\frac{2\pi kr}{N}\right)} \right) \quad (2.40)$$

Autospectrum, in other words autospectral density, is expressed as;

$$S_{xx_k} = \frac{x_k^* x_k}{\Delta f} \quad (2.41)$$

where  $\Delta f$  is frequency resolution,  $x_k^*$  is complex conjugate of  $x_k$ . Autospectrum can be simplified as;

$$S_{xx}(f) = \frac{x^*(f)x(f)}{\Delta f} = \frac{|x(f)|^2}{\Delta f} \quad (2.42)$$

Frequency resolution is also defined as;

$$\Delta f = \frac{1}{T} \quad (2.43)$$

where T is the measurement period.

To understand the philosophy behind Fourier Transform, a basic illustration is included here in Figure 2.13 where the time domain signal has basically three harmonic components. If the signal is decomposed to the three harmonic components, pure sinusoidal signals will be obtained. Moreover, each separated

signal components have individual frequencies. As a summary, Fourier analysis provides a tool to transform a signal from time domain to frequency domain.

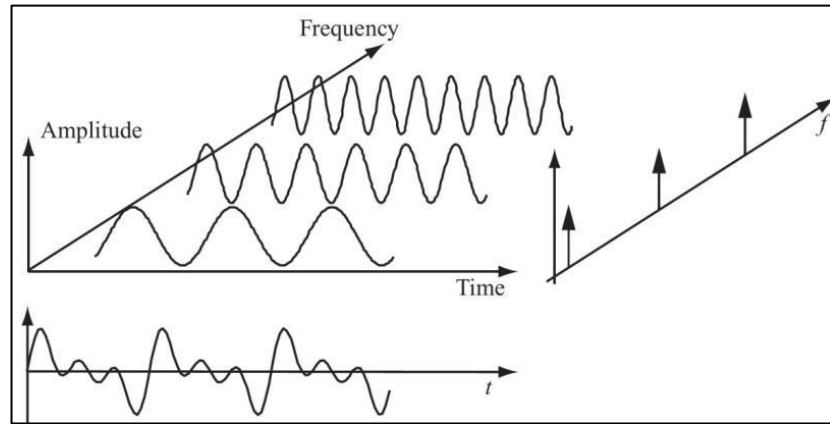


**Figure 2.13 :** Time and frequency domain [38].

### 2.5.3 Cepstrum analysis

Cepstrum is defined as the inverse Fourier transform of the logarithm of a spectrum. The main idea behind cepstrum analysis is to determine the frequency repetitions in a spectrum. Cepstrum analysis is commonly used for gear fault detection [38]. Consequently, Power Cepstrum is inverse Fourier Transform of the logarithm of Auto Power Spectrum. The Power Cepstrum of a signal  $x(t)$  is denoted as [38, 39];

$$c_{px}(\tau) = IFFT[\log S_{xx}] \quad (2.44)$$

where  $\tau$  is referred to as quefrequency. Cepstrum analysis detects periodicities in  $S_{xx}$ . If the analysed signal  $x(t)$  is the input signal,  $y(t)$  is the output signal, then the Cepstrum can sometimes separate the input spectrum from the linear system frequency response. If  $x(t)$  is the input signal,  $y(t)$  is the output signal and the linear system has Frequency Response Function (FRF)  $H(f)$ . Then, for a linear system, the auto spectrum of the output can be written as [38];

$$S_{yy}(f) = |H(f)|^2 S_{xx}(f) \quad (2.45)$$

By the way,  $c_{py}(\tau)$  becomes as [38];

$$c_{py}(\tau) = IFFT[\log |H|^2] + IFFT[\log(S_{xx})] \quad (2.46)$$

where  $c_{py}(\tau)$  denotes Power Cepstrum of system's output.

## 2.5.4 Envelope analysis

“Envelope analysis”, also called amplitude demodulation technique, is useful for detecting periodic impact excitations which can excite vibration modes at higher frequencies [40]. This technique is mostly used for detecting impact repetition frequency when individual impacts create resonant responses. As stated in previous section, firing order is the main impact source of torsional excitation in internal combustion engines, and torsional excitation dominates the gear impacts. Moreover, impacts can lead to higher frequency excitations. In addition, the most significant impact repetition frequency becomes firing order in the engine. Therefore, identification of impact source is becoming important.

A time domain signal can be demodulated by Hilbert transform which is commonly used in envelope analysis [40].

### 2.5.4.1 Hilbert transform

The Hilbert transform shows the relationship between the real and imaginary components of the Fourier transform of one-sided signal. Hilbert transform of a time function is defined as [40];

$$H\{x(t)\} = \frac{1}{\pi} \int_{-\infty}^{+\infty} x(\tau) \frac{1}{t - \tau} d\tau \quad (2.47)$$

where  $t$  is time,  $x(t)$  is time domain signal, and  $H\{x(t)\}$  is the Hilbert transform of  $x(t)$ . By using the Hilbert transform and time domain signal, the analytic signal  $A(t)e^{i\phi(t)}$  is defined as [40];

$$A(t)e^{i\phi(t)} = x(t) + iH[x(t)] \quad (2.48)$$

where  $A(t)$  is amplitude modulation function in other words envelope of the signal. Complex analytic signal  $A(t)e^{i\phi(t)}$  is decomposed into its amplitude and phase components. By the way,  $A(t)$  amplitude modulation and  $\phi(t)$  phasing modulation are obtained as [40];

$$A(t) = \sqrt{x(t)^2 + H[x(t)]^2} \quad (2.49)$$

$$\phi(t) = \arctan \frac{H[x(t)]}{x(t)} \quad (2.50)$$

### 3. NUMERICAL ANALYSIS OF GEARTRAIN IMPACTS

Torsional vibrations of gear shafts and impacts between gears are considered to be main reasons of geartrain impact noise in heavy-duty (HD) diesel engines. In this section, two methods are used for numerical analyses of geartrain impacts. They are namely "the impact impulse analysis of geartrain" and "torsional vibration analysis of crankshaft". A 12.7-liter HD diesel engine CAE model is used for the numerical analyses. Geartrain system CAD model of this 12.7-liter HD diesel engine with crankshaft and camshaft is shown in Figure 3.1.

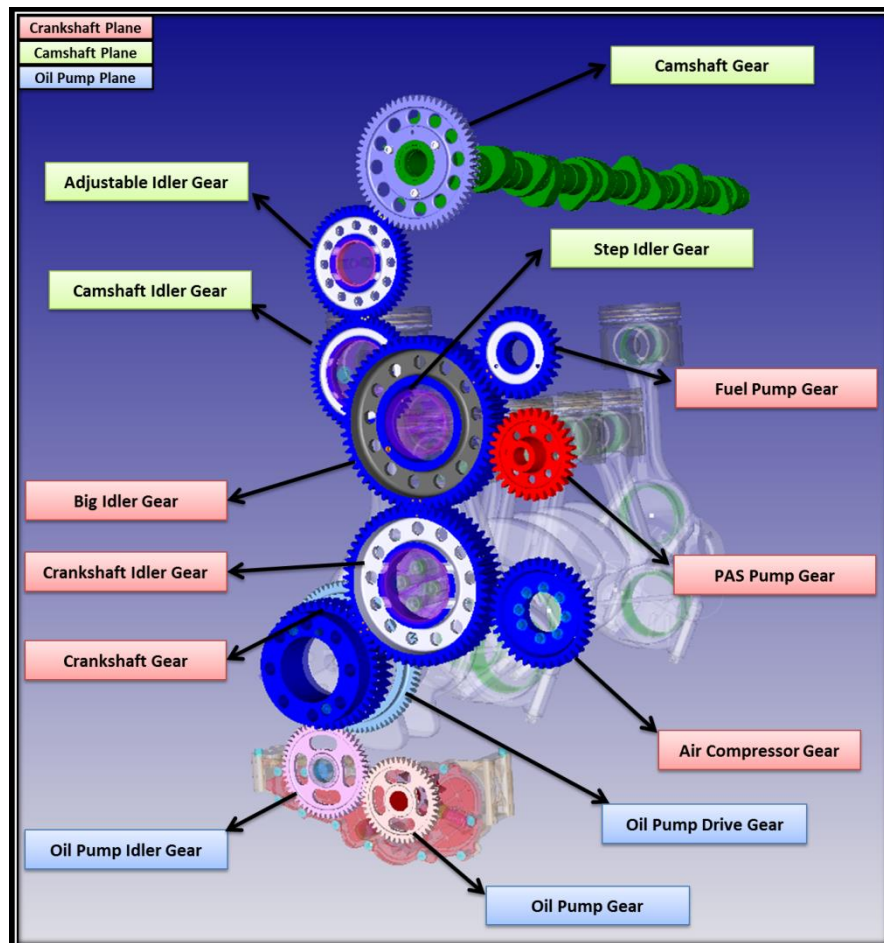


**Figure 3.1** : Geartrain system of a 12.7 liter engine.

There are ten gears between crankshaft and camshaft in this geartrain system. There are three more gears (oil pump drive gear, oil pump idler gear and oil pump gear)

belonging to lubrication system of the engine, which are located at the bottom side of the crankshaft. It is worth stating that the gears which belong to the lubrication system are not accepted as part of the geartrain system. However, they have contribution on geartrain impact and meshing noise. The geartrain including the lubrication system has three gear planes which are named as camshaft plane, crankshaft plane and oil pump plane. Camshaft plane consists of four gears which are camshaft gear, adjustable idler gear, camshaft gear and step idler gear. Crankshaft plane, on the other hand, has six gears which are named as crankshaft gear, crankshaft idler gear, big idler gear, fuel pump gear, power assisted steering (PAS) gear and air compressor gear. The last group, the oil pump plane contains three gears: oilpump drive gear, oil pump idler gear and oil pump gear. Step idler and big idler are located on the same axis. Similarly, oil pump drive gear and crankshaft gear are located on the same axis with crankshaft gear. Step idler and oil pump drive gear provide differentiation of three planes by changing the peripheral speed of gears on the same axes. For instance, the existence of three different planes leads to three different meshing frequencies during rotation of gear wheels. Multiplying engine order of geartrain planes by engine speed can also yield gear meshing frequency. Engine orders of three geartrain planes are calculated by multiplying the teeth numbers by speed ratio of gears with respect to engine speed. Engine orders of this three gear planes are as determined to be as follows: engine order of camshaft plane is 30, crankshaft plane is 45 and oil pump plane is 80 in the geartrain system.

### 3.1 Geartrain Impact Impulse Method

The so-called "Geartrain impact impulse method" is a correlative calculation method for quantifying gear impact (rattle) noise. Contact forces between gears and acoustical relevant contact time (ARCT) are used in order to calculate impact impulses [41]. Actually, AVL Excite, which is a multibody dynamics analysis software, uses this method in its Timing Drive module. According to AVL Excite Timing Drive guideline, the impact impulse equation is expressed as [41];

$$I = \int_{ARCT} F dt \quad (3.1)$$

where I is the impact impulse for a gear mesh, F is the contact force between gears.

It is also accepted that very low contact force and contact velocity make no contribution to impacts, hence threshold values for force and velocity are defined and impacts are evaluated whether they exceed these threshold values [41].

Acoustic Relevant Contact Time (ARCT) value is recommended as 0.0005 second by AVL Excite Timing Drive guideline. ARCT contact time is taken into account up to peak force time [41]. A sample contact force between gears as function of time is shown in Figure 3.2. In addition, impact impulse is calculated by evaluating the definite integral equation (Eq.(3.1)) between 0 and 0.0005 seconds.

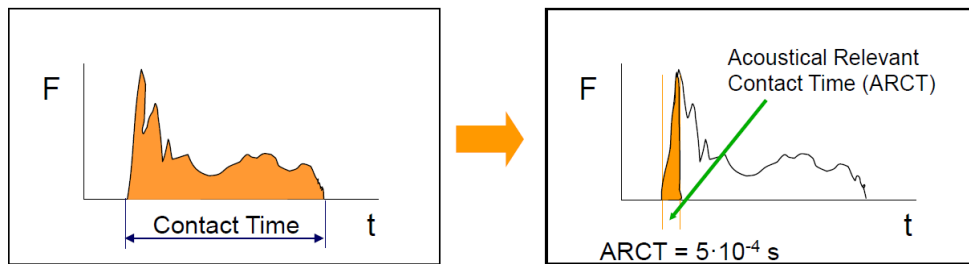


**Figure 3.2 :** Acoustic relevant contact time [41].

Crankshaft torque, speed irregularity, other geartrain components such as fuel pump and camshaft torque, are the main input of this geartrain multibody dynamic system. Losing contact in gear meshes due to angular vibration leads to impacts between gears and as a result, creating impact impulses.

A geartrain model is built by using mechanical elements in AVL Excite for impact impulse analysis. Then, the effects of fuel pump phasing, engine speed, PAS pump torque gear backlash on geartrain impact noise are analyzed and critical gear meshes for impact noise are determined with the help of geartrain impact impulse method. These four effects are in fact considered to be major contributors to geartrain impact noise.

### 3.1.1 Geartrain modelling in AVL Excite Timing Drive

AVL EXCITE Timing Drive software uses multi-body dynamics theory for dynamic analyses of geartrain systems. Essentially, a mechanical system consists of mass, spring and damper elements. For a damped MDOF system with N degrees of freedom, the governing equation of motion is written in matrix form as;

$$[M]\{\ddot{x}(t)\} + [C]\{\dot{x}(t)\} + [K]\{x(t)\} = \{F(t)\} \quad (3.2)$$

where  $[M]$  is mass matrix,  $[C]$  is damping matrix and  $[K]$  is stiffness matrix. Moreover,  $\{F(t)\}$  represents force vector as an input and  $\{x(t)\}$  stands for displacement vector as an output.

Geartrain model is built with elements such as shafts, gears, bearings and rotational excitations. All elements have input and output pins for connections with other elements. Lumped mass system with equivalent dynamic characteristics is used in geartrain modelling. Motions, forces and torques of the elements in geartrain system are calculated in time domain by systematic integrations which is also called Predictor / Corrector method. Forces, torques and speed irregularities at gears and shafts are main input parameters. The deflections, velocities, accelerations, forces and torques in the timing drive elements can be computed by using this software. Periodically varying meshing stiffnesses, in other words changing backlashes in the tooth meshes, are also considered a factor on dynamic characteristic of geartrain system in AVL Excite Timing Drive software [42].

Shaft elements are considered like beam elements based on finite element theory and, they consist of mass, spring and damper elements. Shaft elements also have torsional and bending motions. Furthermore, Shaft/Gear (SHGE) element is used for modelling a gear which is connected to a shaft. SHGE elements have radial, axial and rotational degrees of freedoms [41, 42].

Gear elements are modelled as mass and moment of inertia. Masses are joined by spring and damper elements with the consideration of stiffness and damping of gear meshes. Gear elements represent a rigid body and a gear mesh unit that describes the meshing contact between the actual element and its predecessor. The important point is that the gear meshes are expressed by backlash, stiffness, damping and gear geometry properties. Variable mesh stiffness during contact and viscous damping in the backlash are also non-linear properties of gear meshes. For gear impact analysis, constant meshing stiffness is used instead of varying meshing stiffness which can be used for gear whine noise analysis [41, 42].

In geartrain modelling, there are two fundamental bearing elements which are described as radial bearing elements and thrust bearing elements. It is important to note that bearing elements are accepted as massless elements. Bearing elements define the connection between a rigid body part of a shaft and the fixed ground.



### 3.1.2 Determination of critical gear meshes

In a geartrain system, there are some gear meshes which have higher impact noise contribution compared to other gear meshes. Gear mesh names with corresponding mesh number are given in Table 3.1. Impact impulse method provides a tool in order to determine critical gear meshes.

**Table 3.1** : Names of gear meshes.

<b>Mesh #</b>	<b>Gear Mesh</b>
Mesh1	Crankshaft Gear- Crankshaft Idler Gear
Mesh2	Crankshaft Idler Gear - Air Compressor Gear
Mesh3	Crankshaft Idler Gear - Big Idler Gear
Mesh4	Step Idler Gear- Fuel Pump Gear
Mesh5	Step Idler Gear- Camshaft Idler
Mesh6	Camshaft Idler Gear - Adjustable Idler Gear
Mesh7	Adjustable Idler Gear - Camshaft Gear
Mesh8	Step Idler Gear - PAS Pump Gear

First of all, impact impulses are calculated for all gear meshes and the total impact impulse is obtained by summing up individual impact impulses. Then, the impact impulse for each gear mesh is divided by the total impact impulse in order to obtain impact impulse contribution for individual gear meshes. Finally, impact impulse percentage of each gear meshes are calculated.

For the determination of critical gear meshes, it is necessity to define a baseline condition. The baseline condition for the 12.7 liter HD engine can be described as follows: backlash values for all meshes are chosen as 0.23 mm, power assisted steering pump torque is selected as 0 Nm and fuel pump phasing angle is chosen as 0 degree. Moreover, the range of engine speed is considered to be between 600 rpm to 2200 rpm. Furthermore, all the loads for the geartrain system are defined for full load engine condition. In fact, crankshaft speed irregularities, valvetrain loads and fuel pump torque are provided to the system for full load condition. Then, the total impact impulses and impact impulses of individual gear meshes are calculated. Impact impulse contributions of individual meshes are presented in Figure 3.4 as a percentage. According to the presented results, gear mesh 1 is identified as the critical gear mesh for all speeds. Mesh3, mesh4, mesh5 have also more impact contributions compared to other gear meshes. It is understood that torque fluctuation of each component directly affects their connected mesh.

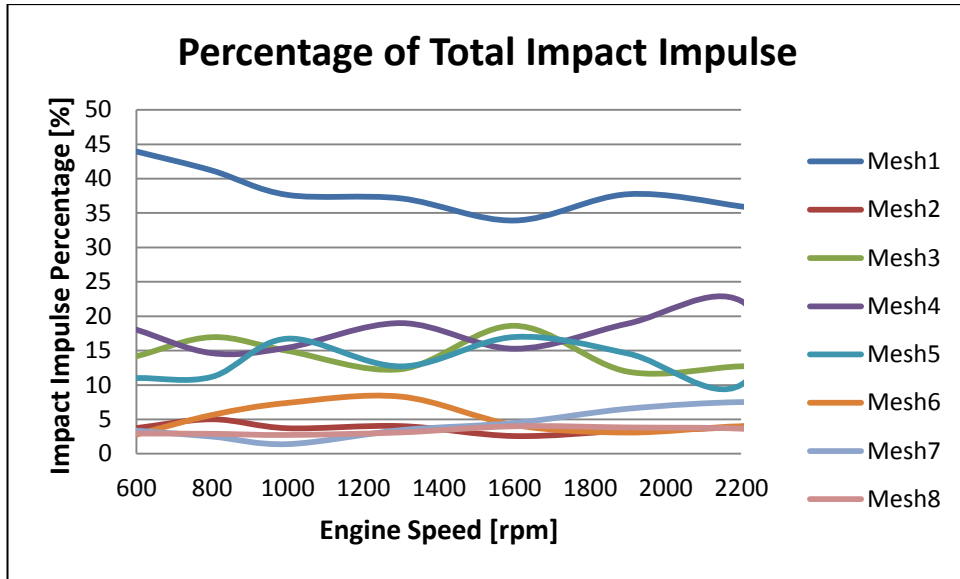


**Figure 3.4 :** Determination of critical gear meshes.

### 3.1.3 Effect of engine speed on impact impulses

Engine speed has significant effect on impact impulses. In section 3.1.2, impact impulses for each mesh and total impact impulses have already been calculated. In Figure 3.5, total impact impulses are shown from 600 rpm to 2200 rpm. Moreover, an allowable total impact impulse limit is also expressed by AVL, a level which is not supposed to be exceeded. As can be seen from Figure 3.5, this limit is set at 70 N.s level. It is also seen that the total impact impulses increase with respect to engine speed until engine rated speed which refers to the speed of maximum power.

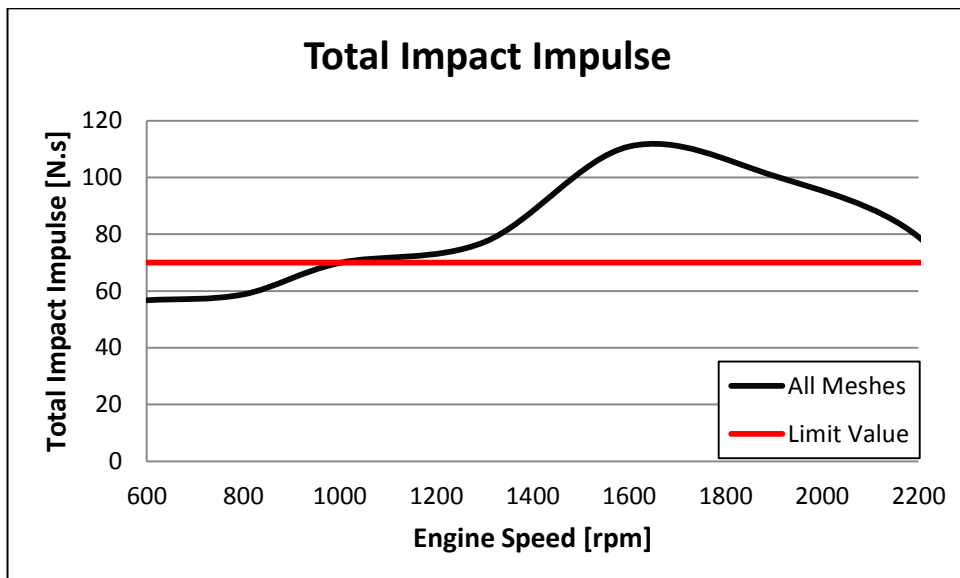


**Figure 3.5 :** Engine speed effect on total impact impulse.

### 3.1.4 Backlash effect on impact impulses

According to Crocker, there is a relationship between gear impact noise and gear backlash [4]. For geartrain analyses, backlash value is specified to describe the gear mesh properties in AVL Excite Timing software. According to AVL Excite Timing Drive Software guideline, backlash has significant effect on gear mesh stiffness which in turn, can change the impact impulse values. In this section, the effects of two different backlash values (0.23 mm and 0.19 mm) on total impact impulse are investigated for all gear meshes. In Figure 3.6, analysis results show that total impact impulses increase as the backlash value increases: 0.19 mm backlash value yields less total impact impulse than 0.23 mm does. Moreover, reaching the value of total impact impulse threshold (70 N.s) is approximately shifted from 1000 rpm to 1350 rpm if the the backlash value is decreased from 0.23 mm to 0.19 mm. As expected, results clearly indicate that higher backlash value yields higher levels of impact impulses.

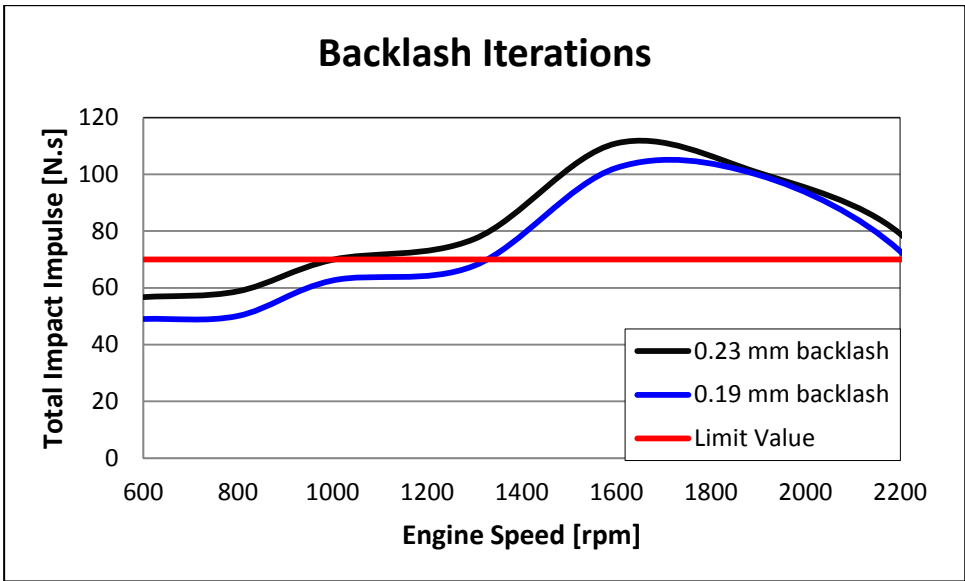
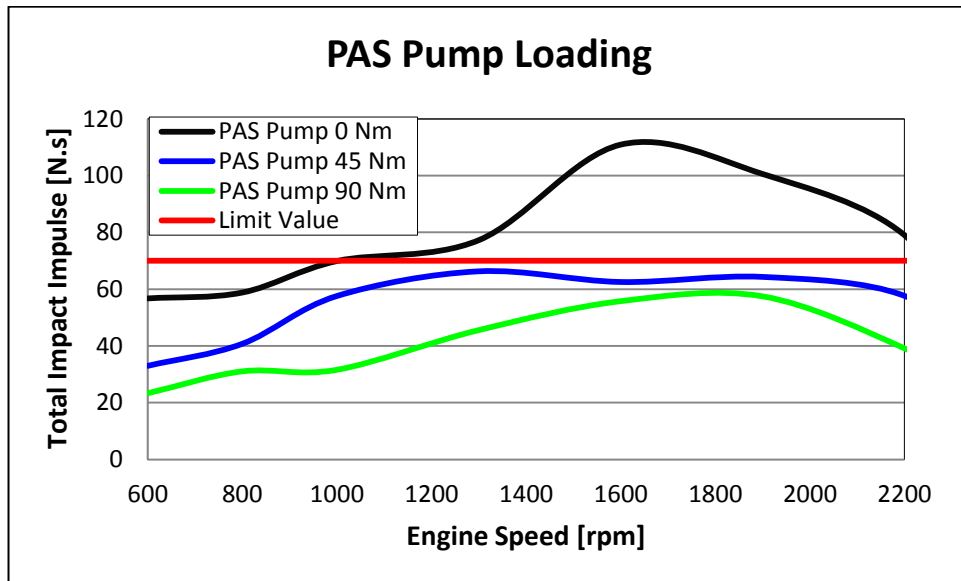


Figure 3.6 : Backlash effect on total impact impulse.

### 3.1.5 Effect of gear loading on impact impulses

Loading gears has significant effect on gear impact noise due to the nature of gear impact mechanism. Loading gears helps to decrease total torque on geartrain system. For the simulation, power assisted steering (PAS) pump load is chosen either 0 Nm or 45 Nm or 90 Nm as constant values, which means that there is no torque fluctuation on PAS pump torque. For instance, if the driver does not turn the steering

wheel, PAS pump does not demand any input torque. On the other hand, if the driver starts to turn the steering wheel, PAS pump will demand torque and it will increase up to 90 Nm which is nearly measured PAS pump needed torque value. In the AVL Excite Timing Software, PAS pump torque value is defined as a constant friction torque which means reverse torque application to the geartrain system. By the way, geartrain dynamic model is run for three cases. In Figure 3.7, the total impact impulse results are shown for three torque levels, i.e.: 0 Nm, 45 Nm and 90 Nm.



**Figure 3.7 :** PAS pump loading effect on total impact impulse.

Loading PAS pump shows that loading gear has the highest effect on impact impulses according to the experimental test results. Inspection of Figure 3.7 reveals that by loading PAS pump, total impact impulse value decreases significantly under the threshold total impact value. It is seen that the torque level on the system has very significant effect on the total impact impulses. It is also clear that loading the gears with constant torque is beneficial for reducing gear impact noise. However loading some gears with components such as power assisted steering pump is not a practical solution because loading gear may mean unnecessary power consumption. Therefore, loading gear is not an acceptable solution for reducing gear impact noise.

### 3.1.6 Effect of fuel pump phasing on impact impulses

Fuel pump phasing means changing the assembly position of the crankshaft and fuel pump relative to each other. In other words, it is changing the timing between fuel pump plunger and crankshaft piston. It is suggested in the literature that fuel pump

has higher effect on geartrain impact noise due to the torque alteration [3, 4, 5, 7]. Actually, fuel pump requires higher torque fluctuations during a working cycle, therefore high levels of torque variations occur between the timing gears and fuel pump gear, and this leads to impacts between gears as well as impact noise [26]. Timing of the fuel pump torque curve with respect to engine crankshaft torque curve can be shifted by fuel pump phasing. For some phasing angles, impacts can increase due to the torque timing. However, it can also cause decreasing speed fluctuation in some phasing angles due to torque cancellation. Therefore, impact noise can be reduced by fuel pump phasing. Nine different fuel pump phasing angles are investigated so as to establish the effect of fuel pump phasing on gear impact. By changing the fuel pump working time as well as torque peak time with respect to engine torque peak time in the model, fuel pump phasing process is achieved. In Figure 3.8, the total impact impulse values corresponding to individual phasing angles are presented with respect to engine speed and this plot provides valuable information about the effects of phasing angle on total impact impulses. Inspection of this figure reveals that there is a nodal point around 1450 rpm and the total impact impulse behavior of phasing angles changes with respect to this nodal point. It is seen that after this nodal point, 84 degrees and 72 degrees phasing angles have higher impact contribution on geartrain compared to other phasing angles. However, before this nodal point, 24 and 36 degree phasing angles have higher impact contribution on geartrain. Consequently, the results show that fuel pump phasing can have both negative and positive effects on geartrain impact noise.

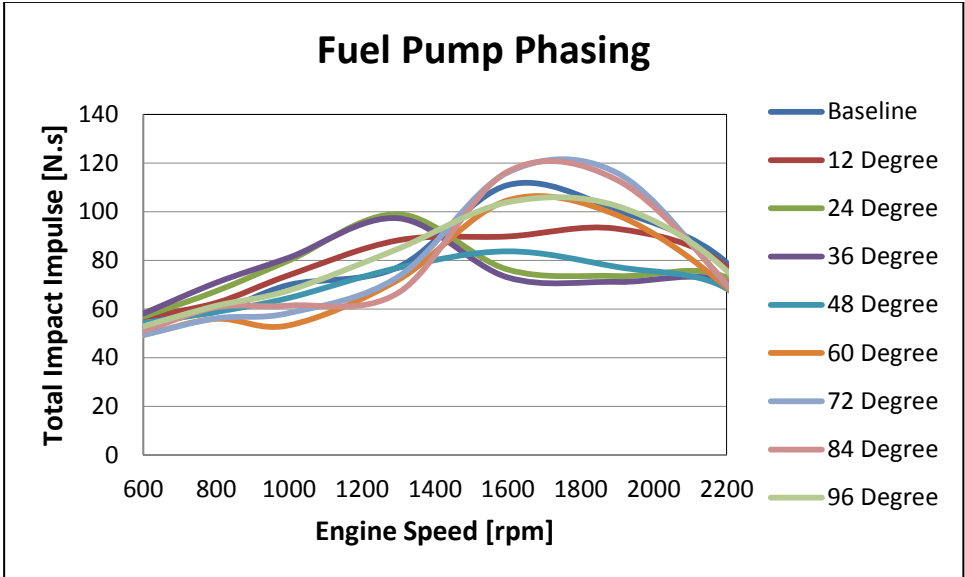


**Figure 3.8 :** Fuel pump phasing effect on total impact impulse.

### 3.2 Torsional Vibration Analysis of Crankshaft

Torsional vibration of crankshaft is one the most important main source of geartrain impact noise. Combustion process has a significant effect on this torsional vibration. The main aim of this study here is to show the torsional vibration characteristics of a six cylinder heavy-duty diesel engine.

#### 3.2.1 Multi-body engine model

In this study, torsional vibration analysis and design of 12.7 liter heavy-duty diesel engine cranktrain were done by using AVL Excite software. The background theory of torsional vibration is presented in AVL Excite Designer Theory [43].

A lumped mass system with torsional spring and damping is used for cranktrain modelling in AVL Excite software. The engine model shown in Figure 3.9 includes the crankshaft, main bearings, conrods, pistons, big end and small end bearings. All the geometrical data are also described in the cranktrain model. After modelling the cranktrain system, there is only one additional thing; cylinder pressure is needed as an input data. Dynamic equations of the system can be solved by using cylinder pressures and engine model [44].

In this study, actual cylinder pressure data at 550 rpm, which are measured in engine dynamometer, are used in this model. A 1D torsional model is established for cranktrain dynamic model. In addition, cranktrain torsional vibration analysis is done at 550 rpm engine speed only.

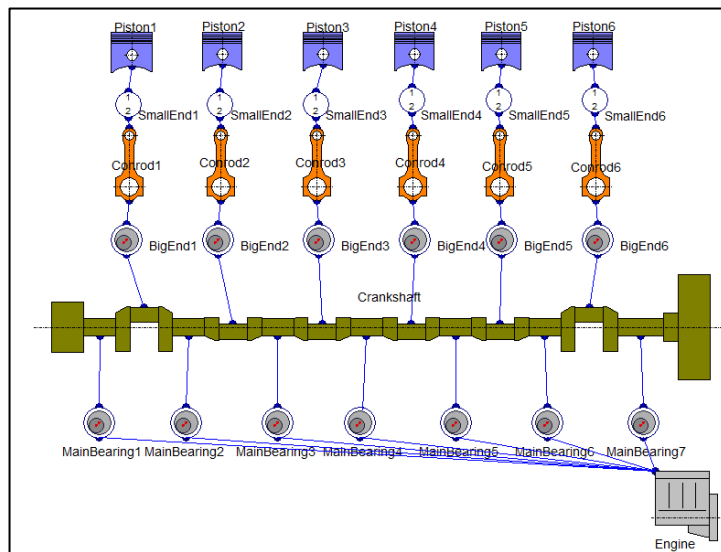


**Figure 3.9 :** Multi-body engine model [44].

### 3.2.2 Multi-body dynamic analysis result

Two important results that are torque fluctuation and angular acceleration are obtained by solving the multibody engine model. The torque fluctuation in Figure 3.10 and angular acceleration in Figure 3.11 are calculated by using cranktrain dynamic analysis.

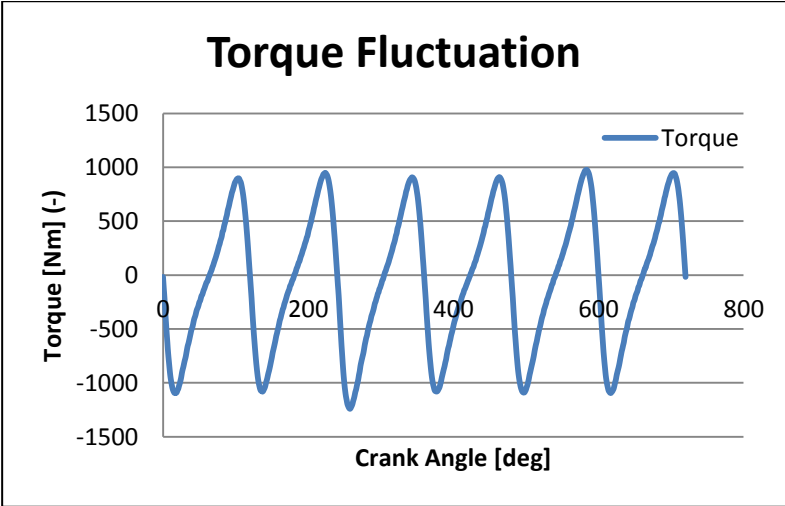


Figure 3.10 : Torque fluctuation of crankshaft.

It is observed that cranktrain has significant torque fluctuations at engine idle speed 550 rpm. This is not an unexpected result; internal combustion engines cannot produce constant torque due to their principle of operation. Sequential combustion process leads to torque variation which is the primary reason why torsional modes are excited. Torque fluctuation is also one of the most important contributors to geartrain impacts.

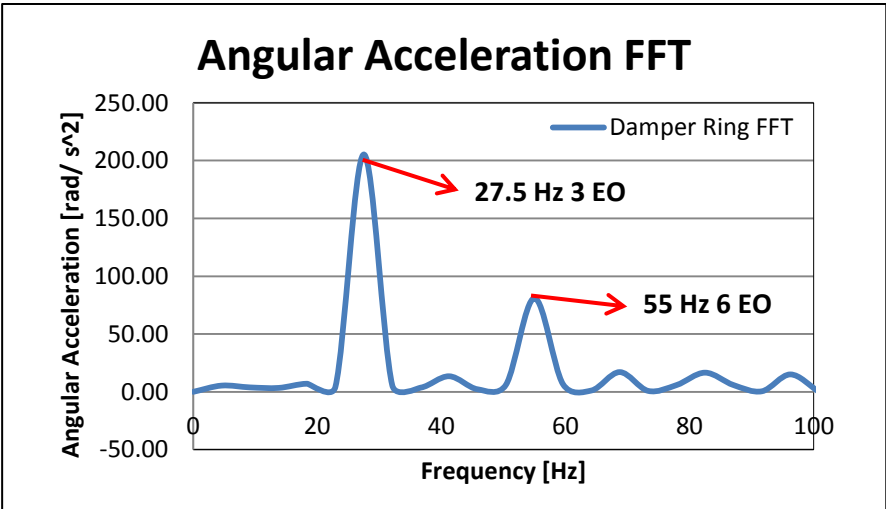


Figure 3.11 : Angular acceleration FFT of crankshaft damper ring.

In Figure 3.11, angular acceleration spectrum shows some peak frequencies: 27.5 Hz and 55 Hz. 27.5 Hz corresponds to 3<sup>rd</sup> engine order and 55 Hz corresponds to 6<sup>th</sup> engine order at 550 rpm engine speed. Engine order is also calculated as;

$$\text{Combustion Frequency} = \frac{\text{Engine Speed}}{60} \times \text{Cylinder Number} \times 0.5 \quad (3.3)$$

where the engine speed is 550 rpm and cylinder number is 6. Accordingly, the combustion frequency is calculated as 27.5 Hz. In addition, 55 Hz is a harmonic of 27.5 Hz. They are also called as firing or combustion orders.

From this study, it is concluded that combustion orders dominate torsional vibrations of crankshaft. By the way, these frequencies and orders directly affect torsional vibrations of crankshaft and they indirectly affect geartrain impacts. Combustion orders are considered as the dominating factor on geartrain impact.



#### 4. EXPERIMENTAL STUDY OF GEARTRAIN IMPACT NOISE

Experimental measurements are generally accepted as reliable studies because more accurate results can be obtained by experimental studies compared to numerical CAE analyses. In this chapter, NVH measurements on a 12.7 liter heavy-duty (HD) diesel engine, which is also modelled via CAE analysis as described in chapter 3, are presented in order to determine influential parameters on geartrain impact noise. Test results are going to be expressed under four main subsections which are named as "engine dynamometer noise and vibration tests", "investigation of housing effect", "vehicle exterior noise tests" and "advanced signal processing applications". Maximum power of this 12.7 liter engine is 460 PS. Detailed information about the tested engine is presented in Table 4.1.

**Table 4.1 :** Engine specification.

Engine Type	Diesel
Engine Displacement	12.7 liter
Number of Cylinders	6
Cylinder Arrangement	Inline
Bore	130 mm
Stroke	160 mm
Compression Ratio	17:1
Emission Level	EU6
Aspiration	Turbocharged
Fuel Injection System	CRS
Fuel Delivery	Direct Injection
Coolant	Liquid
Camshaft Position	SOHC
Engine timing sysem	Gear drive
Valves per cylinder	4
Firing Order	1,5,3,6,2,4
Maximum Power	460 PS
Maximum Torque	2300 Nm
Maximum Engine Speed	2100 rpm
Minimum Egnine Speed	550 rpm
Rated Speed	1900 rpm

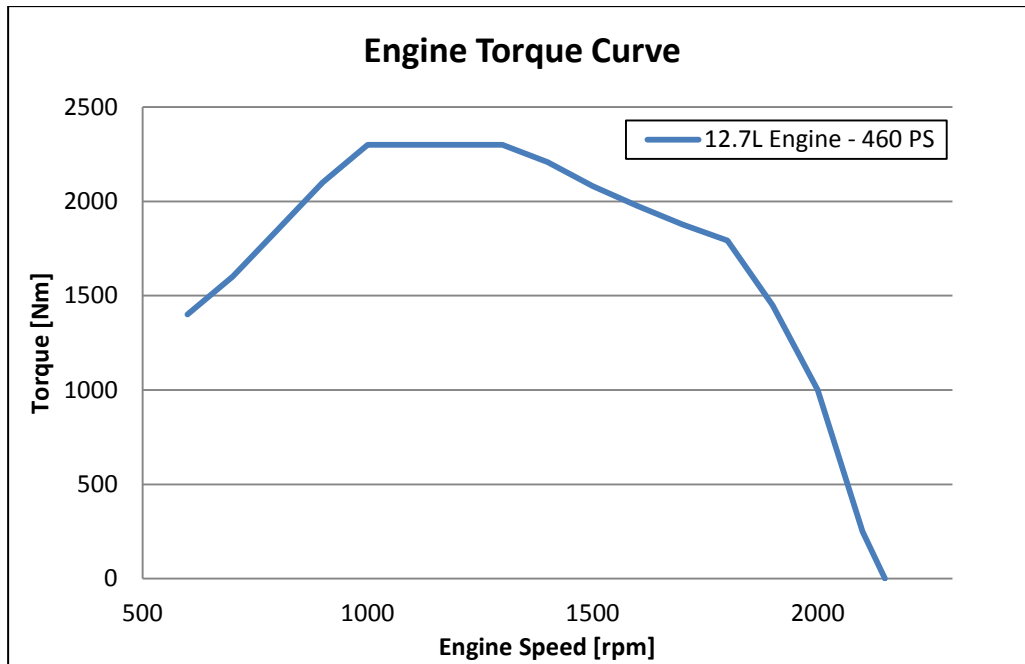


**Figure 4.1 :** Torque curve of 12.7L HD diesel engine.

#### **4.1 Engine Dynamometer Noise & Vibration Tests**

Engine dynamometer tests are needed to meet noise and emission legislation and this requires performing many tests in engine dynamometer. As concerned with these legislations, engine acoustic dynamometer tests are essential requirements to meet noise legislation for automotive companies. In fact, engine overall noise level has become more important for engine manufacturers due to the competitions in automotive industry. Moreover, significant NVH improvements on engines can be made with the support of dynamometer tests before the mass production. Mainly, engine dynamometer tests are performed for measuring power, torque and engine parameters (temperature, pressure etc.) at different speeds and load conditions, such as full load (WOT), no load (CT) and part load (POT) conditions. Cylinder pressure sensors, temperature sensors, accelerometers and microphones are essentially used transducers in acoustic dynamometer. For this purpose, a 6 cylinder 12.7 liter heavy-duty diesel engine without the transmission unit has been tested in semi-anechoic chamber by using these transducers. In addition, NVH measurements on this HD engine were performed for full load speed sweep, no load speed sweep and idle operating conditions. Three run average were used for calculations such as sound pressure level, power, torque etc. A schematic representation of the semi-anechoic chamber is shown in Figure 4.2

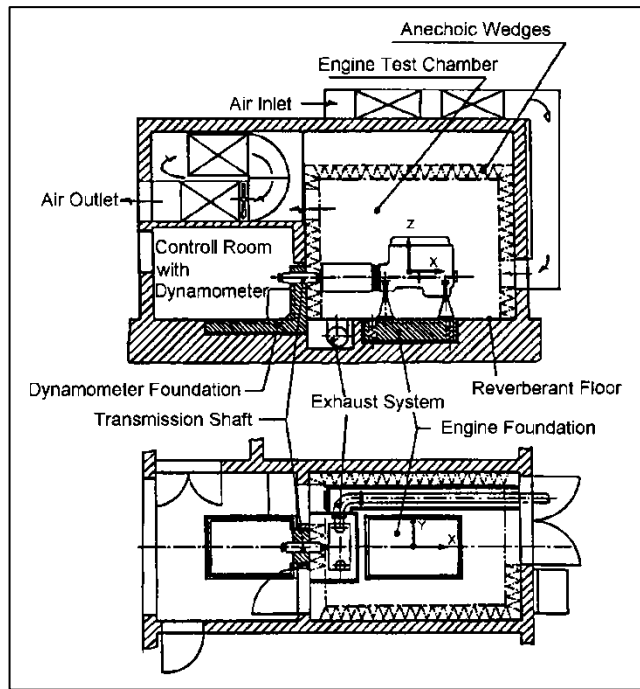


**Figure 4.2 :** Semi-anechoic test cell with low-noise engine test bench [26].

According to AVL Acoustics book [26], a standardized measurement procedure for machinery noise emission, which is named as DIN 45635, is used for the engine noise measurements in semi-anechoic chambers. A reference box is established by pointing the outermost part of the engine, which provides to determine the microphone location. Microphones are basically located 1 meter away from the the outermost part of the engine and centered to the related surface of the reference box. In semi-anechoic chambers, four microphones are used for the determination of the overall engine noise level [26]. The top view of the 12.7 liter HD engine dynamometer configuration is shown in Figure 4.3.

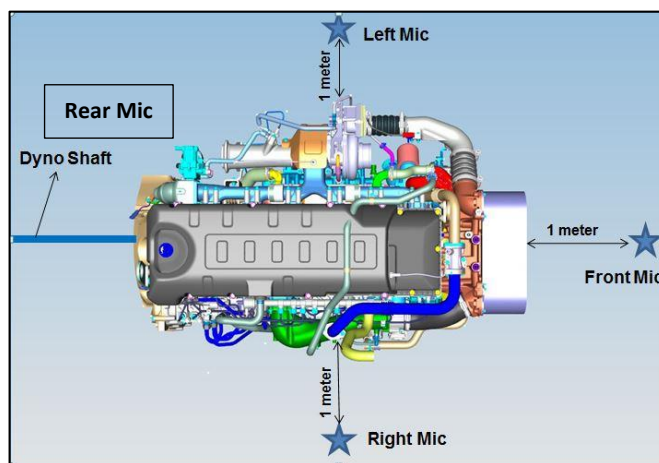


**Figure 4.3 :** Engine dynamometer configuration of 12.7 liter HD diesel engine.

Sound pressure data were collected on five different microphone positions in 12.7 liter engine dyno tests, the measurements locations being: engine left side, engine right side, engine front side, engine top side and engine rear side. Microphone locations are seen in Figure 4.4.

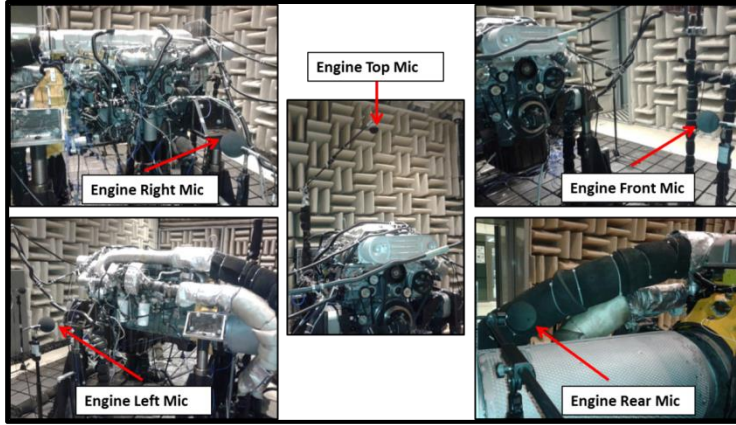


**Figure 4.4 :** Microphone positions in engine dynamometer.

All microphones except the rear microphone are located 1 meter away from the outside of the engine in acoustic chamber based on DIN 45635. However, rear microphone was located 0.8 meter away from the outside of the engine. In addition, rear microphone, which is not used in engine overall sound pressure level calculations, was also used in order to make detail analysis of the geartrain impact noise. The formulation of the average sound pressure level is expressed as [17];

$$L_{P_{average}} = 10 \log_{10} \left[ \frac{1}{N} \sum_{i=1}^N 10^{(L_{P_n}/10)} \right] \quad (4.1)$$

where N is number of microphone positions and  $L_{P_n}$  is sound pressure level at related microphone position. As it is mentioned in reference [17], average sound pressure level of an engine in semi-anechoic room is calculated by using left mic, right mic, front mic and top mic data hence this average sound pressure level is shortly named as four mic average SPL in engine NVH literature. Related to four mic average description, formulation of average sound pressure level is rewritten as;

$$L_{P_{4mic}} = 10 \log_{10} \left( \left( 10^{L_{P_{Front}}/10} + 10^{L_{P_{Left}}/10} + 10^{L_{P_{Right}}/10} + 10^{L_{P_{Top}}/10} \right) / 4 \right) \quad (4.2)$$

#### 4.1.1 Vibration and acoustic measurement comparisons

It is known that if there is no sound reflection in a field, free field microphones are best for such measurements. In such cases, microphone should be perpendicular to moving direction of sound waves [17]. Therefore, free field microphones are used in semi-anechoic chambers. Brüel & Kjaer 4188 type free field microphones [45] were used in engine dynamometer tests for this purpose. Moreover, PCB Piezotronics HT 356B21 model ICP accelerometers [46] were used in the engine tests due to high surface temperature of the heavy-duty engine. Furthermore, HT 356B21 model accelerometers have higher temperature strength whose operational temperature can be up to 163 °C. Noise, vibration, cylinder pressure, engine torque and engine speed data were collected by 64 - channel LMS SCADAS 310 - UTP data acquisition system [47]. The free field microphone and integrated circuit piezoelectric accelerometer are demonstrated in Figure 4.5.

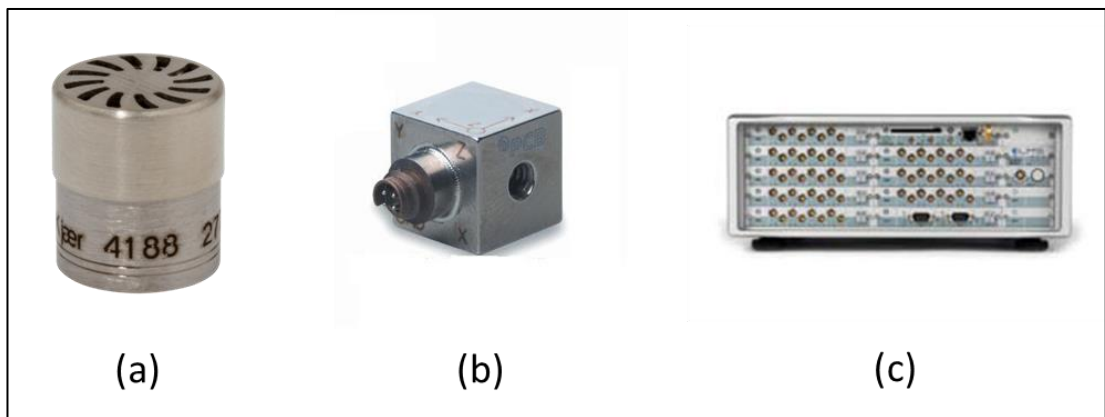


**Figure 4.5 :** (a) Brüel & Kjaer microphone Type 4188 [45]. (b) PCB Piezotronics ICP accelerometer Model HT 356B21 [46]. (c) LMS SCADAS 310 - UTP data acquisition system [47].

In 12.7 liter engine, geartrain is located at the rear side of the engine. That's why microphones, particularly located in the rear, left and right sides, are important for the investigation of geartrain impact noise. Geartrain housing and flywheel housing are determined as the best accelerometer locations in order to investigate geartrain impact noise of the HD engine. Accelerometer location of flywheel housing and geartrain housing are illustrated in Figure 4.6. Gear impact noise can be observed at higher frequencies. Dominant impact frequencies of the 12.7 liter engine were observed between a frequency range of 1000 Hz to 6000 Hz which are the sources of broadband noise. On the other hand, impacts have also contributions beyond these

frequencies due to the nature of hammering process. Rattle noise is remarkably audible at idle operating condition based on subjective and objective measurements.

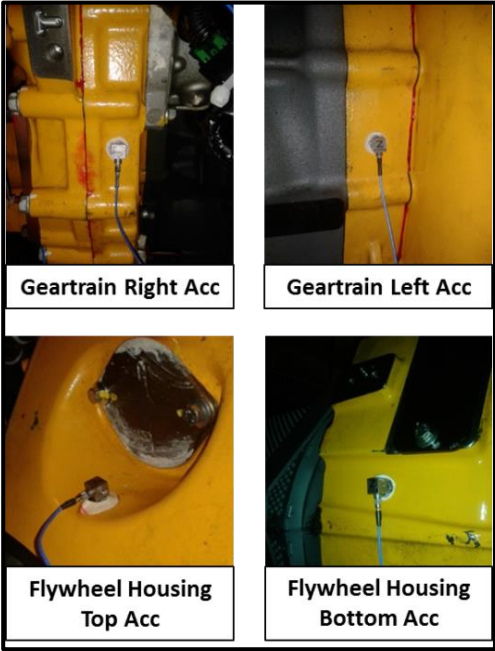


**Figure 4.6 :** Accelerometer locations on engine.

It can be said that engine rear side microphone and flywheel housing bottom side accelerometer give good correlation between 1500 Hz and 3000 Hz at engine idle speed (550 rpm) based on waterfall FFT diagrams presented in Figure 4.7.

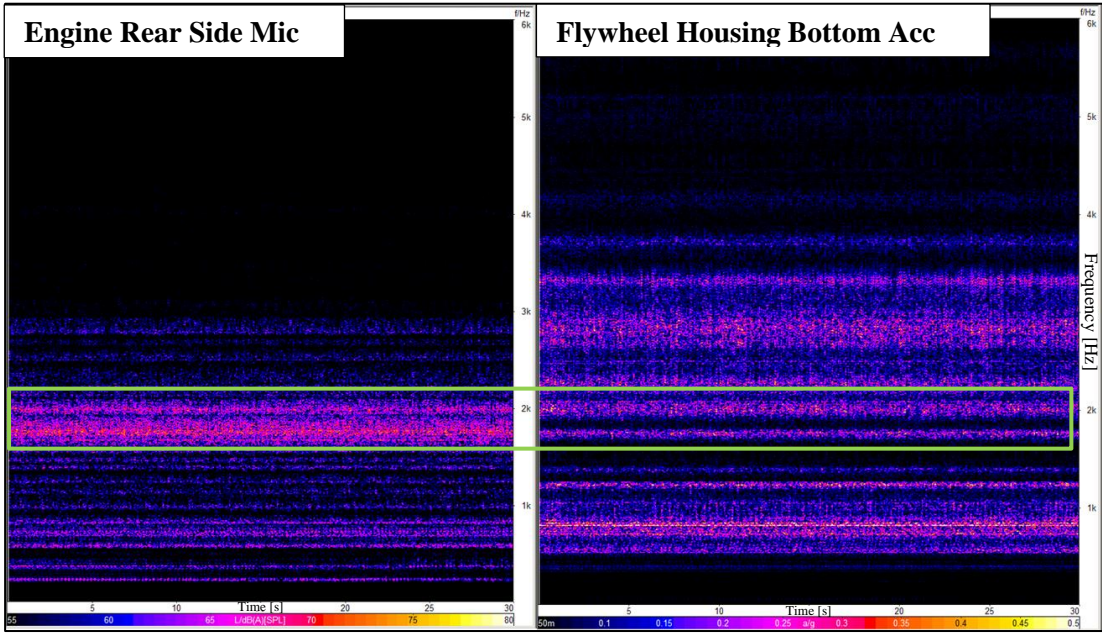


**Figure 4.7 :** Waterfall FFT vs time diagram of engine rear side mic and flywheel housing bottom accelerometer.

In addition, engine left side microphone data and geartrain left side accelerometer data show similar trends around 2000 Hz at engine idle speed according to Figure 4.8.

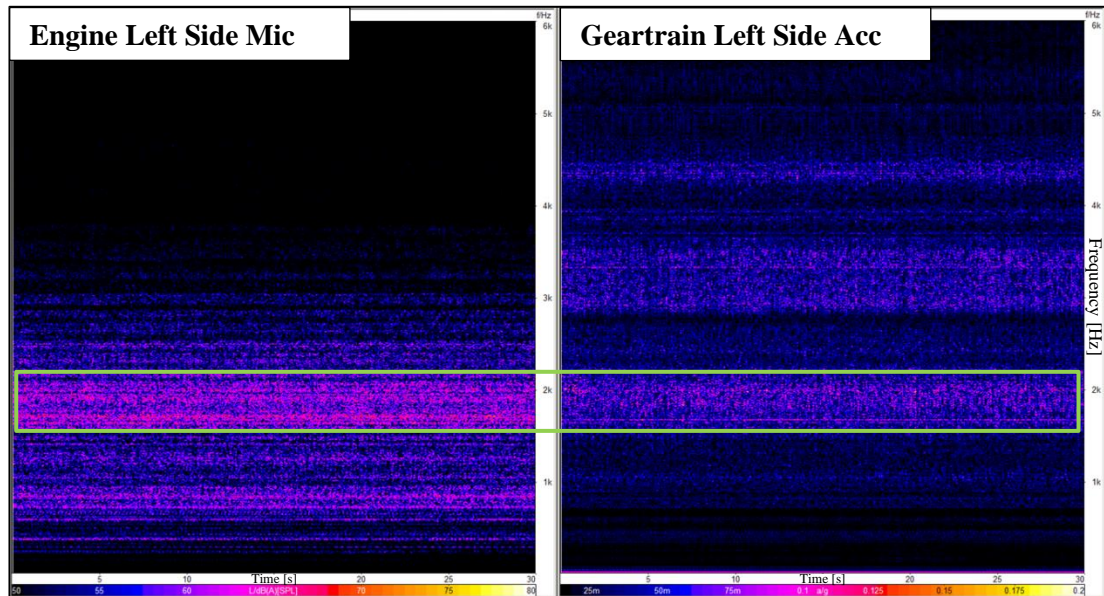


**Figure 4.8 :** Waterfall FFT vs time diagram of engine left side mic and geartrain housing left accelerometer.

Likewise, geartrain right side accelerometer and engine right side microphone prove the broadband frequency characteristic of the rattle noise. Narrowband lower frequencies below 1000 Hz can be seen in waterfall FFT diagrams which are related to engine orders. Moreover, some of them are gear meshing frequencies which are related to Geartrain 1<sup>st</sup> and 2<sup>nd</sup> plane, oilpump drive gear plane, oil pump internal gear and fuel pump internal gear. In Table 4.2, fundamental gear meshing frequencies at 550 rpm idle speed and engine orders are shown.

**Table 4.2 :** Geartrain meshing frequency.

	Gear Meshing Frequency at Idle [Hz]	Engine Order
Geartrain 1st Plane	412.5	45
Geartrain 2nd Plane	275	30
Oil Pump Drive Gear Plane	733.3	80
Oil Pump Internal Gear	150	16.4
Fuel Pump Internal Gear	151.25	16.5

#### 4.1.2 Acoustic camera measurements

“Acoustic camera visualizes the origin and intensity of sound waves using an array of microphones and sophisticated signal-processing algorithms. The principle underlying such devices is to record audio signals from an array of microphones and to compute the intensity of sound pressure for well-defined points in space; this approach enables visualization of sound sources.” [48].



**Figure 4.9 :** HEAD VISOR acoustic camera [49].

In this experimental study, HEAD VISOR acoustic camera [49] shown in Figure 4.9 is used in order to determine the sound sources of 12.7 liter engine. It is a useful tool for locating, visualizing, quantizing and auralizing of sound sources.

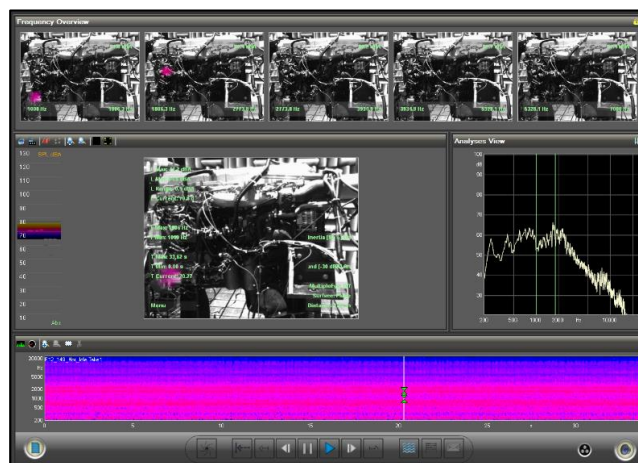


**Figure 4.10 :** Screenshot of HEAD VISOR software.

Acoustic camera measurement were made for the engine right side, left side and front side in engine dynamometer. Measurements from engine right side and left side are displayed because geartrain side can be seen at right side and left side of the engine by acoustic camera. Engine rear side could not be measured by acoustic camera due to the space limitation at the rear side. In addition, acoustic camera measurement were made at engine idle speed (550 rpm) and run for thirty seconds.

Acoustic camera software shows that the most critical peak is determined between 1621 Hz and 1748 Hz at engine right side and the current sound pressure level between this interval is measured as 68 dB(A). Geartrain is detected as sound source of this peak based on acoustic camera visualization at engine left side. Sound source detection of this peak is seen in Figure 4.11.

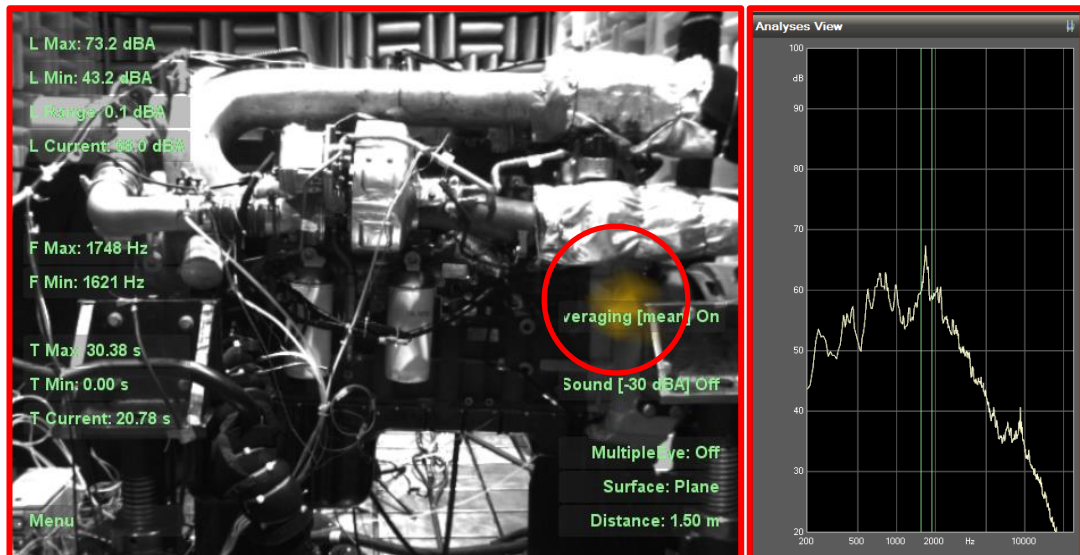


**Figure 4.11** : Engine left side critical peak.

As can be seen from Figure 4.12, there is also another peak between 1597 Hz and 1748 Hz at engine right side. The current sound pressure level is measured as 66.5 dB(A). In a similar manner, geartrain is determined as a suspected sound source based on acoustic camera measurements of the engine right side. In Figure 4.11, geartrain is shown as sound source.

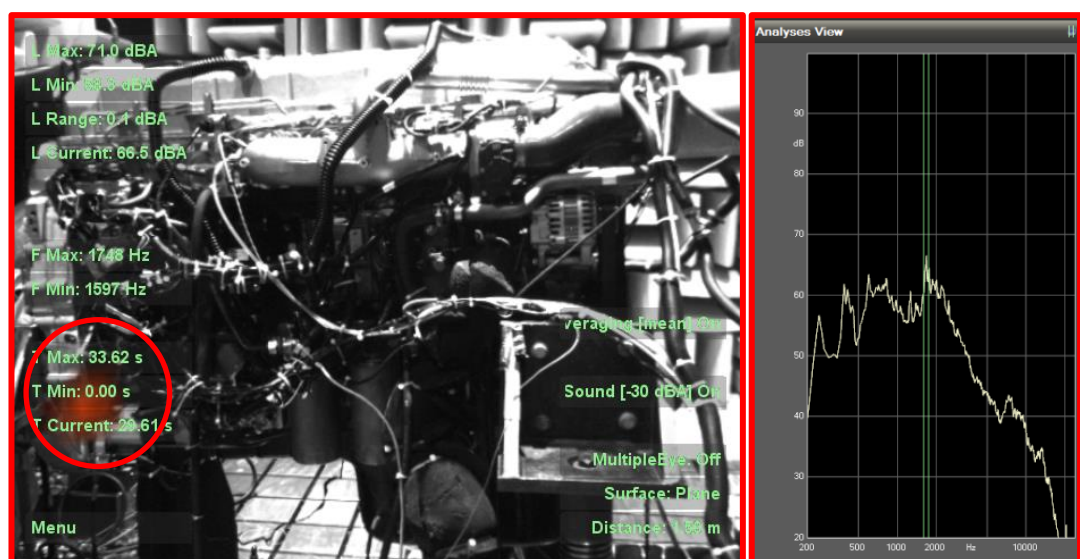


**Figure 4.12** : Engine right side critical peak.

As a summary, the most critical frequency is measured to be nearly the same at engine right and left sides, which can be accepted between 1621 Hz and 1748 Hz. The geartrain is also determined as the main sound source at this critical frequency.

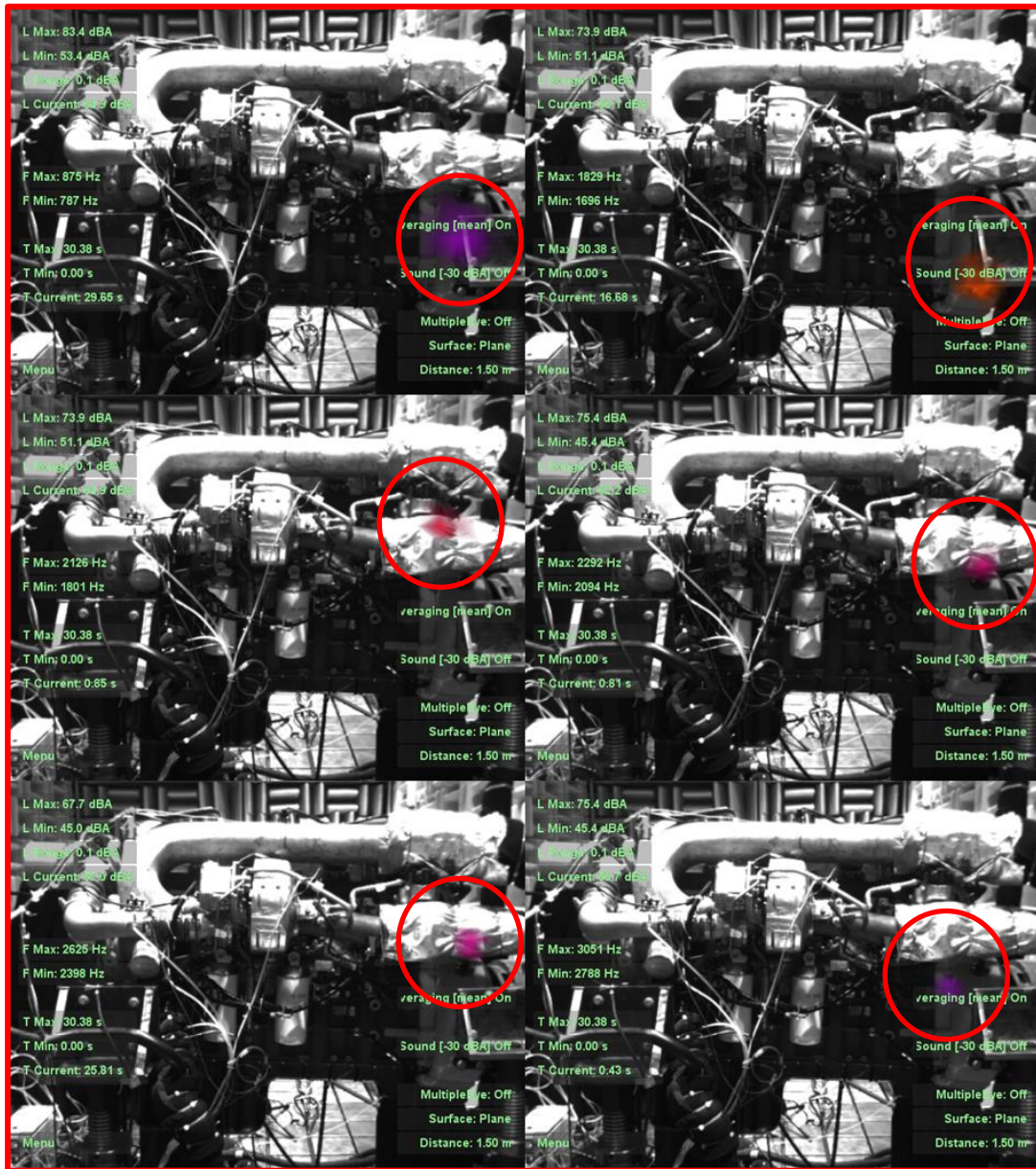


**Figure 4.13 :** Engine left side acoustic camera result.

Other measured significant frequencies by acoustic camera are displayed in Figure 4.13. Peak frequency intervals of 787 Hz – 875 Hz, 1696 Hz – 1829 Hz, 1801 Hz – 2126 Hz, 2094 – 2292 Hz, 2398 Hz – 2625 Hz and 2788 – 3051 Hz are determined as noise contributor at engine left side. The results show the rear side as a sound source. The results show that engine right side also contributes to the rattle noise with geartrain. Moreover, there are important peaks in the interval between

1215 Hz – 1313 Hz, 1333 Hz – 1459 Hz, 1722 Hz – 1829 Hz, 1942 Hz, 2094 Hz, 2126 Hz – 2362 Hz and 2830 Hz– 3144 Hz. As shown in Figure 4.14, geartrain is found to be a main noise source at these frequency intervals. Therefore, it can be inferred that geartrain is a potential noise contributor at this frequency intervals.

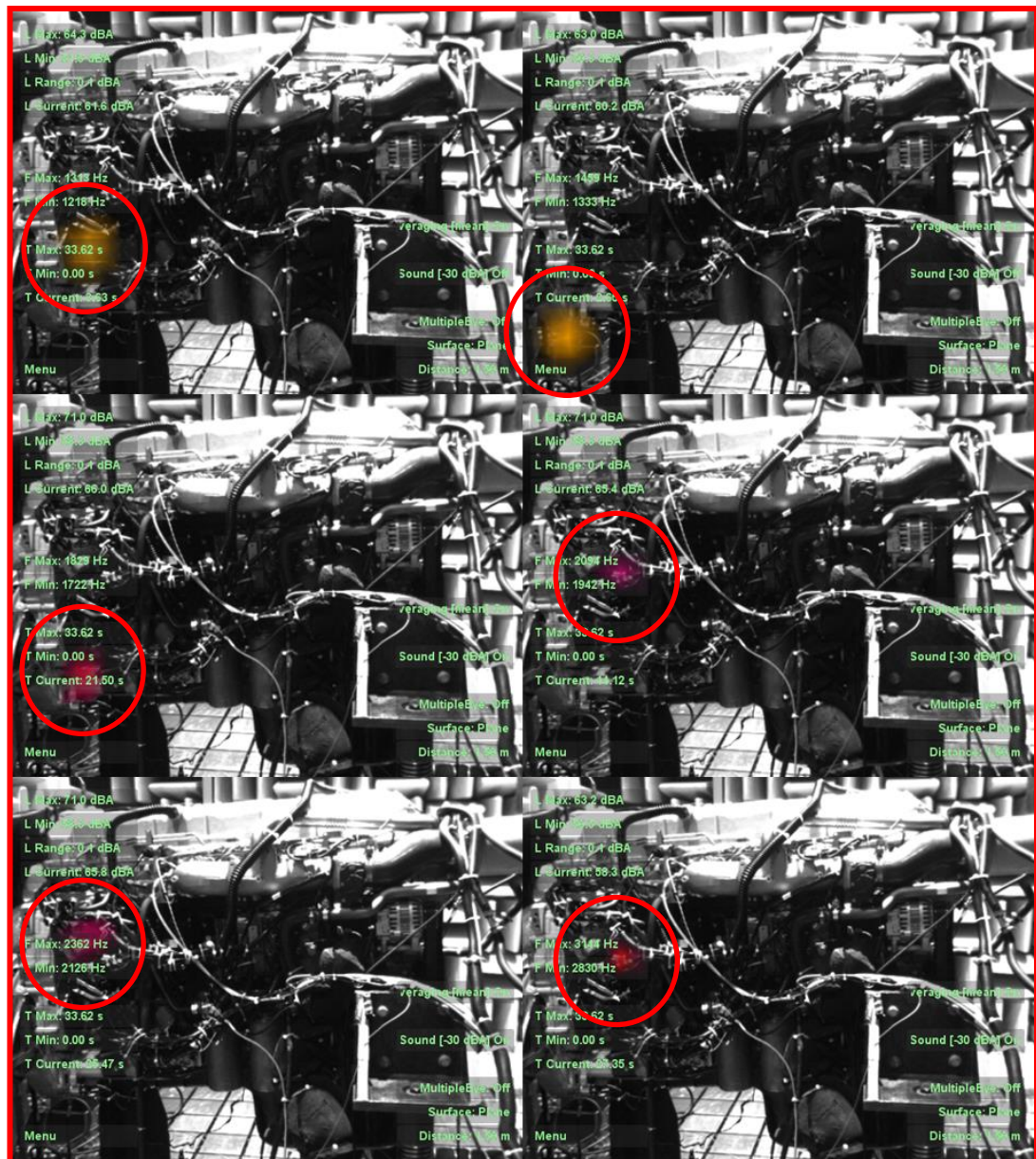


**Figure 4.14 :** Engine right side acoustic camera result.

In summary, acoustic camera measurements from both engine right side and engine left side prove that geartrain is the main noise source at idle speed. As stated before, rattling noise is more audible at idle speed due to the fact that combustion noise and other mechanical noise has lower contributions at idle speed. This is also the reason why acoustic camera measurements were made at idle speed.

### 4.1.3 Investigation of backlash effect

In this section, two different backlash values (which are defined as minimum and maximum) between oil pump gear and oil pump idler gear in 12.7 liter HD diesel engine are compared in order to assess the effect of backlash on gear rattle noise. It is known that backlash has significant effect on gear rattle noise based on Crocker graph [4]. It is expected that rattle noise will increase if the backlash value between gears increases. In Figure 4.15, oil pump with its gears are presented and in Table 4.3 minimum and maximum backlash values between oil pump gears are listed. First of all, it is worth stating that the maximum and the minimum backlash values between oil pump gear and oil pump idler gear were identified by providing different tolerances in oil pump gear shafts. Engine sound pressure level was calculated for hot idle condition by using 1/3 octave band. Frequencies between 100 Hz and 10 kHz are used for calculating 1/3 octave sound pressure level. In addition, full load speed sweep test and no load speed sweep test were used for calculating the sound pressure level at different engine speeds. Sound pressure levels were calculated by using three run average for each engine operating condition.

**Table 4.3 :** Oilpump backlash value.

<b>Gear Pair</b>	<b>Min Backlash</b>	<b>Max Backlash</b>
Oilpump Gear - Oilpump Idler	103 micron	215 micron

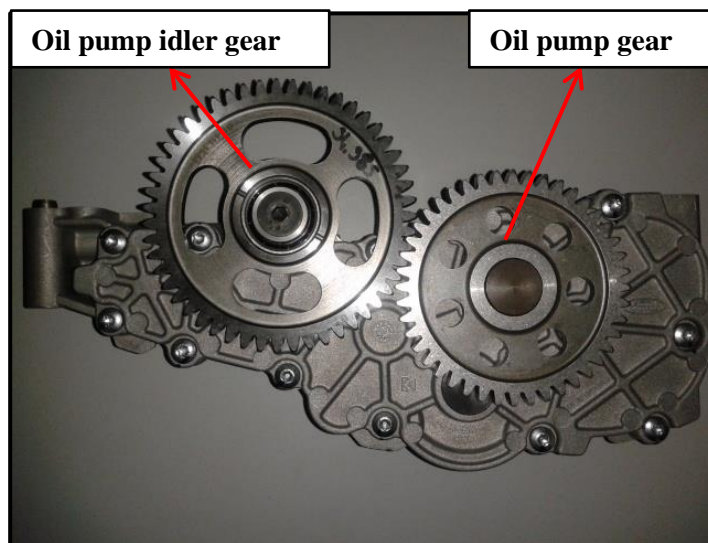


**Figure 4.15 :** Oilpump gears of 12.7 liter HD diesel engine.

Objectively and subjectively, it has been observed that oil pump with minimum backlash causes less rattle noise compared to oil pump with maximum backlash according to the measurements in semi-anechoic acoustic chamber under hot idle, full load and no load speed sweep conditions. In Table 4.4, sound pressure levels of individual microphones and four mic average are shown for idle operating condition.

**Table 4.4 :** Hot idle sound pressure level of backlash iterations.

Sound Pressure Level dB(A)		
	Min Backlash	Max Backlash
<b>4 Mic Average</b>	81.34	81.62
<b>Rear Mic</b>	85.14	85.83
<b>Front Mic</b>	79.04	79.39
<b>Left Mic</b>	82.08	82.53
<b>Right Mic</b>	82.49	82.64
<b>Top Mic</b>	81.00	81.17

Although the hot idle four mic average radiated noise difference between minimum and maximum backlash oil pump is 0.28 decibel, sound pressure level difference between maximum and minimum backlash oil pump is 0.69 decibel at engine rear mic. Sound pressure level difference between minimum and maximum backlash value is higher at engine rear side compared to other sides since gear train is the main suspected component for rattle noise. Briefly, it is seen that backlash has slight effect on radiation of rattle noise at idle speed due to changing backlash in only one mesh.

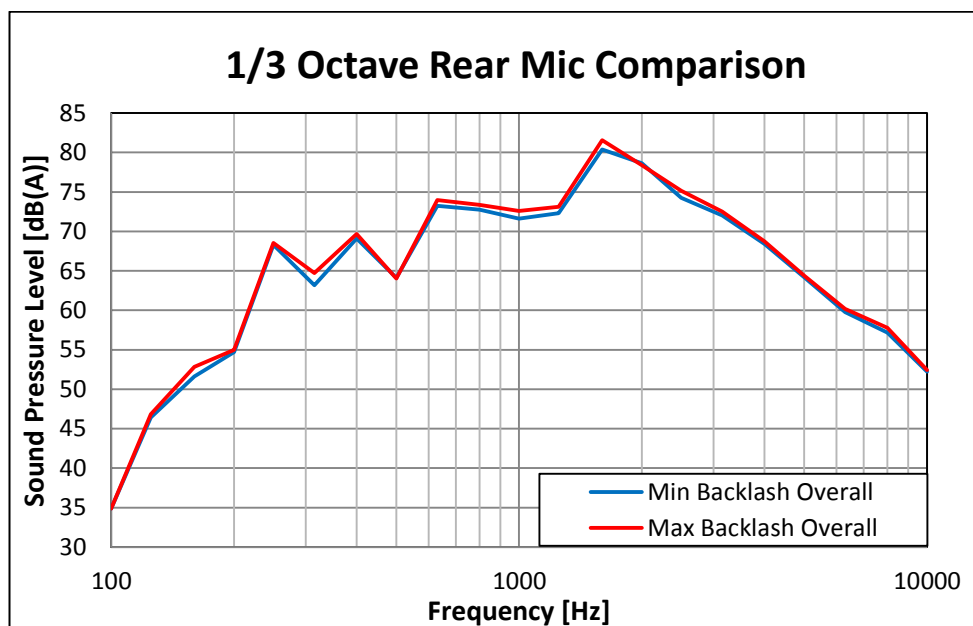


**Figure 4.16 :** Engine rear microphone 1/3 octave of oil pump backlash iterations.

Backlash effect at higher frequencies can be seen based in Figure 4.17. Moreover, minimum backlash value between gears appears to provide lower amplitudes at higher frequencies relative to maximum backlash measurement, which can be seen in Figure 4.17. Left mic color map also yields similar result in Figure 4.18 as well.

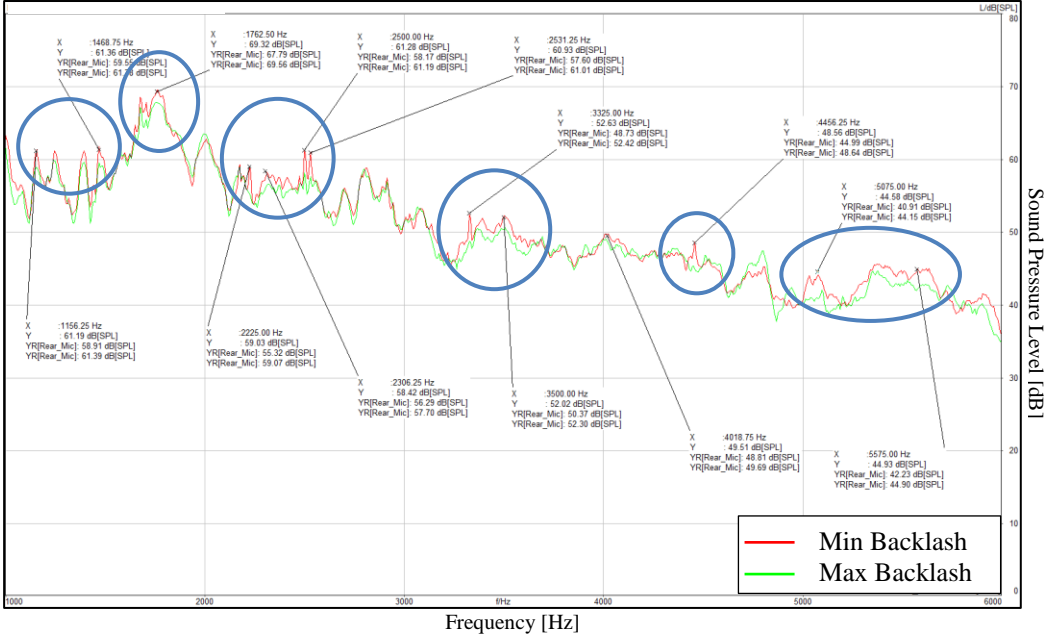


**Figure 4.17 :** Engine rear microphone FFT of oil pump backlash iterations.

In fact, there are significant improvements at broadband frequencies in a wide range from 1 kHz to 6 kHz according to Figure 4.17 and Figure 4.18. There are also improvements at frequencies higher than 6 kHz but the improvements are minor compared to those within a frequency range between 1 kHz and 6 kHz.

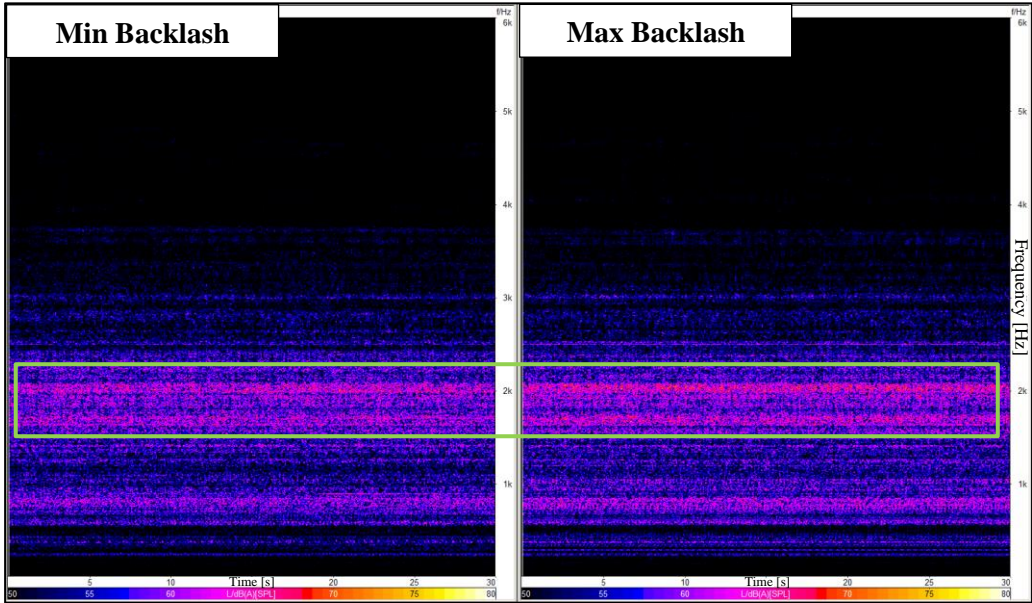


**Figure 4.18 :** Engine left mic waterfall FFT diagram of oil pump backlash iterations.

Full load speed sweep tests are another important measurements in order to assess the backlash effect on rattle noise. Sound pressure level difference between maximum and minimum backlash iteration reaches up to 0.67 dB (A) level at rear mic for full load speed test. Maximum SPL differences of other microphones are tabulated in Table 4.5.

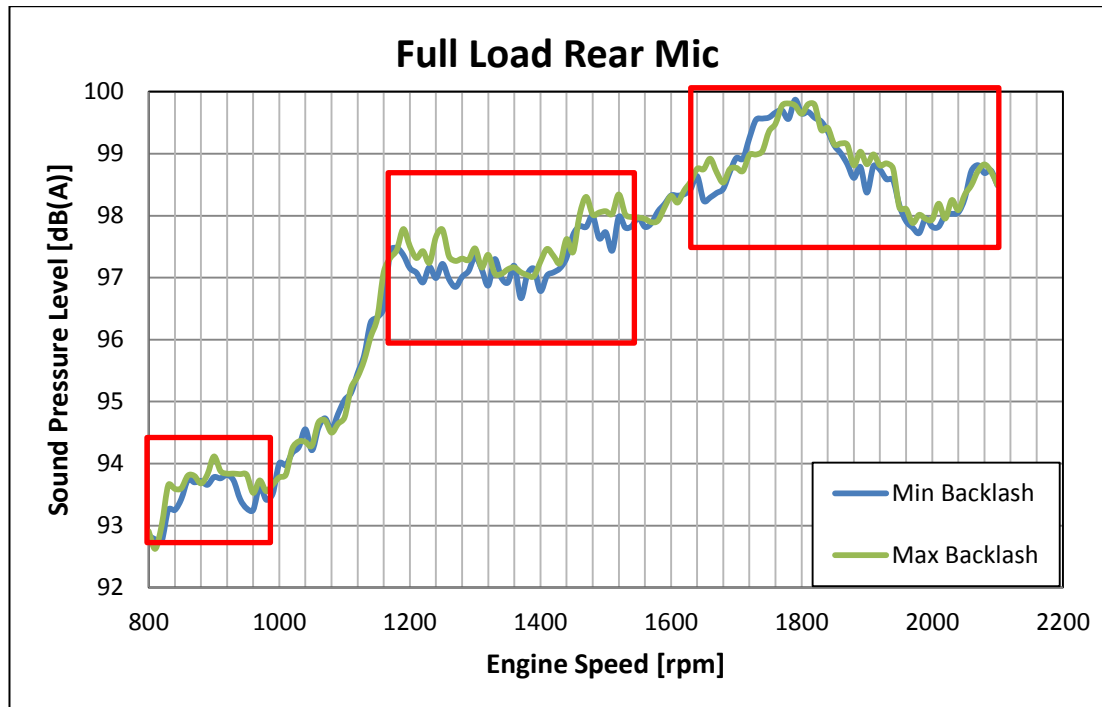


**Figure 4.19 :** Oilpump backlash iteration comparison at engine rear microphone.

Referring to Figure 4.19, it is seen that the differences between SPL are more obvious around certain ranges of engine speeds. The results from rear mic indicates that using minimum backlash yields slightly lower sound pressure level between 800 rpm – 1000 rpm, 1200 rpm – 1500 rpm and 1700 rpm – 2100 rpm intervals.

**Table 4.5 :** Full load speed sweep sound pressure level of backlash iterations.

SPL Difference dB(A)	4 Mic	Rear	Left	Front	Right	Top
<b>Maximum Difference</b>	0.49	0.67	0.76	0.72	0.69	0.60
<b>Minimum Difference</b>	-0.29	-0.56	-0.61	-0.34	-0.54	-0.38

As a summary, it can be said that the backlash effect has minor effect on SPL because SPL differences corresponding to minimum and maximum backlash values are less than 1 dB (A) for all mics. On the other hand, decreasing backlash between oil pump gears can lead to increase of backlash between oilpump idler gear and crankshaft gear. That’s probably the reason why changing backlash between oil pump gears only in geartrain has minor effect on engine overall noise level.

#### 4.1.4 Fuel pump phasing

Fuel injection pump phasing is essentially important for minimising the cylinder-to-cylinder pressure variation and fuel quantity variation. In addition, geartrain impact noise can be reduced by fuel pump phasing which has significant effect on geartrain dynamics. However, fuel injection pump phasing process may result in both beneficial and adverse effects on geartrain impact noise due to the importance of timing between “generated torque on crankshaft via combustion process” and the “required torque by fuel injection pump”, both of which play important role on speed fluctuations in geartrain system. Considering geartrain rattle noise, optimisation of fuel pump phasing is carried out during the engine development phase. Although the fuel injection system has indirect effects on impact, geartrain impact noise can be significantly reduced by choosing best fuel pump phasing angle.

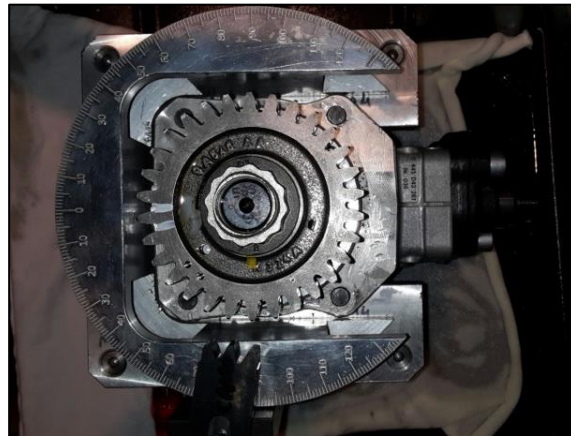


**Figure 4.20 :** Fuel pump phasing tool.

Fuel pump phasing is achieved by changing the assembly position of the fuel pump with respect to the engine. New phasing angle can be determined by turning the fuel pump gear in anti clockwise or clockwise by the help of phasing tool shown in Figure 4.20.

A. Rust gave brief information about the fuel injection phasing effect on geartrain impact noise and he indicated that the excitation of gear rattle noise in a timing drive depends on the backlash and the speed fluctuation at each gear mesh. The speed fluctuation at a gear mesh is the result of the superposition of all speed and torque fluctuations of all gear train members. For this superposition, the phase of synchronous contributions (like the torque fluctuation of the fuel pump) decides whether the speed fluctuation amplitudes are summed up or are partly cancelled.

Lowest gear rattle noise is obtained, if the optimum phase setting is achieved, yielding maximum unbalanced torque cancellation. This optimum phase setting can be determined either by tests or by a simulation of the gear train dynamics. In most cases, the ratio between pump speed and crankshaft speed is 0.5. If the ratio would be any number, then the resulting superposition of speed fluctuation amplitudes would vary in time between maximum summing-up (high rattle noise) and maximum cancellation (low rattle noise) [50].

In our 12.7 liter engine, the drive ratio between pump speed and crankshaft is 1.5 and fuel pump has two plunger. In this study, nine different phasing angles in anti clockwise starting from 0 (baseline) degree to 96 degrees with 12 degrees step were tried in order to assess the effect of fuel pump phasing on geartrain rattle noise. Actually, 12 degrees case corresponds to one tooth since the fuel pump gear has thirty teeth. By dividing  $360^\circ$  to 30 teeth, 12 degrees can be easily obtained for one tooth. Phasing tests are carried out under full load, no load and idle situation in engine dyno. Four mic average and rear mic sound pressure level for nine different phasing angles are revealed in Figure 4.21 and 4.22. Test result show that 12 degree phasing angle is determined as the best case and 72 degree is determined as the worst case under full load speed sweep based on 4 mic average and all mic result. Four mic average and rear mic result is shown in Figure 4.21 and Figure 4.22.

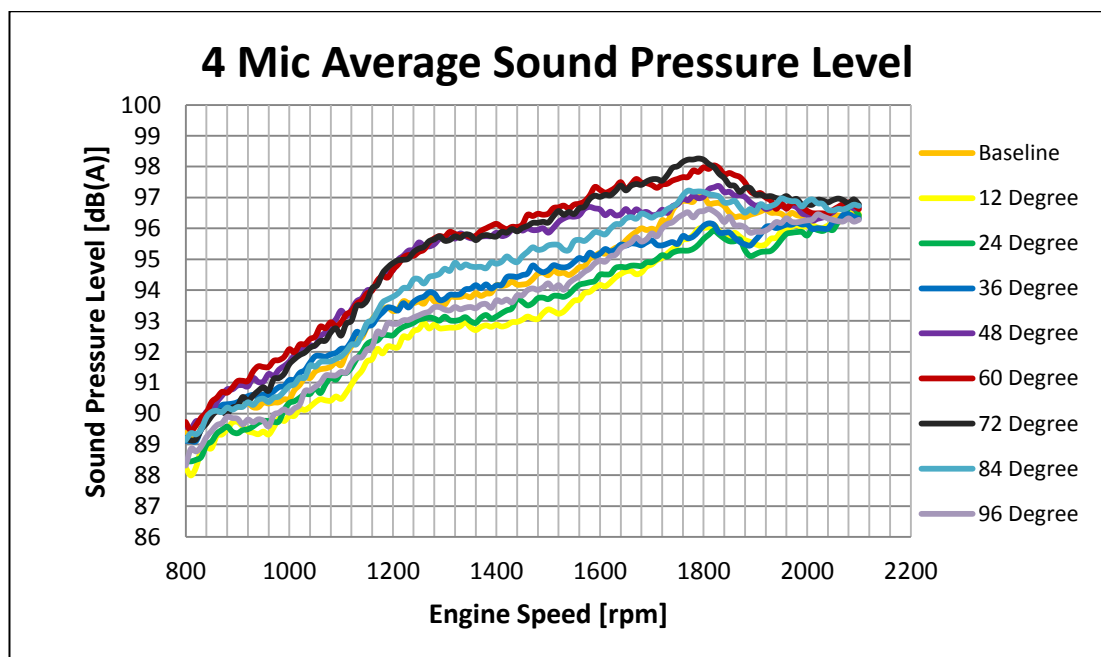


**Figure 4.21 :** Full load test 4 microphone average sound pressure level of phasing angles.

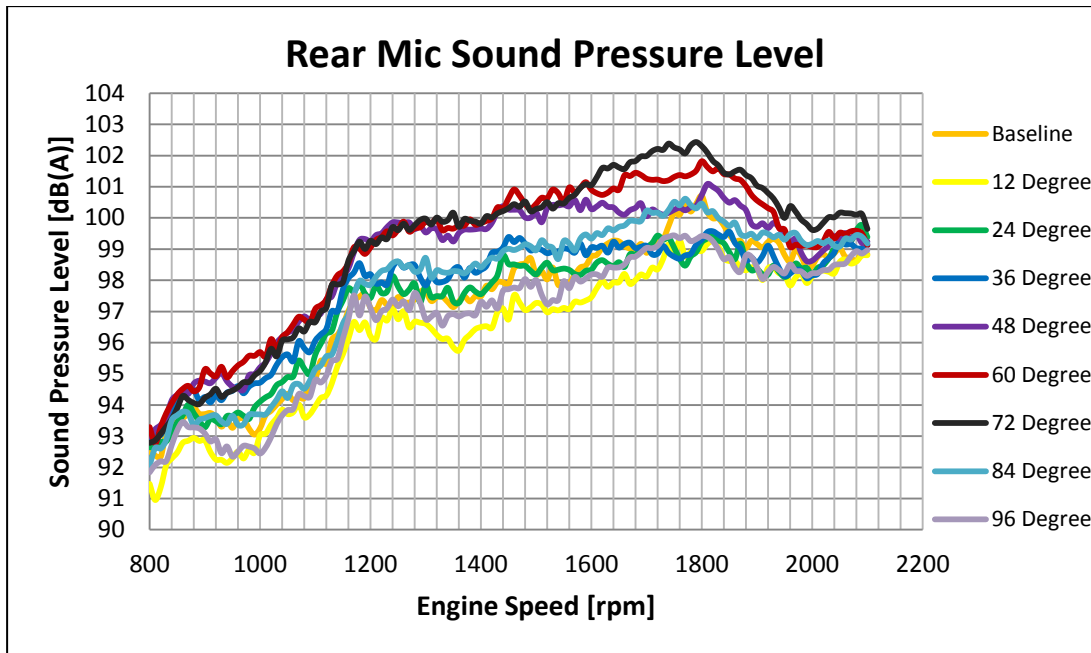


**Figure 4.22 :** Full load test rear microphone sound pressure level of phasing angles.

Four mic average sound pressure level difference between the best case (12 degree) and the worst case (72 degree) nearly reaches up to 3.3 decibel in full load speed sweep test. Moreover, rear mic SPL difference between the best and the worst cases reaches up to 4.3 decibel in full load speed sweep test. Furthermore, sound pressure level difference between the worst and the best case is reaching up to 3.5 decibel for the left mic, 4.5 decibel for the right mic, 2.8 decibel for the front mic and 3 decibel for the top mic based on full load speed sweep test. All mics results prove that the largest change of sound pressure level occurs in engine rear side that means fuel pump phasing has major effect on geartrain noise. Additionally, significant SPL differences are observed in engine rear mic, left mic and right mic results.

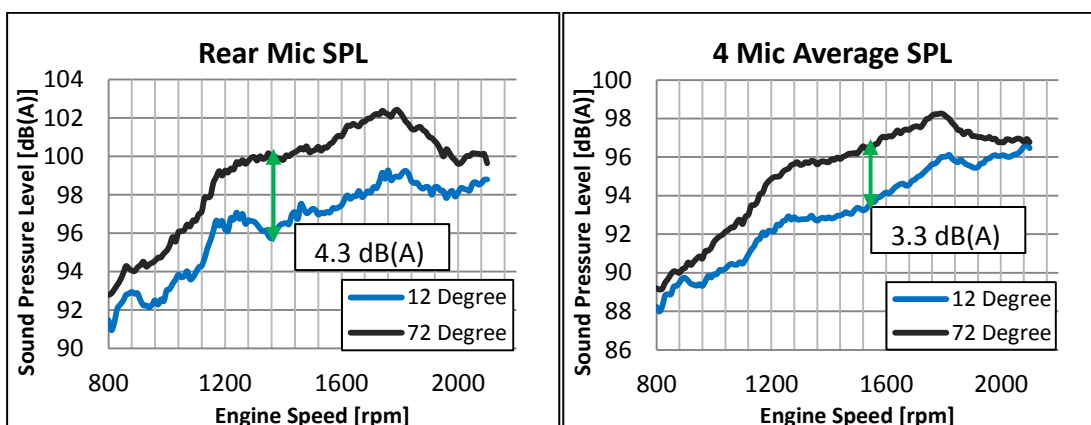


**Figure 4.23 :** Fuel pump phasing noise contribution on rear mic and four mic average.

Common rail pressure and engine torque level are other important parameters for fuel pump phasing test because pump phasing should not affect rail pressure or engine torque level. In other words, these two parameters should not change. Considering this case, rail pressure and engine torque level were measured and they are presented in Figure 4.24 and Figure 4.25. It is proven that no change is observed for common rail pressure and engine torque level with respect to fuel pump phasing angle.

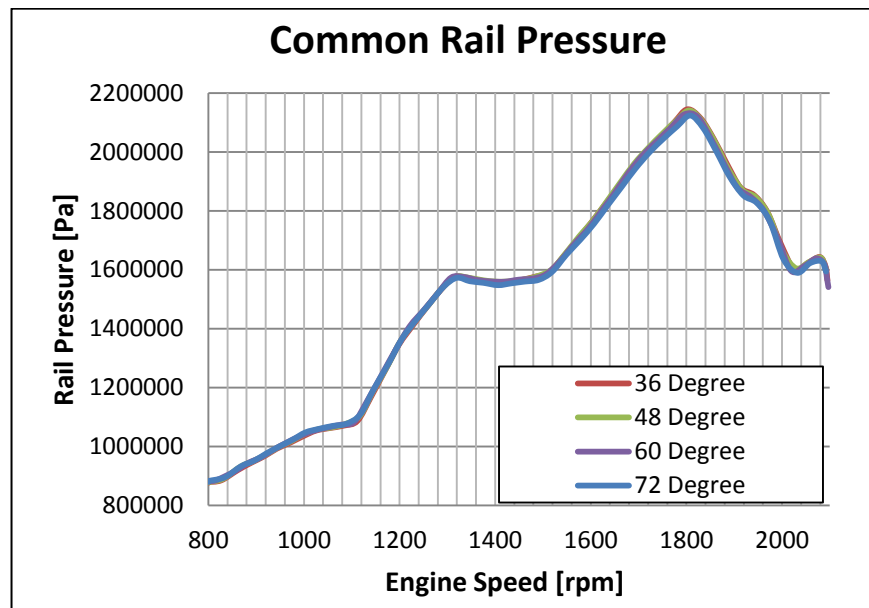


**Figure 4.24 :** Engine rail pressure for different phasing angles.

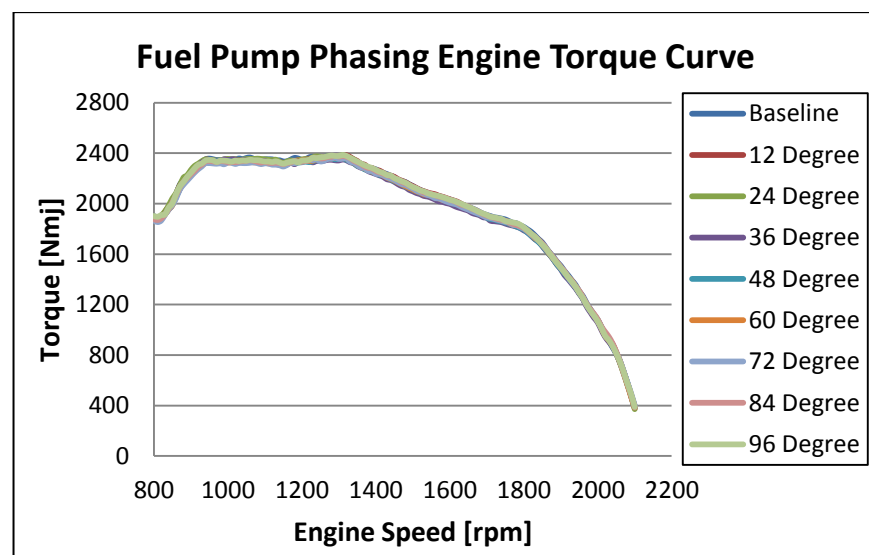


**Figure 4.25 :** Engine torque level for different phasing angles.

Rail pressure was only measured from 36 degrees to 72 degrees. However, engine torque level was measured for all nine phasing angles. No significant rail pressure

and torque level difference are observed, as seen in Figure 4.24 and Figure 4.25. These results also prove that sound pressure level differences between different phasing angles are due to the geartrain impacts.

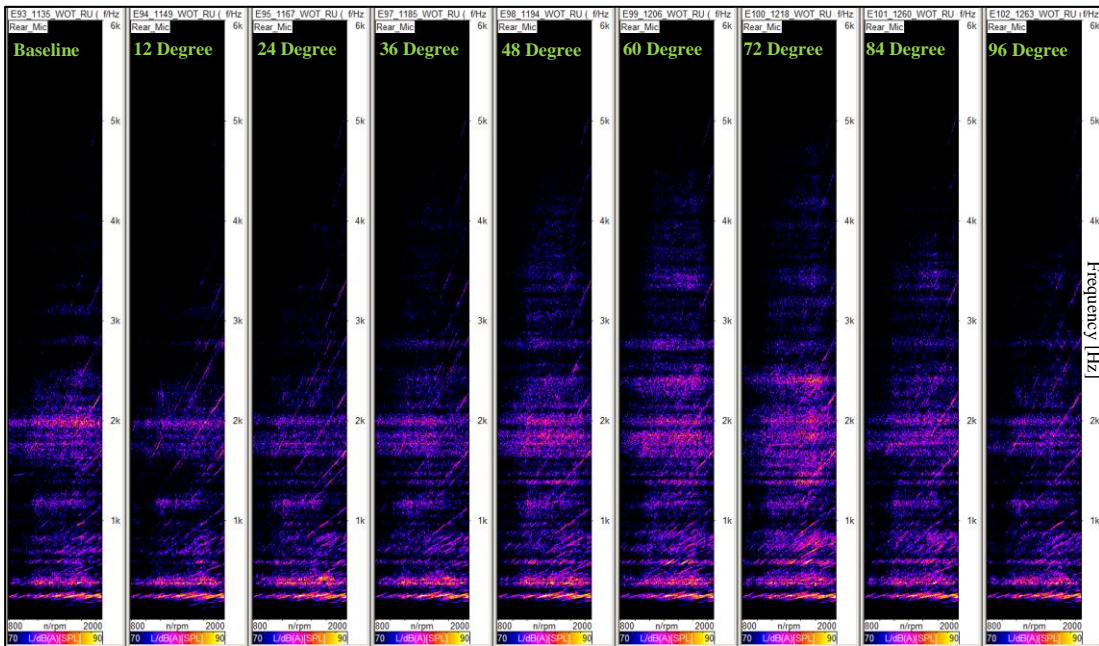


**Figure 4.26 :** Fuel pump phasing full load speed sweep test FFT vs rpm campbell diagram of engine rear microphone.

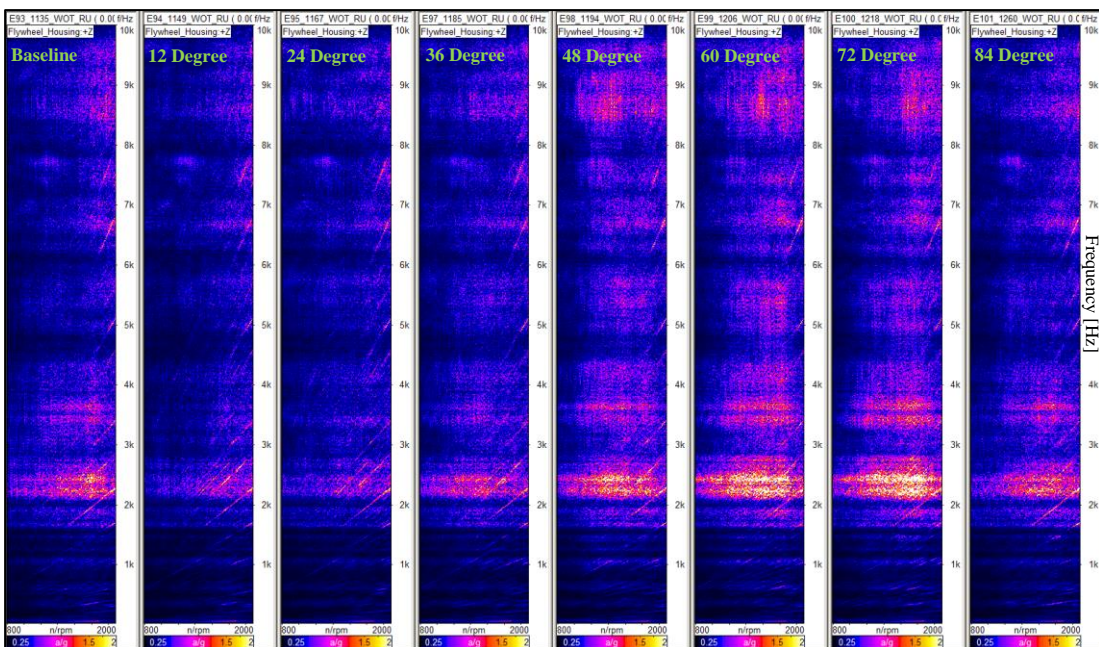


**Figure 4.27 :** Fuel pump phasing full load speed sweep test FFT vs rpm campbell diagram of flywheel housing accelerometer.

Full load speed sweep tests show that vibration levels of geartrain housing and flywheel housing change as the fuel pump phasing angle is changes and this means

fuel pump phasing has direct effect on geartrain noise. Also, results show that phasing have significant effect on resonance frequencies in full load speed sweep test according to microphone and accelerometer measurements. As seen in Figure 4.26 and 4.27, phasing effect on resonance frequencies is also seen at rear microphone and flywheel housing accelerometer. Geartrain impacts are also observed at higher frequencies from 1 kHz to 10 kHz. Obviously, fuel pump phasing provides improvements at higher frequencies in a wide frequency range.

There is less SPL difference in hot idle tests compared to speed sweep tests. Hot idle SPL results are shown in Figure 4.28 for rear microphone and four microphone average. Baseline is determined as the best case for engine rear microphone SPL and 60 degree phasing angle is determined as the best case based on four mic average using idle radiated noise measurements. On the other hand, 24 degree phasing angle is determined to be the worst case using either engine rear microphone or four-microphone average. Sound pressure level difference between the best and the worst cases reaches up to 1.4 decibel when rear mic data are used. 0.5 decibel difference is obtained when four mic average is used, that is not a remarkable SPL difference. Although baseline is the best case for hot idle radiated noise, 12 degree phasing angle is determined as best phasing angle for full load test.

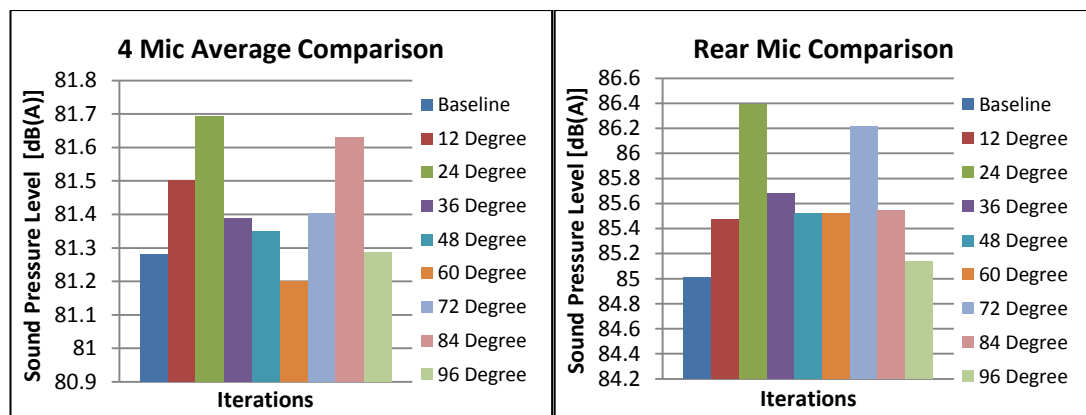


**Figure 4.28 :** Fuel pump phasing idle SPL of rear mic and four mic average.

In conclusion, fuel pump phasing has major effect on geartrain impact noise when the engine is running at full load. Moreover, the effects of fuel pump phasing are seen on both acoustic and vibration measurements. Broadband noise characteristic of impact noise can be detected in acoustic and vibration campbell diagrams of different phasing angles.

### 4.1.5 Torsional vibration measurement of crankshaft

Crankshaft torsional vibration is another significant factor on gear impacts. In this experimental study, measurements were made under full load condition from torsional vibration damper (TVD) which is located at one end of the engine. Torsional vibration measurement is conducted at rotation axis of the crankshaft. TVD is shown in Figure 4.29.



**Figure 4.29 :** Torsional vibration damper of 12.7 liter engine.

Torsional vibration measurements for full load speed sweep test presented in Figure 4.30 show that third engine order component dominates the torsional vibrations. Additionally, it is known that six times firing occurs during combustion cycle of a six cylinder engine within two revolutions of the crankshaft. This is the reason why the third engine order component is very significant in the vibration spectrum. Third engine order is also known as combustion order of 6 six cylinder engines.

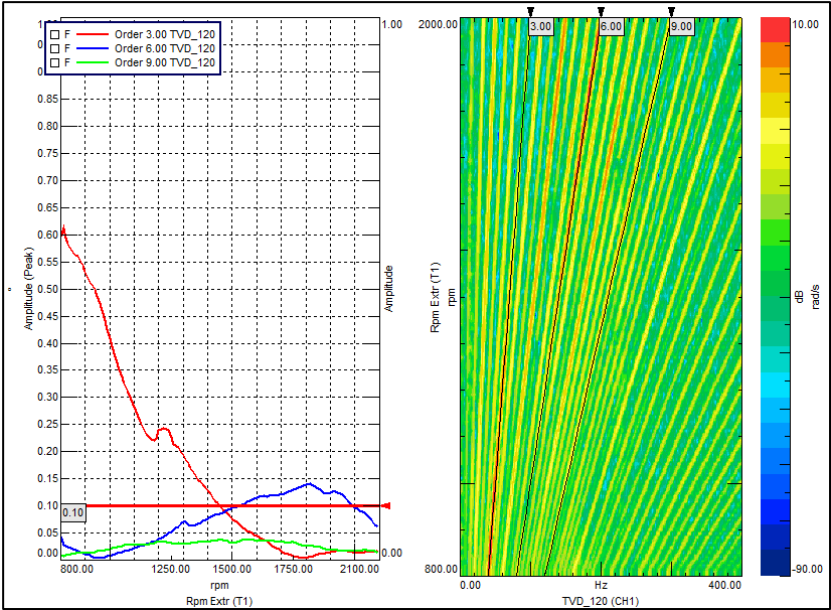


**Figure 4.30 :** Torsional vibration measurements of 12.7 liter HD engine.

#### **4.1.6 Cylinder pressure variation effect on torsional vibrations**

Cylinder pressures in internal combustion engines change continuously during the combustion cycle. This is the main reason for torsional vibrations of crankshafts and drive systems. Moreover, there are some other factors such as cylinder peak pressure variations between cylinders in internal combustion engines. It is also in the literature that cylinder to cylinder peak pressure variation leads to torsional vibrations in internal combustion engines [51, 52].

It has been known that fuel injection pump cannot supply the same injection pressure and fuel quantity to each cylinder, resulting in pressure variations between cylinders. This also amplifies torsional vibrations of crankshafts. Therefore, it is expected that geartrain impacts are affected from cylinder to cylinder pressure variations. Indeed, product development engineers try to minimize these variations in order to minimize torsional vibration related problems. Fuel injection pump phasing has effects on both cylinder pressure variation and injected fuel quantity as well its effect on geartrain dynamics. Fuel injection pump phasing is tried in different phasing angles in order to minimize cylinder pressure variations. Moreover, injected fuel quantity directly affects cylinder pressure. That's why optimizing fuel injection pump phasing plays very significant role on cylinder pressure variations.

In this section, measurements and assessments of cylinder-to-cylinder pressure variations are presented in idle condition for detailed analysis of idle rattle noise. Cylinder pressure measurements were taken from only four cylinders which are cylinder numbers 1, 2, 5 and 6. Cylinder pressure measurement from other two cylinders could not be made due to the lack of adequate cylinder pressure sensors. As an additional information, cylinder number ordering (1-6) starts from engine front side (accessory drive) to engine rear side (timing drive). Cylinder pressures of 12.7 liter engine were measured in engine dynamometer by PFP sensors which can operate at elevated temperatures compatible with cylinder temperatures. In Figure 4.31, cylinder pressure graph are seen with their peak values. Obviously, cylinder peak pressures are not the same for all the cylinders (cylinders 1, 2, 5, 6). Percentages of cylinder pressure variations were calculated with respect to average cylinder pressure described below.

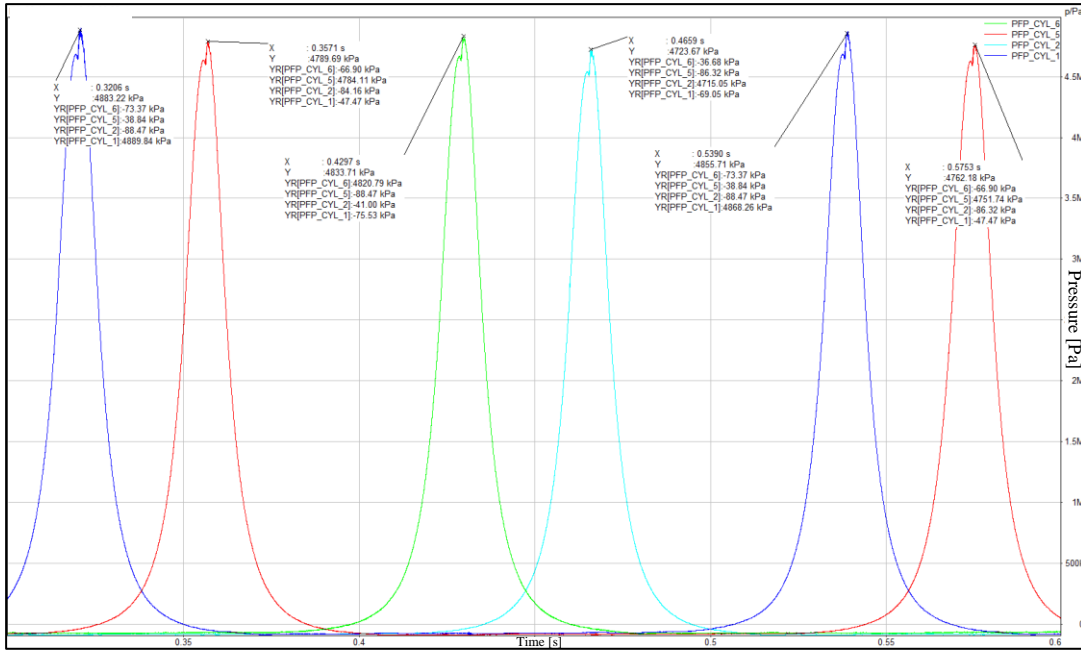


**Figure 4.31** : Cylinder pressures of cylinders 1, 2, 5, 6.

Average cylinder pressure is calculated by using cylinder peak pressures from idle test, measurement period being thirty seconds. Average pressure is expressed as;

$$Average\ Pressure = \left[ \sum_{i=1}^N Pressure(i) \right] / N \quad (4.3)$$

where N is the number of cylinders. After the calculation of average pressure by using equation 4.3, cylinder pressure variation is calculated as;

$$Pressure\ Variation(i) = \frac{|Average\ Pressure - Pressure(i)|}{Average\ Pressure} \quad (4.4)$$

Cylinder to cylinder peak pressure variations for cylinders 1, 2, 5, 6 are listed in Table 4.6 where average peak pressure is calculated as 4735442 Pa. According to cylinder pressure measurements from cylinders 1, 2, 5, 6, maximum cylinder to cylinder variation is calculated nearly as % 2. Crankshaft torsional vibration can be reduced by minimising this pressure variation between cylinders.

**Table 4.6** : Cylinder to cylinder peak pressure variation

Cylinder Number	Cylinder 6	Cylinder 5	Cylinder 2	Cylinder 1
Max Cylinder Pressure [Pa]	4771684	4713135.5	4639337	4817611.5
Cylinder pressure variation %	0.77	0.47	2.03	1.74

## 4.2 Investigation of Housing Effect

As stated in reference [14 – 16] gear housings have significant effect on sound transmission of geartrain impact noise in engines. Housing effect is shown by frequency response function (FRF) measurements in section 4.2.1.

### 4.2.1 Housing FRF measurements

In this section, some details of the modal tests of three different flywheel housings, which are named as A, B and C, in free-free boundary condition are presented so as to demonstrate the housing transmission effect on geartrain impact noise. The so-called A, B and C flywheel housings differ from each other in their geometries and ribs. Different designs of flywheel housing are shown in Figure 4.32.

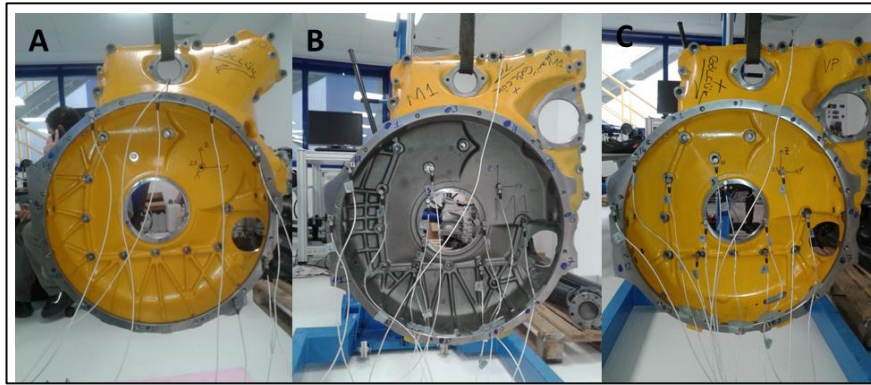


**Figure 4.32 :** Different flywheel housing designs.

24 accelerometer locations and 6 hammer locations were determined on the flywheel housing for impact test. The same accelerometer and hammer locations were marked for all A, B, C flywheel housings. Red points are determined as accelerometer locations and blue points are determined as hammer locations in Figure 4.33.

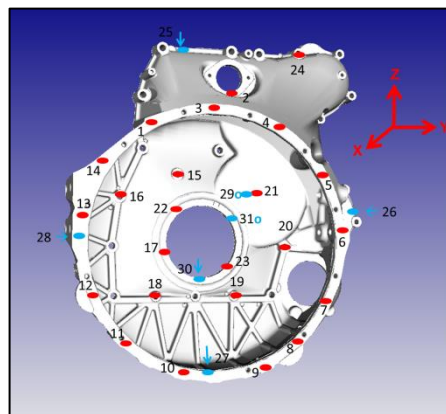


**Figure 4.33 :** Flywheel housing FRF measurement accelerometer locations.

All collected FRF were summed in X, Y, Z directions separately. In addition, structural behaviour of flywheel housing were determined based on 24 accelerometer locations and 6 force locations. On the other hand, FRF measurement could be done up to 5000 Hz due to the excitation limitation of the flywheel housings.

According to flywheel housing impact test results, it can be inferred that, within 1.5 kHz to 3.0 kHz, flywheel housing B and C have better structural behavior than flywheel housing A in the sense that the levels of the sums of FRFs of B and C are lower than that of flywheel housing A. In Figure 4.34, it is seen that there is a strong peak around 1740 Hz for the flywheel housing A. It has the highest amplitude compared to other peaks. Moreover, critical peak between 1621 Hz and 1748 Hz had been detected from flywheel side before by acoustic camera measurement. Thus, this peak within this frequency range is also detected from FRF measurements of the housing. Only Y direction FRF sum of flywheel housings are shown in Figure 4.34.

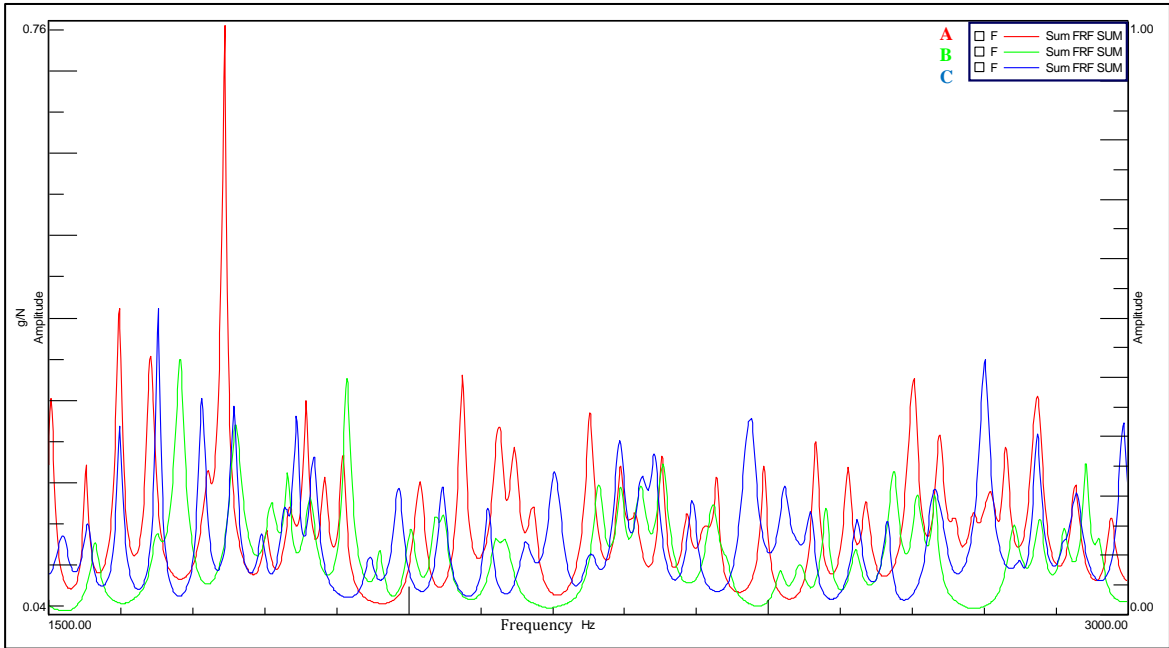


**Figure 4.34 :** Flywheel housings in Y direction: FRF sum.

As a brief summary, tests are performed and some results are presented here so as to determine if there is any correlation between the housing natural frequencies and the frequencies at which peak noise levels are detected by acoustic camera. There seems to be such a correlation between 1621-1748 Hz for flywheel housing A. Furthermore, it is found that the dynamic behavior of individual flywheel housings can be significantly different from each other.

### 4.3 Vehicle Exterior Noise Tests

Instead of using engine dynamometer, NVH measurements are also made on vehicles. However, apart from pass-by noise tests, there is not a standart engine NVH test procedure for vehicles. Error states of engine noise can be assessed on vehicles after finishing the engine dynamometer tests. In this section, based on vehicle test results, the effects of gear loading, idler gear backlash and idle speed on geartrain impact noise are discussed. NVH measurement on vehicles were done by using accelerometers and microphones, as in the engine dynamometer tests. Engine rear, left and right sides were used as microphone locations and geartrain housing, flywheel housing, engine head and valve cover were used as accelerometer locations. The same microphone and accelerometer locations were used for gear loading and idle speed tests. However, in backlash test, only three microphones, locations of which are not necessarily the same with those in other vehicle test, and no accelerometer were used. The backlash tests were performed at 550 rpm idle speed.



**Figure 4.35 :** Microphones locations for gear loading and idle speed changing test.

Accelerometers locations in vehicle tests were the same as those during engine dynamometer tests. In Figure 4.35 and Figure 4.36 microphone locations were shown for vehicle tests.



**Figure 4.36 :** Microphones locations for adjustable idler gear backlash test.

#### 4.3.1 Gear loading effect

Loading gears may cause both positive and negative effects on geartrain noise depending on torque load characteristics. The main principle is that the transmitted

torque through to a geartrain is reduced by reverse (demanding) torque loading via gears, hence impact forces between gears can be reduced by gear loading. It is expected that if the net torque on geartrain is decreased, impact energy between gears will be reduced. In other words, the decrease of impact force between gears leads to reduction of gear impact noise. On the other hand, gear meshing noise will increase due to the higher contact forces between gears. Consequently, gear loading has a reverse effect between gear meshing noise and impact noise. This effect can be explained as a trade-off curve, which implies reverse effect. Another important point for geartrain impact noise reduction is that, whenever possible, constant load is desirable. It is known that higher levels of torque fluctuations in the system encourage geartrain impacts, leading to higher levels of geartrain impact noise.

In this experiment, gear loading is achieved by loading power assisted pump gear, which is located in the right side of the geartrain. Power assisted steering (PAS) pump operates under constant loading torque hence it is expected to reduce geartrain impacts. First of all, steering wheel of the vehicle was rotated manually in order to load the PAS pump gear with nominally constant torque. It has been proven by tests that loading a gear with constant torque has significant effect on geartrain impact noise. Moreover, experimental results show that loading PAS pump gear increases gear meshing noise although gear impact noise decreases. It is the main point of this experiment. On the other hand, a study was done for air compressor gear loading which worked under alternating torque. It shows that alternating torque on the gear leads to increase of geartrain impact noise.

PAS pump is located on the right side of the engine, hence higher noise contribution from PAS pump is expected from the right hand side of the engine. Therefore, waterfall diagrams are obtained using the engine right mic and results are presented in figures 4.37 and 4.38. Frequency scale is up to 6 kHz in Figure 4.37 and it is up to 1 kHz in Figure 4.38. Two different scales are chosen in order to show the reverse noise effect of gear loading. In Figure 4.37, it is clearly seen that the amplitudes of broadband noise levels decrease when the PAS pump is loaded, i.e., when the steering wheel is rotated. As the steering wheel is operated in a cyclic manner (steering wheel is rotated for a few seconds and then stopped and this process is repeated again), gear impacts also occur in a cyclic manner. This is identified and labeled as "rattle islands" in Figure 4.37. The main reason for these impacts (or rattle

islands) is that PAS pump gear is not loaded when the steering wheel is stopped to rotate. As a result, impact noise decreases when the PAS gear is loaded and increases when it is unloaded.

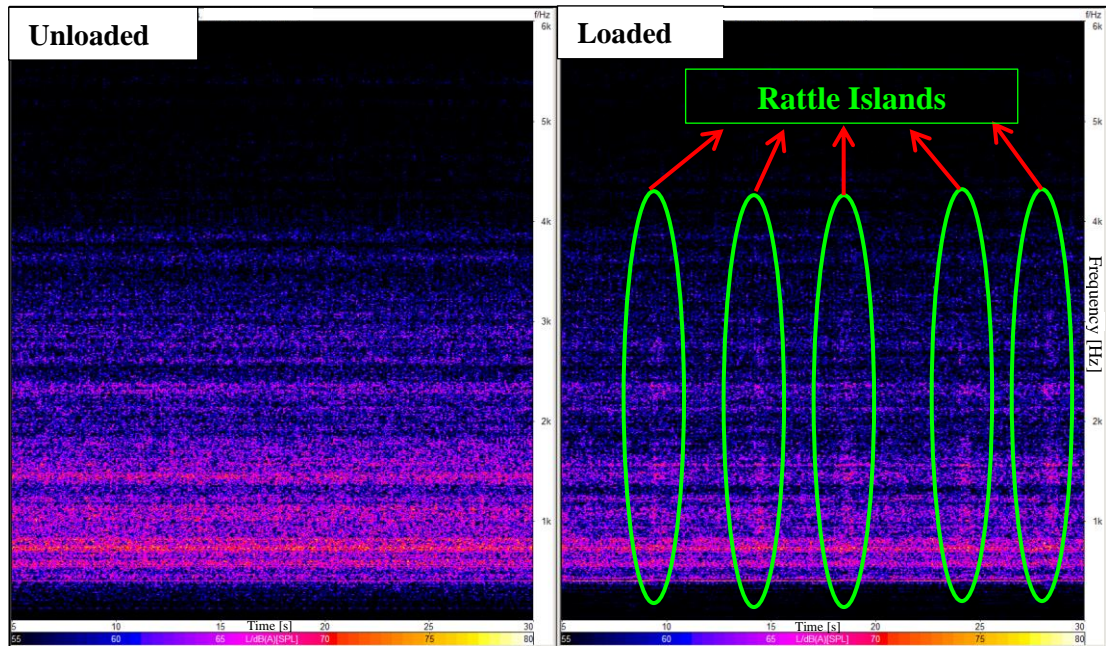


**Figure 4.37** : Right mic waterfall FFT diagram of gear loading (impact noise).

By the way, the meshing frequency of the pas pump gear is 412.5 Hz. It is seen clearly in the Figure 4.38 that PAS pump gear loading increases the gear meshing noise of PAS pump gear at 412.5 Hz meshing frequency.

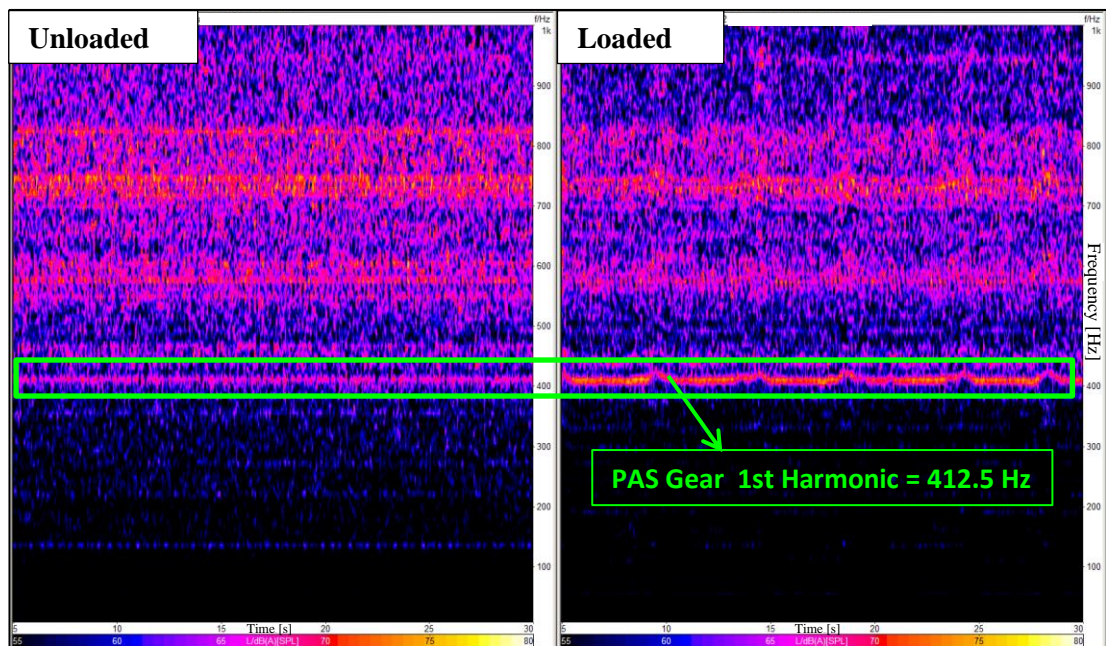


**Figure 4.38** : Right mic waterfall FFT diagram of gear loading (meshing noise).

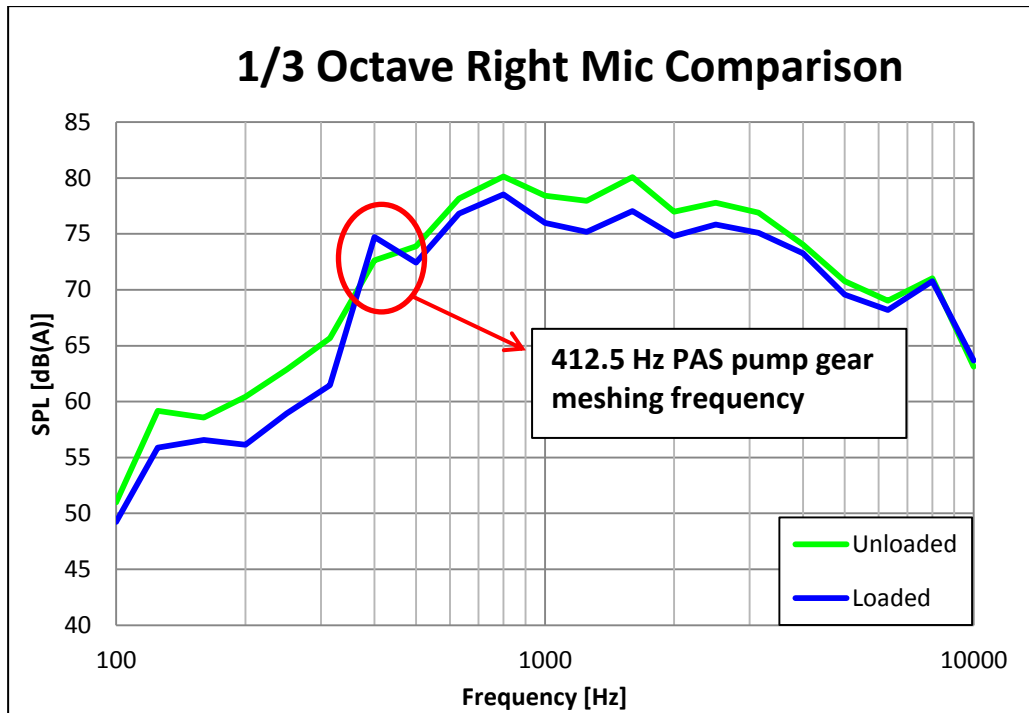


**Figure 4.39 :** 1/3 octave comparison of PAS pump gear loading.

The 3rd octave plot in Figure 4.39 compared noise levels when PAS pump is loaded and unloaded. It is seen that, relative to the unloaded case, PAS pump loading reduces the noise level significantly. However, this plot also shows that gear loading leads to increase noise amplitude at PAS pump gear meshing frequency which is calculated as 412.5 Hz for engine idle speed (550 rpm). Table 4.7 provides information about PAS pump gear loading effect on sound pressure level based on three microphone measurements. It is seen that sound pressure level differences are very significant between unloaded and loaded cases. Despite the increase of gear meshing noise, the maximum SPL difference is calculated as nearly 1.79 dB(A) at the right hand side microphone of the vehicle.

**Table 4.7 :** Sound pressure level comparison of gear loading.

	Rear Mic dB(A)	Left Mic dB(A)	Right Mic dB(A)
<b>Unloaded</b>	93.16	89.18	88.27
<b>Loaded</b>	91.81	87.96	86.49
<b>Difference</b>	1.35	1.21	1.79

As a summary, the reverse effects between gear impact and meshing noise are shown with waterfall diagrams. It is clearly seen from waterfall diagrams that gear meshing noise has a narrowband tonal noise characteristic and gear impact noise has a broadband noise characteristic.

### 4.3.2 Adjustable idler backlash changing effect

Adjustable idler gear, which is a movable gear, is located between camshaft gear and camshaft idler gear in the geartrain. Adjustable idler gear has no shaft connection as its function is just power transmission from camshaft idler to camshaft gear in the geartrain system. In Figure 4.40, adjustable idler with its connected gears are shown.

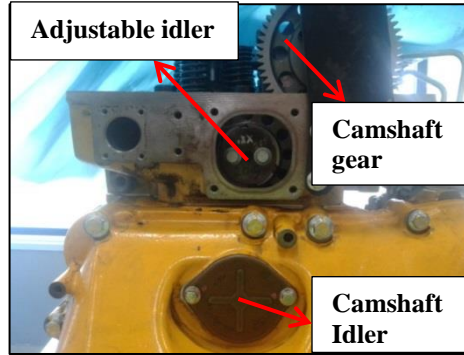


**Figure 4.40 :** Adjustable idler of 12.7 liter engine.

In this section, using three microphone positions (rear, left and right sides), backlash effect on sound pressure level of vehicle was investigated by changing the position of adjustable idler gear. Two different backlash values, named as maximum and minimum, were used in order to show backlash effect on gear impact noise. Minimum backlash value between camshaft gear and camshaft idler gear is measured as 100 microns and maximum backlash value between camshaft gear and camshaft idler gear is measured as 230 microns. In Table 4.8, sound pressure levels corresponding to the maximum and minimum backlash values at three microphone positions are listed. It is seen that there are significant sound pressure level differences between the sound pressure levels corresponding to the maximum and the minimum backlash values at the rear and the right microphones. However, sound pressure level at the left microphone position is almost unchanged. The highest sound pressure level difference is observed as 6.4 decibel at the rear microphone position of the vehicle. Rear microphone 1/3 octave comparisons and waterfall diagram are also shown in Figure 4.41 and 4.42, respectively.

**Table 4.8 :** Sound pressure level comparison of idler backlash effect.

	Rear Mic dB(A)	Left Mic dB(A)	Right Mic dB(A)
<b>Min Backlash</b>	88.15	90.67	88.24
<b>Max Backlash</b>	94.55	90.78	91.87
<b>Difference</b>	6.40	0.11	3.63

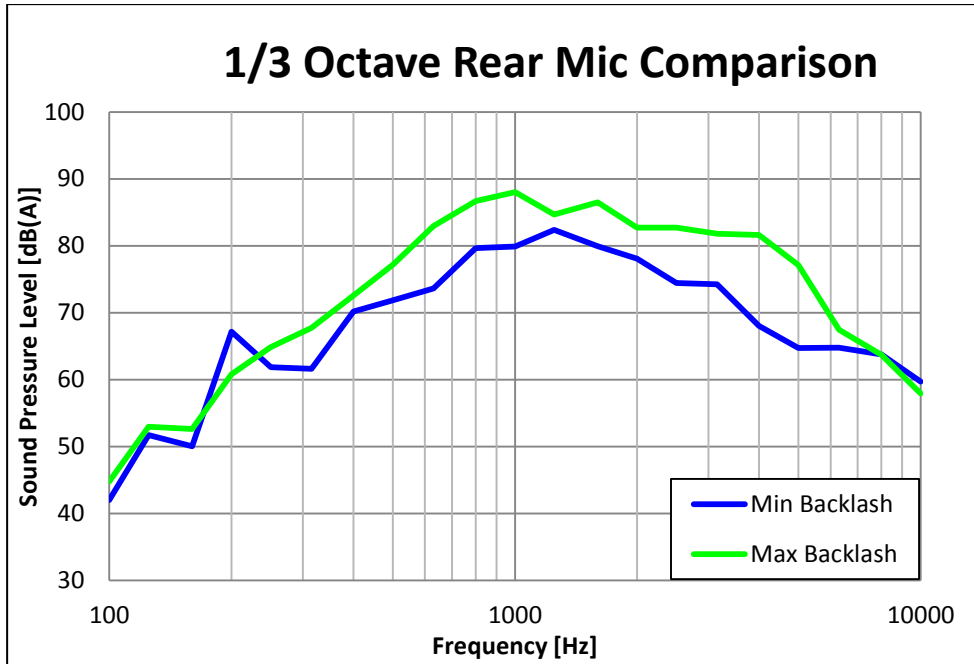


**Figure 4.41 :** 1/3 octave comparison of maximum and minimum idler backlash.

Results show that impact noise significantly increases when the backlash value between camshaft gear and camshaft idler gear increases. Actually, torque fluctuation of camshaft dominates impacts and it directly affects impacts between camshaft gear and camshaft idler gear. Therefore, a change in backlash value between these gears can significantly influence the gear impact noise.

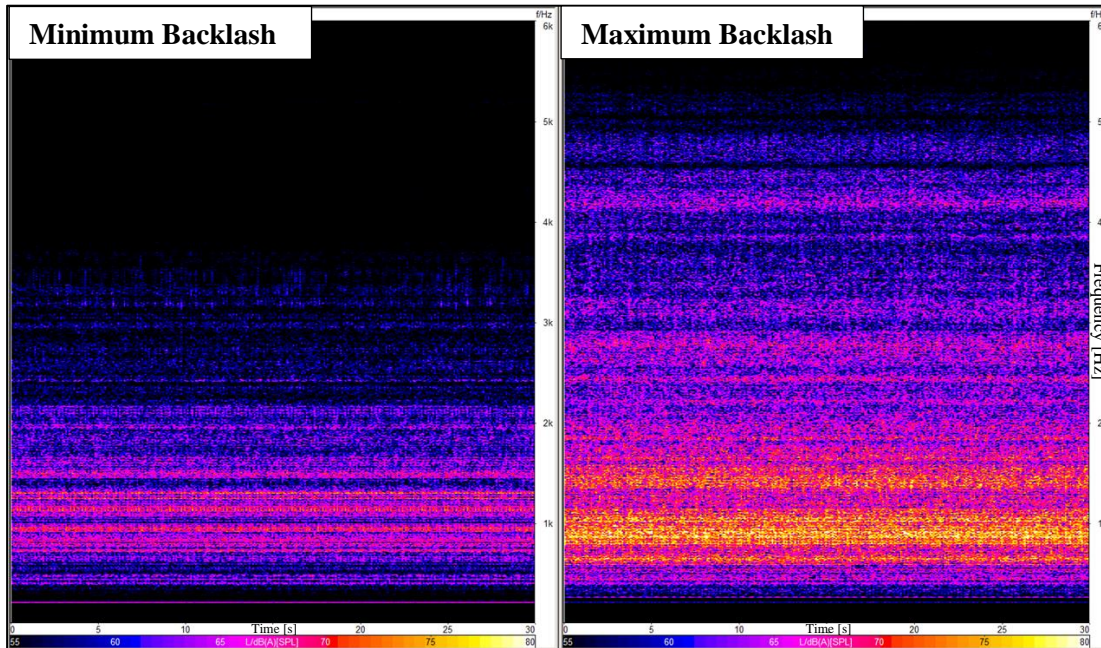


**Figure 4.42 :** Rear mic waterfall FFT diagram of idler backlash effect.

### 4.3.3 Effect of idle speed

Idle speed is an important design parameter for vehicles, which can cause resonance problems at low speeds and higher fuel consumption at higher speeds. Therefore, selection of idle speed is a design optimization problem for car manufacturers. In addition, engine firing frequency, which depends on engine speed, should be higher than the natural frequencies of the rigid body modes of the suspended engine over the mounts in order to prevent resonance risks. Idle speed has also significant effect on gear impacts. Changing idle speed can lead to higher resonance amplitudes of gear impacts. In this experiment, six different idle speeds, from 550 rpm to 800 rpm with 50-rpm increment, were tried on vehicle in order to determine impact noise signature. Waterfall FFT diagram of the rear microphone for different idle speeds are shown in Figure 4.43. It is clearly seen that gear impact noise frequencies do not change with the increase of idle speed. However, it is obvious that impact noise level increases with respect to engine idle speed. Also, resonance frequencies around 4400 Hz, 2500 Hz, 2200 Hz, 1500 Hz, 1200 Hz are seen in Figure 4.43. It is known from previous experiences that geartrain impact noise is observed at frequencies higher than 1000 Hz.

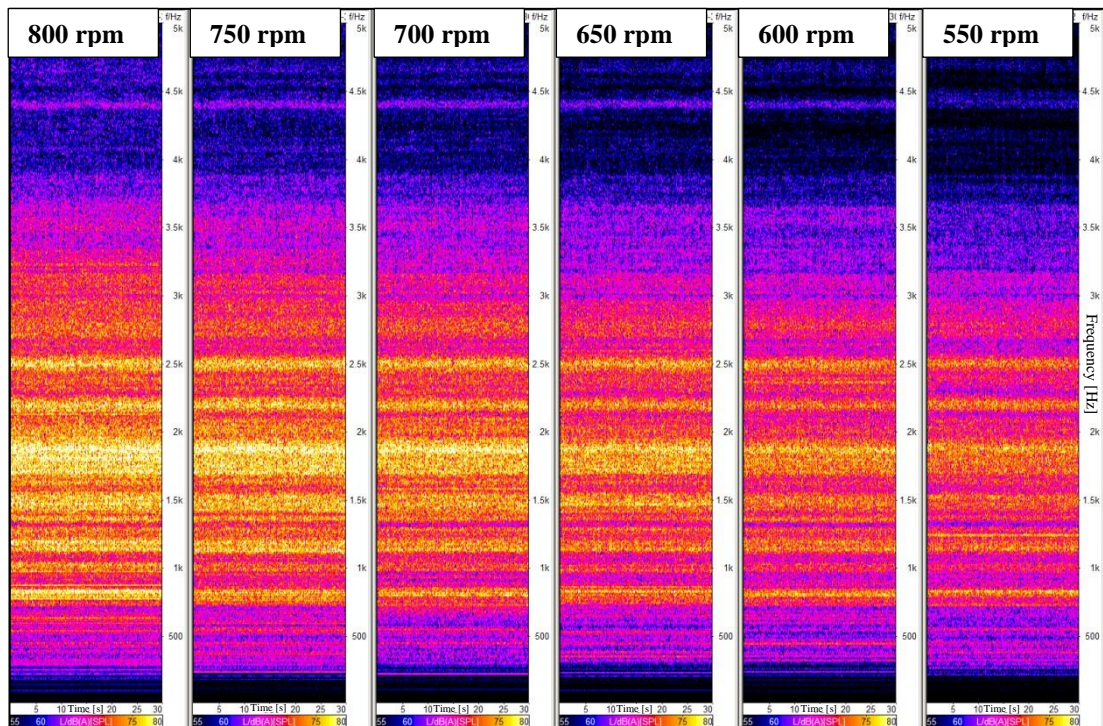


**Figure 4.43 :** Rear mic waterfall FFT diagram of idler backlash effect.

### 4.4 Advanced Signal Processing Applications

There are various methods that can be used to determine gear faults or source of gear noise. However, geartrain impact noise is not a classical gear noise problem due to the fact that firing (combustion) born impacts, which excite geartrain impact noise, play critical role on geartrain impact noise. Therefore, cyclic firing order is important in the analysis of geartrain impact noise. In this section, time domain signal analysis as well as envelope analysis, modulation frequency analysis and cepstrum analysis are shown in some details. All the theory about these analysis methods except modulation frequency analysis are introduced in the chapter 2, section 2.5. The effects of firing frequency effects on gear impact are discussed in this part.

Engine dynamometer hot idle data are used for advanced analyses. Engine rear microphone and flywheel housing accelerometer data are used for detail analyses. Instrumentation locations can be seen in chapter 4, section 4.4.1. As explained in section 4.1, idle speed of this engine is 550 rpm. For a six cylinder engine, firing order is “3”, hence the engine firing frequency is calculated as 27.5 Hz.

#### 4.4.1 Time domain signal analysis of hot idle data

Time domain analyses are important as they can provide various properties of signals including statistical properties, amplitude information, peakiness as well as some repetitions in signals. As can be seen in Figure 4.44, time domain microphone and accelerometer signals can easily reveal that the engine is operating with impacts.

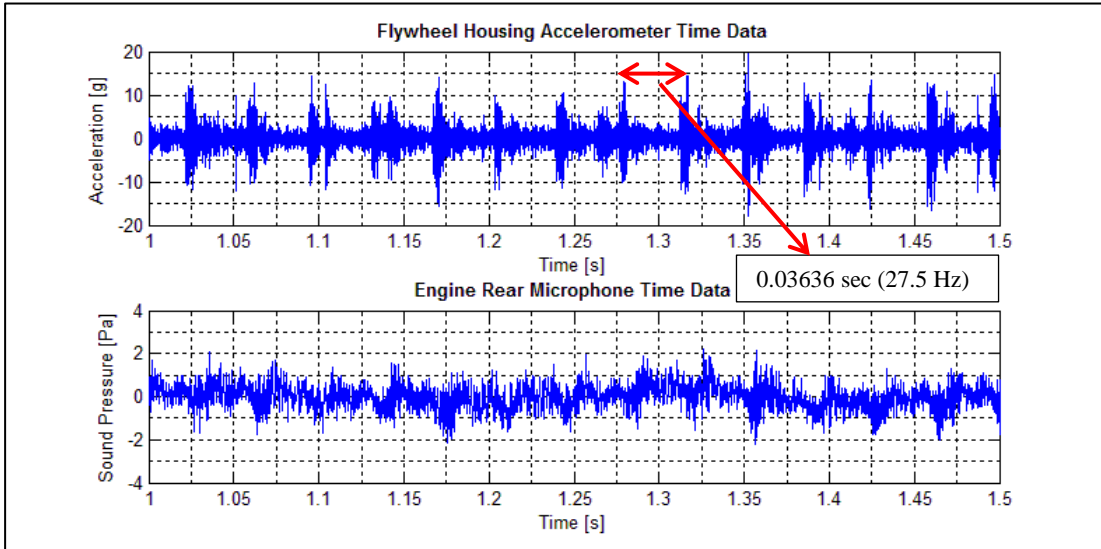


Figure 4.44 : Time domain signals of accelerometer and microphone data.

According to flywheel housing accelerometer data, the obvious impact repetition is calculated as 0.03636 seconds which refers to 27.5 Hz firing frequency. On the other hand, impacts are more clear in accelerometer data compared to that of microphone. Briefly, it is observed that impact repetition of firing frequency excites the system and creates higher frequency vibrations in engine and in its components. This impact repetition can be analyzed by using modulation analysis techniques such as envelope analysis and modulation frequency analysis.

#### 4.4.2 Envelope analysis of hot idle data

Envelope analysis is one of the modulation analysis methods, which is also referred to as amplitude modulation. In MATLAB program, envelope analysis code is written by using Hilbert Transform, original time domain signal and Fast Fourier Transform. First of all, an analytic signal is obtained by complex sum of Hilbert Transform and original time domain signal. Second, the envelope spectrum is obtained by using analytic signal via Fast Fourier Transform.

In Figure 4.45, envelope spectrum of accelerometer and microphone data are shown where firing frequency and its harmonics are clearly seen.

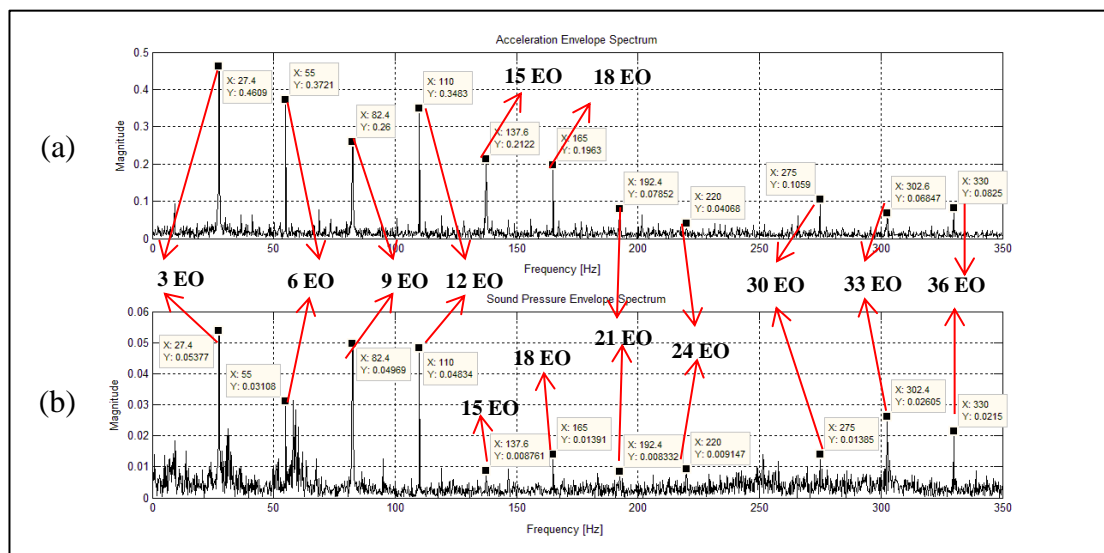


**Figure 4.45 :** Envelope spectra of accelerometer (a) and microphone (b) data.

According to envelope spectrum result, it is seen that firing order has higher harmonics. Especially, 3 EO, 6 EO, 9 EO, 12 EO, 15 EO and 18 EO are dominant.

From section 4.1.4, sound pressure level of the best and the worst phasing angle cases for engine rear microphone are selected where best case is baseline and worst

case is 24 degrees phasing angle. By the way, these two cases are compared by using their envelope spectrums and FFT spectrums. According to envelope spectrum results, seen in Figure 4.46, firing harmonics such as 3 EO, 6 EO, 9 EO, 12 EO, 15 EO, 18 EO and others are affected from phasing angle.

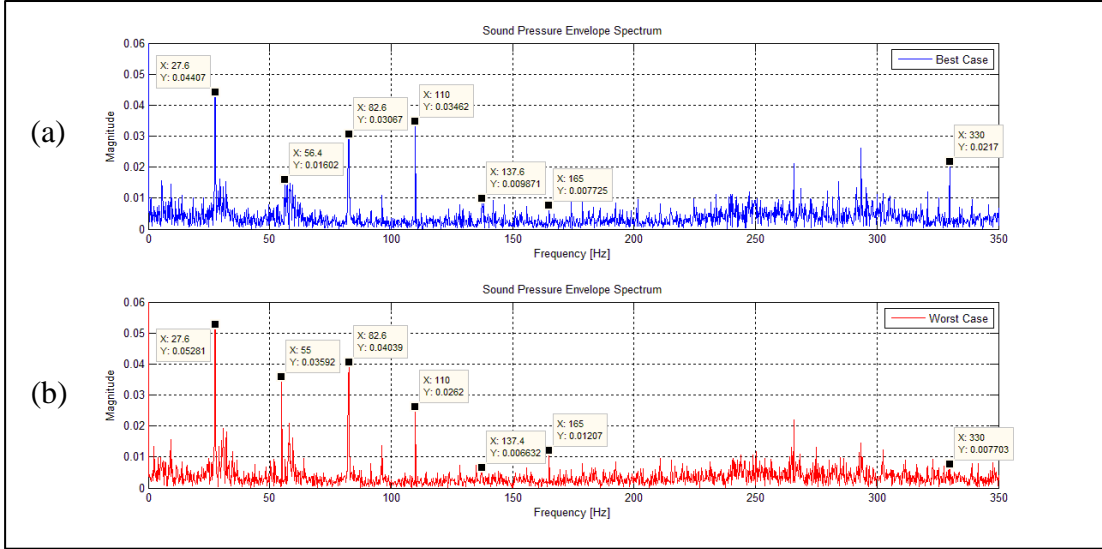


**Figure 4.46 :** Envelope spectrums of fuel pump phasing data: the best case (a) and the worst case (b).

FFT spectrums of fuel pump phasing data are presented in Figure 4.47. It is seen that the amplitudes of the worst case of phasing angle leads to higher amplitudes than those of the best case of phasing angle. It is seen that fuel pump phasing affects the amplitude spectrum.

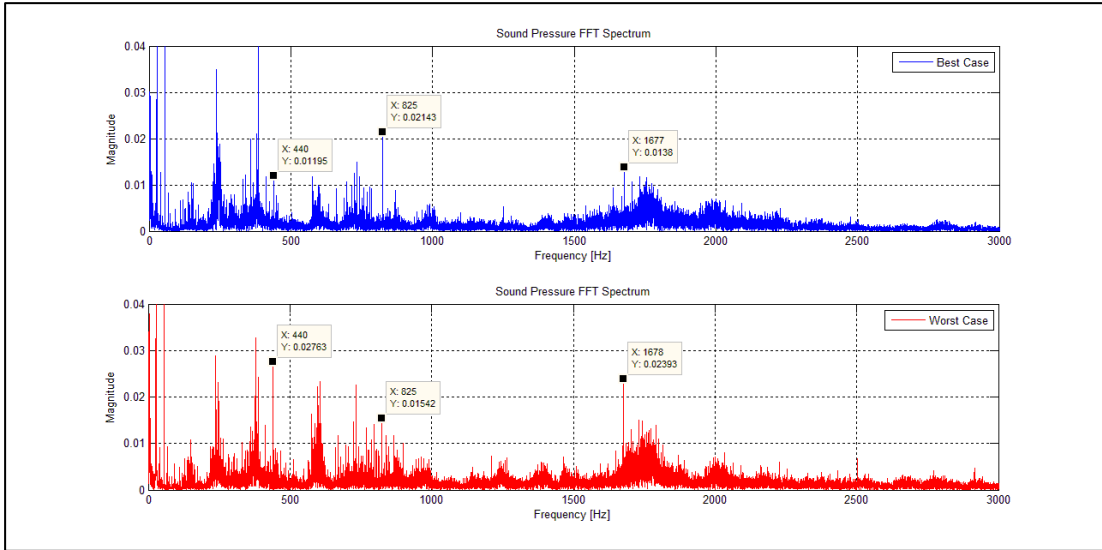


**Figure 4.47 :** FFT spectrums of fuel pump phasing data: the best case (a) and the worst case (b).

### 4.4.3 Modulation frequency analysis of hot idle data

Bodden et. al. [18] explains modulation frequency analysis on gear rattle in detail. Interested reader may refer to the background theory in their paper [18]. In this section, an application of Bodden et. al.'s analysis method on geartrain impact noise is presented. Their analysis program is called "ModFil" which is very useful for modulation frequency analysis as well as sound quality analysis. The analysis method proposed by Bodden et. al is useful for diesel knocking and gear rattle analyses. The main objective of this study in this section is to show the modulation frequency of gear impacts.

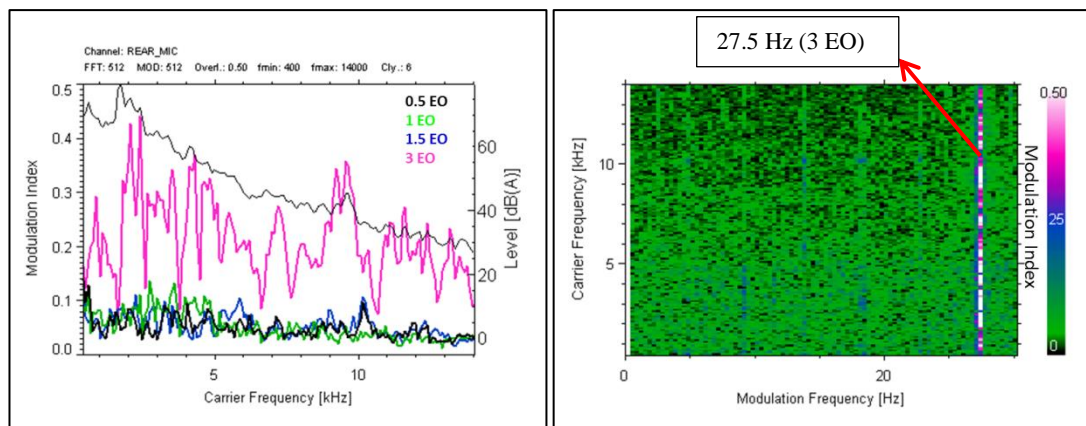


**Figure 4.48 :** Modulation frequency analysis of microphone data.

There are two important frequencies for modulation analysis: modulation frequency and carrier frequency. The main background philosophy of modulation analysis is that modulation frequency carries higher frequencies which are called as carrier frequencies. For an impact noise investigation, impact repetition refers to the modulation frequency and resonance frequencies due to the excitation represent carrier frequencies. Moreover, modulation index, which is another significant description, defines modulation depth. If modulation depth becomes "1", this means that hundred percent modulation is provided.

In Figure 4.48, a modulation frequency analysis is shown with a waterfall diagram and its graphical representation. According to the waterfall diagram, third engine order (3 EO) is clearly seen as a modulation frequency, which highly dominates the gear impacts. By taking into account this modulation frequency analysis, it can be inferred that gear impact noise is excited by firing born periodic impacts.

#### 4.4.4 Cepstrum analysis of hot idle data

Cepstrum analysis is a useful technique to identify periodic harmonics in a spectrum. Therefore, it is commonly used for gear fault detection. In classical cepstrum analysis, cepstrum procedure is applied to Fourier spectrum. However, a variation of the cepstrum analysis is adopted in this thesis. Instead of using the amplitude spectrum, envelope spectrum of the time signal is used in the cepstrum analysis and this procedure is named here as "cepslope". This yielded much clear detection of the harmonics in the envelope spectrum. In Figure 4.49 and 4.50, power cepstrum of the envelope spectrum are presented for accelerometer and microphone data. As seen, 3 EO and its subharmonics are clearly observed in cepstrum envelope analyses.

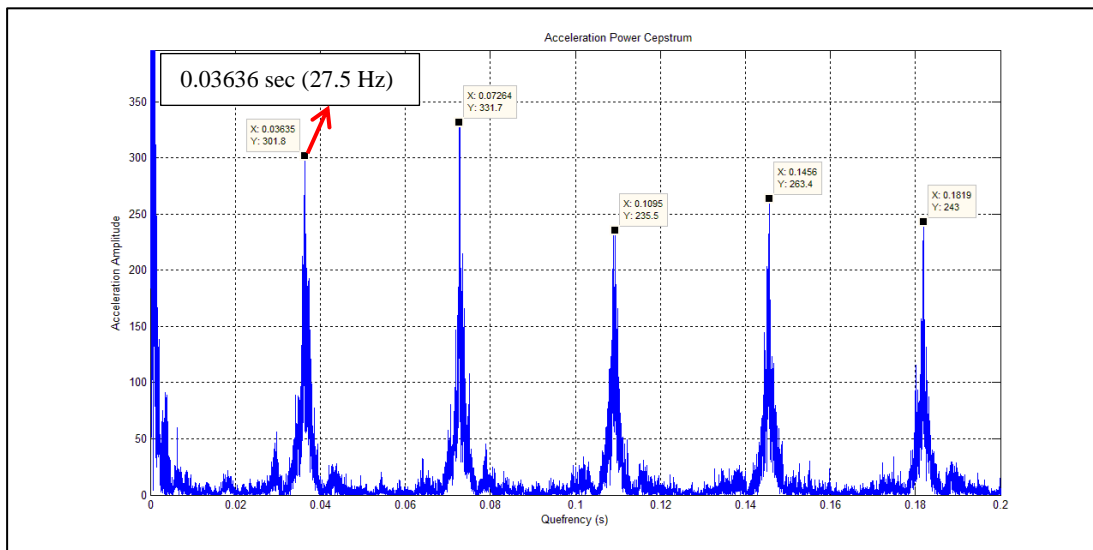


Figure 4.49 : Cepsrum envelope (Cepslope) analysis of accelerometer data.

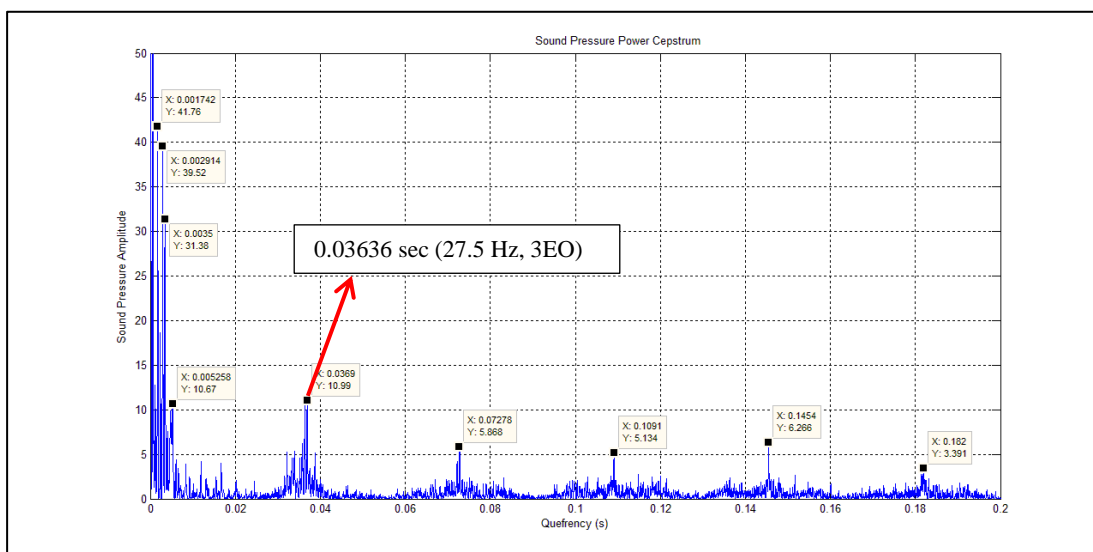


Figure 4.50 : Cepsrum envelope (Cepslope) analysis of microphone data.

## **5. CONCLUSIONS AND RECOMMENDATIONS**

### **5.1 Conclusions**

The main goal of this thesis is to identify the effective parameters on geartrain impact noise in heavy-duty diesel engines. Numerical and experimental studies are carried and results are compared for this purpose.

First of all, geartrain impact impulse method shows that crankshaft gear and crankshaft idler gear mesh appears to be the most critical gear mesh for gear impacts. However, it was not possible to detect the critical gear mesh for gear impacts by experimental studies. By using impact impulse method, gear loading with power assisted steering pump and fuel pump phasing are determined as significant factors on gear impacts. According to geartrain impact impulse analysis, gear loading directly reduces impact impulses, however the effects of fuel pump phasing is somewhat complicated as it depends both on phasing angle and engine speed. Generally, fuel pump phasing and gear loading have more influence on impact impulse compared to backlash effect. Moreover, experimental studies conducted for fuel pump phasing and gear loading yield similar result when compared to those predicted by numerical analysis. Experimental results suggest that fuel pump phasing has strong effect on gear impact noise in full load conditions. Also, it is found that gear loading has significant effect on gear impact noise in hot idle condition. On the other hand, backlash appears to have minor effect on geartrain impact noise according to results obtained by using various oilpump backlash values. However, significant noise effect is observed when idler backlash value is changed in vehicle test. Therefore, chosen gear mesh is important in order to see backlash effect on gear impact noise. Furthermore, changing backlash value of all gear meshes would be beneficial in order to see backlash effect clearly on gear impact noise.

Second, torsional vibration analyses are conducted using both numerical analyses and experimental studies. According to numerical and experimental analyses, torsional vibration analyses show that combustion order, especially the third engine

order, dominates crankshaft torsional vibrations. It is also known from literature survey that torsional vibration is the main excitation mechanism of gear impacts. Thus, torsional vibration characteristic of crankshaft is determined by both numerical and experimental studies. It can be inferred that improvement on combustion process will help to reduce geartrain impacts. Moreover, envelope analysis shows the repetition of combustion orders in the envelope spectrum, suggesting that combustion order is one of the most significant parameter affecting gear impacts. Furthermore, third engine order, which is fundamental order of combustion, is determined as critical order according to cepstrum (cepstrum + envelope) analysis. Numerical and experimental studies also show that combustion order has strong effect on crankshaft torsional vibrations. Torsional vibrations and gear impacts appear to be coupled with each other.

In engine acoustic dynamometer, significant noise source is detected from the heavy-duty engine surface by using acoustic camera at hot idle speed. Acoustic camera results show the rear side of the heavy-duty engine as the highest noise contributor. Additionally, geartrain is located at engine rear side hence geartrain is the main suspected component for impact noise. Moreover, microphone and accelerometer measurements reveal the broadband noise characteristics of impact noise according to waterfall diagrams. Impact noise is observed in a wide frequency range. Good correlations between acoustic camera results and microphone & accelerometer results are obtained for geartrain impact noise at impact frequencies.

FRF test also give information about housing effect on impact noise. It shows that design of housing has significant effect on structural behavior of housing, which can also lead to higher noise radiation from housing surface due to the gear impacts.

Cylinder pressure variations of six cylinder heavy duty engine is also investigated in engine dynamometer. Results show that cylinder to cylinder pressure variations occur in the engine, which can be significant in heavy-duty engines and these pressure variation could also affect crankshaft torsional vibrations.

## **5.2 Future Reccomendations**

Further CAE analyses could give more information about gear impacts. It is known that torsional vibrations have crucial effect on gear impact noise. Therefore, full

torsional modal analysis of geartrain system can be carried out by using appropriate CAE software. Moreover, geartrain modal tests can be performed experimentally for the determination of natural frequencies of torsional modes. Experimental modal analysis will provide more accurate information about torsional behavior of the system. Torsional excitation of the system for modal testing purposes appears to be somewhat difficult, hence improvements can be made in this area.

In order to investigate the effects of camshaft damper and torsional spring on gear impacts, CAE analyses can be conducted by using impact impulse method in AVL Excite software. Gear contact has nonlinear time dependent mesh stiffness according to gear dynamics theory. However, AVL Excite uses constant mesh stiffness for impact impulse analysis. Therefore, nonlinear time dependent mesh stiffness model can be applied in AVL Excite software in order to obtain more precise impact impulse result. Furthermore, a new mesh stiffness model can be developed by including frictional effects as well.

Gear quality definitely affects the geartrain impact noise. Thus, its effect can experimentally investigated by using gears with different levels of quality in engine geartrain system.

Time domain analyses alone may not provide detailed information about geartrain impact noise characteristics. Therefore, such analyses should be followed by frequency domain analyses including envelope analysis. No impact and impact cases may be simulated and for the determination of the geartrain impact noise characteristics in diesel engines.

Fuel pump phasing effects are explained in the theory as well as in numerical and experimental studies. However, its effect on gear impacts could not be revealed by using detail torque and speed measurements. Torque and speed measurements of fuel pump can be compared with engine torque and speed measurements as a function of engine crank angle.

A rattle (impact) index will be helpful for the assessment of rattle noise level in NVH studies. For instance, rattle index can be developed based on engine specific hence rattle noise level will be estimated by the help of this index before the mass production of engines.

Effect of gear housing is investigated in this thesis by impact test. Moreover, sound transmission loss calculation of different gear housing can be performed for rattle noise analysis.

Another recommendation for future studies could be obtaining acoustic transfer functions of geartrain by applying impact to gear teeth with a hammer and measuring sound pressure level with a microphone, yielding sound pressure level due to impact force at the gear teeth. This may provide a model for the determination of gear impact noise at critical frequencies.

Finally, the author of this thesis wishes to offer geartrain design recommendations concerning gear impact noise. It is believed that the recommendations listed below would be helpful for reducing geartrain impact noise in diesel engines:

- ✓ Reducing the number of gear meshes.
- ✓ Reducing gear backlash as well as most critical gear mesh backlash value. Also, controlling axial tolerances of gears.
- ✓ Optimizing fuel pump phasing angle: It can increase or decrease gear impact excitation with respect to baseline condition.
- ✓ Using anti-backlash (scissor) gear for critical gear meshes: It would be helpful for ensuring all time gear contact. However, it decreases the efficiency of transmission, as it absorbs (dissipates) energy.
- ✓ Using torsional vibration damper in critical gear meshes such as in crankshaft, fuel pump and camshaft gear meshes in order to prevent impact excitation.
- ✓ Reducing torsional excitation by controlling combustion process and crankshaft geometry.
- ✓ Gear property: Using high gear quality, using helical gear due to higher contact ratio, using spur gears with high addendum teeth, using small production tolerances in order to reduce gear impact noise.
- ✓ Stiffening of gear housing by using ribs: Ribs location should be optimized.
- ✓ Increasing rotational inertia of gears.

## REFERENCES

- [1] **Rust, A.** (2012). NVH Workshop, Kocaeli, Turkey.
- [2] **Doğan, S. N.** (1999). Loose part vibration in vehicle transmissions - Gear rattle, *Tr. J. of Engineering and Environmental Science*, Vol. 23, pp. 439-454.
- [3] **Esmaeli, M. and Subramaniam, A.** (2011). Engine Timing Geartrain Concepts and Proposals for Gear rattle Noise Reduction in Commercial Vehicles, *M.Sc. Thesis*, Chalmers University of Technology, Gothenburg, Sweden.
- [4] **Crocker, M. D., Amphlett, S. A., and Barnard, A. I.** (1995). Heavy Duty Diesel Engine Gear Train Modelling to Reduce Radiated Noise, *SAE Technical Paper Series*, No: 951315.
- [5] **Wilhelm, M., Laurin, S., Schmillen, K., and Spessert, B.** (1990). Structure Vibration Excitation by Timing Gear Impacts, *SAE Technical Paper Series*, No: 900011.
- [6] **Bailey, G. and Fussner, D.** (2011). A Multi-Variable Experimental Study of Diesel Geartrain Rattle, *SAE International*, No: 2011-01-1561.
- [7] **Gao, Z., Saine, K., and Wollström, M.** (2009). Gear Noise Analysis for a Large Diesel Engine, *The 16<sup>th</sup> International Congress on Sound and Vibration*, Kraków, Poland, July 5-9.
- [8] **Glyniadakis, G. V., Souza, A. B., Pecula, M. M., and Rodrigues, M. C.** (2010). Diesel Engine Air Compressor Rattle Noise, *SAE International*, No: 2010-01-1540.
- [9] **Ozguven, H. N. and Houser, D. R.** (1988). Mathematical Models Used in Gear Dynamics – A Review, *Journal of Sound and Vibration*, Vol. 121, No.3, pp. 384–411.
- [10] **Singh, R., Houser, D. R., and Kahraman, A.** (1990). Non-Linear Dynamic Analysis of Geared Systems, *NASA Contractor Report*, Ohio State University, Columbus, Ohio, USA, No: 4338.
- [11] **Rodriguez, J., Keribar, R., and Fialek, G.** (2005). A Geartrain Model with Dynamic or Quasi-Static Formulation for Variable Mesh Stiffness, *SAE Technical Paper Series*, No: 2005-01-1649.
- [12] **Rivola, A., Milandri, M., and Mucchi, E.** (2006). A Geartrain Model for the Dynamic Analysis of a Motorbike Timing System, *Proceedings of ISMA 2006 Multi-Body Dynamics and Control*, pp. 2689–2703.
- [13] **Carbonelli, A., Perret-Liaudet, J., and Rigaud, E.** (2014). Hammering noise modelling – Nonlinear dynamics of a multi-stage gear train, *International Gear Conference*, Lyon, France, pp. 447–456.

- [14] **Singh, R., Lim, T. C., and Zakrajsek, J. J.** (1989). Modal Analysis of Gear Housing and Mounts, *NASA Technical Memorandum*, Ohio, USA, No: 101445.
- [15] **Schomer, P. D., Hottman, S. D., Kessler, F. M., and Kessler, R. K.** (1987). Expedient Methods for Rattle-Proofing Certain Housing Components, *USA CERL Technical Report*, US Army Corps of Engineers, No: 87/24.
- [16] **Ognjanović, M. and Kostić, S. C.** (2012). Gear Unit Housing Effect on the Noise Generation Caused by Gear Teeth Impacts, *Journal of Mechanical Engineering*, Vol. 58, No. 5, pp. 327–337.
- [17] **Özgülven, H. N.** (2008). *Gürültü Kontrolü: Endüstriyel ve Çevresel Gürültü*, Türk Akustik Derneği, İstanbul.
- [18] **Bodden, M. and Heinrichs, R.** (1999). Analysis of the time structure of gear rattle, *Proceedings of the Internoise 99*, Fort Lauderdale, USA, pp. 1273–1278.
- [19] **Url-1**<<http://science.howstuffworks.com/transport/engines-equipment/gear2.htm>>, date retrieved 27.04.2015.
- [20] **Url-2**<<http://science.howstuffworks.com/transport/engines-equipment/gear3.htm>>, date retrieved 27.04.2015.
- [21] **Yücenur, M. S. and Temiz, V.** (2004). *Dişli Çarklar*, İTÜ Makina Fakültesi, İstanbul, Turkey.
- [22] **Babalık, F. C.** (2009). *Makine Elemanları ve Konstrüksiyon Örnekleri*, Uludağ Üniversitesi, Dora Yayıncılık, Bursa, Turkey.
- [23] **Sahip, Y.** (2012). NVH Evaluation of a High Pressure Fuel Pump MBD Model with Internal Hydraulic Effects and Valve Train System Excitation Parameters, *M.Sc. Thesis*, Istanbul Technical University, Istanbul, Turkey.
- [24] **Barber, A.** (1993). *Handbook of Noise and Vibration Control*, Elsevier Advanced Technology.
- [25] **Gopinath, K. and Mayuram, M. M.** (n.d.). *Machine Design 2*, Indian Institute of Technology Madras.
- [26] **AVL Acoustics** (2005). *Noise and Vibration Training*, Graz, Austria.
- [27] **Xin, Q.** (2011). *Diesel engine system design*, Woodhead Publishing Limited, USA, pp. 759–821.
- [28] **Nilsson, A. I.** (2013). Gear Whine Noise Excitation Model, *M.Sc. Thesis*, Chalmers University of Technology, Gothenburg, Sweden.
- [29] **Houser, D. R., Harianto, J., and Ueda, Y.** (2004). Determining the source of gear whine noise, *Gear Solutions*.
- [30] **Kelly, P. and Menday, M.** (2010). *Tribology and dynamics of engine and powertrain*, Woodhead Publishing Limited, USA, pp. 839–856.
- [31] **Url-3**<<http://upload.wikimedia.org/wikipedia/en/2/2e/Backlash.jpg>>, date retrieved 27.04.2015.

- [32] **Rust, A., Brandl, F. K., and Thien., G. E.** (1992). Investigation of Gear Rattle Phenomena, AVL List GmbH, Graz, Austria.
- [33] **Pasin, F.** (1994). *Mekanik Sistemler Dinamiği*, İTÜ Makina Fakültesi, Istanbul, Turkey.
- [34] **Kahraman, A. and Singh, R.** (1990). Mathematical models Used in Gear Dynamics – A Review, *Journal of Sound and Vibration*, Vol. 142, No.1, pp. 49-75.
- [35] **Xin, Z., Changzheng, C., Jie, L., and Lei, Z** (2015). Dynamic characteristics of a spur gear transmission system for a wind turbine, *International Conference on Automation, Mechanical Control and Computational Engineering (AMCCE 2015)*, Vol. 142, No.1, pp.1985-1990.
- [36] **Mitianiec, W. and Buczek, K.** (2008). Torsional Vibration Analysis of Crankshaft in Heavy Duty Six Cylinder Inline Engine, Wydawnictwo Politechniki Krakowskiej.
- [37] **Guney, İ. A.** (n.d.). *Taşıtlarda Titreşim ve Gürültü*, İTÜ Makina Fakültesi – Otomotiv Anabilim Dalı, Istanbul, Turkey.
- [38] **Brandt, A.** (2011). *Noise and Vibration Analysis: Signal Analysis and Experimental Procedures*, University of Southern Denmark, A John Wiley and Sons, Ltd., Publication.
- [39] **Hansen, H. K. and Herlufsen, H.** (2010). *Envelope and Cepstrum Analyses for Machinery Fault Identification*, Brüel and Kjaer, Nærum, Denmark.
- [40] **Randall, R. B.** (1987). *Frequency Analysis*, Brüel & Kjaer, Denmark.
- [41] **AVL List GmbH** (n.d.). *Excite Timing Drive Training*, Graz, Austria.
- [42] **AVL List GmbH** (2013). *AVL Product Description Excite Timing Drive*, Graz, Austria.
- [43] **AVL List GmbH** (2013). *AVL Excite Designer Theory*, Graz, Austria.
- [44] **Balci, E.** (2013). Influence of Rib Stiffener Design Parameters on the Noise Radiation of an Engine Block, *M.Sc. Thesis*, Istanbul Technical University, Istanbul, Turkey.
- [45] **Url-4** <<http://www.bksv.com/Products/transducers/acoustic/microphones/microphone-cartridges/4188>>, date retrieved 27.04.2015.
- [46] **Url-5** <[http://www.pcb.com/contentstore/docs/PCB\\_Corporate/Vibration/Products/Manuals/HT356B21.pdf](http://www.pcb.com/contentstore/docs/PCB_Corporate/Vibration/Products/Manuals/HT356B21.pdf)>, date retrieved 27.04.2015.
- [47] **Url-6** <[http://portal.tugraz.at/portal/page/portal/Files/i3050/files/labor/Brochure\\_LMS\\_scadas.pdf](http://portal.tugraz.at/portal/page/portal/Files/i3050/files/labor/Brochure_LMS_scadas.pdf)>, date retrieved 27.04.2015.
- [48] **Zimmermann, B. and Studer, C.** (2010). FPGA-based Real-Time Acoustic Camera Prototype, Circuits and Systems (ISCAS), *Proceedings of 2010 IEEE International Symposium*.
- [49] **Url-7** <[https://www.head-acoustics.de/downloads/eng/head\\_visor/D7500\\_HEAD\\_VISOR\\_e.pdf](https://www.head-acoustics.de/downloads/eng/head_visor/D7500_HEAD_VISOR_e.pdf)>, date retrieved 27.04.2015.
- [50] **Rust., A.** (2014). *Gear Rattle Noise Appointment*, Graz, Austria.

- [51] **Bremer, R.**, (1979). A Practical Treatise on Engine Crankshaft Torsional Vibration Control, *SAE Technical Paper Series*, No790763.
- [52] **Feese, T. and Hill, C.** (2009). Prevention of Torsional Vibration Problems in Reciprocating Machinery, *Proceedings of the Thirty-Eighth Turbomachinery Symposium*, Turbomachinery Laboratory, Texas A&M University, College Station, Texas, USA, pp. 213-238.

## **CURRICULUM VITAE**



**Name Surname:** Ali Tatar

**Place and Date of Birth:** Istanbul, 02.05.1990

**E-Mail:** tataric@gmail.com

**B.Sc.:** Istanbul Technical University, Mechanical Engineering (2012)

**B.Sc.:** Istanbul Technical University, Mechatronics Minor (2013)

### **Professional Experience and Rewards:**

Turkish Government Graduate Scholar – Republic of Turkey Ministry of National Education / 2015 – Present

Engine NVH Development Engineer – AVL Turkey / 2013 – 2015